ALMA MATER STUDIORUM - UNIVERSITA' DI BOLOGNA
Dipartimento di Elettronica, Informatica e Sistemistica, sede di Cesena

Dottorato di Ricerca in Bioingegneria

XX CICLO

Settore Scientifico Disciplinare: ING-IND/34

BIOMECHANICAL MODELLING OF HUMAN KNEE DURING LIVING ACTIVITIES

(MODELLAZIONE BIOMECCANICA DEL GINOCCHIO DURANTE ATTIVITA' MOTORIE QUOTIDIANE)

Autore

Ing. Luigi Bertozzi

Coordinatore
Prof. Angelo Cappello

Supervisore
Prof. Angelo Cappello

Correlatore
Prof. Rita Stagni

Controrelatore
Prof. Luca Cristofolini

Esame finale anno 2008

This work is dedicated to my family,

my wife Barbara and my daughter Rita.

Abstract – Italian Version

L'articolazione di ginocchio è una struttura chiave del sistema locomotore umano. Conoscere come ogni singola struttura anatomica contribuisce a determinare la complessa funzione biomeccanica del ginocchio è di fondamentale importanza per lo sviluppo di nuove protesi e di innovative procedure cliniche, chirurgiche e riabilitative. In questo contesto, l'utilizzo di un approccio modellistico è l'unico modo possibile per quantificare la funzione biomeccanica di ogni singola struttura anatomica in condizioni fisiologiche, come ad esempio stimare la forza prodotta dai legamenti crociati durante l'esecuzione di compiti motori quotidiani.

Lo scopo principale di questo studio è stato ottenere un modello di ginocchio altamente specifico di un soggetto selezionato utilizzando tecniche diagnostiche per immagini, come risonanza magnetica e video-fluoroscopia. Utilizzando accurate geometrie ossee e cinematiche articolari acquisite sperimentalmente dal soggetto considerato, sono stati sviluppati modelli 3D dei legamenti crociati e del contatto articolare tra tibia e femore.

Nel modello dei legamenti crociati, ognuno dei due legamenti è stato modellato tramite l'utilizzo di 25 elementi elastici-lineari disposti considerando la naturale torsione anatomica delle fibre. Nel modello sviluppato si è cercato di raggiungere il più alto livello di specificità al soggetto possibile. Infatti, ogni singola molla è stata geometricamente caratterizzata utilizzando dati sperimentali provenienti dal soggetto selezionato, mentre l'unico parametro meccanico del modello, il modulo elastico, è stato considerato da dati sperimentali riportati in letteratura a causa delle misure invasive necessarie per quantificarlo nel soggetto selezionato. Una volta implementato, il modello è stato utilizzato simulando test di stabilità e imponendo i compiti motori eseguiti dal soggetto. I risultati ottenuti sono sempre stati fisiologicamente significativi. Tuttavia, la mancanza di un valore del modulo elastico proveniente dal soggetto selezionato ha generato la necessità di sviluppare una metodologia sperimentale per caratterizzare la meccanica dei legamenti crociati in soggetti viventi e senza misure dirette ed invasive.

Utilizzando i medesimi dati geometrici e cinematici, sono stati anche implementati due modelli per la valutazione del contatto tibio-femorale, uno finalizzato alla stima dell'area di contatto in posizioni statiche (massima estensione con e senza peso corporeo), ed uno finalizzato alla valutazione della posizione del punto di contatto durante i compiti motori eseguiti dal paziente. Questi due diversi approcci sono stati implementati e testati valutando i pro e i contro di ognuno in modo da suggerirne il corretto ambito di utilizzo e possibili miglioramenti futuri.

Il risultato finale di questo studio contribuirà allo sviluppo di avanzate metodologie per la valutazione *in-vivo* della funzione/patologia dell'articolazione di ginocchio, anche durante compiti motori della vita quotidiana. Le metodologie sviluppate saranno così di notevole utilità per lo sviluppo di nuove protesi, strumenti e procedure sia nel campo della ricerca che in campo clinico, chirurgico e riabilitativo.

Abstract

The knee joint is a key structure of the human locomotor system. The knowledge of how each single anatomical structure of the knee contributes to determine the physiological function of the knee, is of fundamental importance for the development of new prostheses and novel clinical, surgical, and rehabilitative procedures. In this context, a modelling approach is necessary to estimate the biomechanic function of each anatomical structure during daily living activities.

The main aim of this study was to obtain a subject-specific model of the knee joint of a selected healthy subject. In particular, 3D models of the cruciate ligaments and of the tibio-femoral articular contact were proposed and developed using accurate bony geometries and kinematics reliably recorded by means of nuclear magnetic resonance and 3D video-fluoroscopy from the selected subject.

Regarding the model of the cruciate ligaments, each ligament was modelled with 25 linear-elastic elements paying particular attention to the anatomical twisting of the fibres. The devised model was as subject-specific as possible. The geometrical parameters were directly estimated from the experimental measurements, whereas the only mechanical parameter of the model, the elastic modulus, had to be considered from the literature because of the invasiveness of the needed measurements. Thus, the developed model was employed for simulations of stability tests and during living activities. Physiologically meaningful results were always obtained. Nevertheless, the lack of subject-specific mechanical characterization induced to design and partially develop a novel experimental method to characterize the mechanics of the human cruciate ligaments in living healthy subjects.

Moreover, using the same subject-specific data, the tibio-femoral articular interaction was modelled investigating the location of the contact point during the execution of daily motor tasks and the contact area at the full extension with and without the whole body weight of the subject. Two different approaches were implemented and their efficiency was evaluated. Thus, pros and cons of each approach were discussed in order to suggest future improvements of this methodologies.

The final results of this study will contribute to produce useful methodologies for the investigation of the *in-vivo* function and pathology of the knee joint during the execution of daily living activities. Thus, the developed methodologies will be useful tools for the development of new prostheses, tools and procedures both in research field and in diagnostic, surgical and rehabilitative fields.

Acknowledgements

The successful completion of this work is the result of the help, cooperation, faith and support of many people.

First of all, I need to thank my supervisor Prof. Angelo Cappello, since without him, none of this work would have been possible. He provided me with the opportunity to make this research happen.

A special thanks to my co-supervisor, Prof. Rita Stagni, for her great patience, constant encouragement, and endless support throughout my doctoral studies. Her patient guidance not only helped me to improve my research skills, but also to become a better person.

For their reviews and comments regarding the manuscript you are holding, I would like to thank Prof. Silvia Fantozzi and Prof. Luca Cristofolini. The suggestions they provided helped me to greatly improve the quality of this document.

I would also extend my sincere appreciations to all my friends who stayed close to me in these years. In particular, I would to thank Luca for the pleasant conversations, the restoring walks and swims, and the hard fought games of chess.

My parents receive my deepest gratitude and love for their many years of support and encouragement.

Last but not the least, I would like to thank my wife for her understanding and love during the past few years, and specially for giving me a beautiful daughter, Rita.

Table of Contents

List of Tables

List of Figures

List of Abbreviations

2D: Two-dimensional
3D: Three-dimensional
A/P: Anterior-Posterior direction/axis
M/L: Medial-Lateral direction/axis
P/D: Proximal-Distal direction/axis
Lg: Longitudinal direction/axis
Fl/Ex: Flexion-Extension angle/rotation
In/Ex: Intra-Extra angle/rotation (**I/E**)
Ab/Ad: Abduction-Adduction angle/rotation

NMR: Nuclear Magnetic Resonance
MRI: Magnetic Resonance Imaging
CT: Computed Tomography
EMG: Electromyography
EEG: Electroencephalography
GFR: Ground Force Reaction

ACL: Anterior Cruciate Ligament
PCL: Posterior Cruciate Ligament
MCL: Medial Collateral Ligament
LCL: Lateral Collateral Ligament

DAEs: Differential Algebraic Equations
RBSM: Rigid Body Spring Model
FEM: Finite Element Method
MH: Modified Hertzian theory
SES: Simplified Elastic Solution
TPS: Thin Plate Splines
NURBS: Non-uniform rational B-splines
RMSE: Root Mean Square Error

Introduction

The human knee joint is an attracting complex of anatomical structures which fascinates anatomists, clinicians and bioengineers. This joint has two apparently contrasting requirements: it must be mobile in order to achieve a large and smooth range of motion, and it must be stable in order to guarantee strong support to loading conditions of the daily living activities. The knee accomplishes these two fundamental requirements by the concurrent actions of different active (i.e. muscles), and passive anatomical structures, such as the *cruciate ligaments*, and by the conformity of the *articular surfaces*. Any injury to any of these anatomical structures alters the function of the whole joint. Thus, a good knowledge of the *in-vivo* biomechanical function of each anatomical sub-unit is of fundamental importance and of great clinical interest for the development of new effective rehabilitative and surgical procedures.

In order to reach this aim, it is possible to use different approaches. Although experimental methods produce direct and reliable measurements of the variables of interest, they are usually quite invasive and can alter physiological conditions and limit generalization. Thus, when the goal is the evaluation of the normal function of the considered organ, invasive measurements should be avoided and a modelling approach might be preferred. Moreover, with the evolution of the medical and the diagnostic technologies, such as MRIs, CTs, EMGs and EEGs, nowadays it is possible to investigate the anatomy and the function of organs and tissues of a living healthy subject with a limited invasiveness.

The aim of this work was to provide novel experimental methodologies for the investigation of the knee joint in living subjects, with particular attention to the subject-specific modelling of the cruciate ligaments and of the tibio-femoral contact. Thus, the objective of this study was to obtain subject-specific models of the cruciate ligaments and of the tibio-femoral articular interaction, which were exploitable during the execution of daily living activities. Each one of these models was designed and developed as a computational tool aimed to investigate the specific functionality/pathology

of the considered anatomical structure of the selected subject. This means that, for example, the model of the cruciate ligament neglected the possibility to evaluate the functionality of other anatomical structures of the knee, such as collaterals, capsule, muscles and bony and cartilaginous interactions. Moreover, each developed model neglected the possibility: i) to export the developed methodology for other similar anatomical structures, because of the specificity of the hypotheses made with respect to the considered anatomical structure, and ii) to generalize the model designed for a specific subject and apply it for other subjects, because of the intrinsic differences in morphological and kinematical data. Finally, since the developed models were aimed to be used in physiological conditions, such as the execution of daily living activities, these models had to be simple and computationally light in order to be executed several times, once for each acquired frame. In this study, the considered kinematics were only the chair rising/sitting and the step up/down motor tasks, but using the developed methodologies and models can be evaluated all those motor tasks in which the knee under analysis can be recorded by means of a video-fluoroscopy.

The terminology used in the present thesis with respect to the biomechanics of knee joint is provided in Chapter 1. In particular, an anatomical description of the main passive and active structures is provided paying a particular attention on the mechanical behaviour of the modelled anatomical structures. Finally, a brief biomechanical description of the two apparently conflicting functions of the physiological knee joint (i.e. stability and mobility) is also proposed.

Through the last two centuries, the problem of the knee modelling has been tackled from different points of view and at different levels of complexity. A thorough state-of-the-art review about knee biomechanics is reported in Chapter 2. A particular attention is focused on methods and tools that can be used in modelling of knee joint and on problems that could arise in this context.

The cruciate ligaments are one of the most attractive anatomical structures of the knee joint because of their mechanical behaviour, which is simple but very effective and hard to reproduce by means of the surgical approach. The interest on these anatomical structures is also demonstrated by almost 8 millions injury-related visits, 478000 total knee replacements and

9000 other repair of cruciate ligaments performed in the USA in 2004 as reported by the American Association of Orthopaedic Surgeons (AAOS). Given the importance of these key structures, a 3D quasi-static model of the human cruciate ligaments is implemented and described in Chapter 3. The devised model is as subject-specific as possible, because it is extensively based on the use of geometrical and kinematical data acquired and computationally reconstructed from a living and healthy selected subject. This model is also used to evaluate the functionality of the cruciate ligaments both during simulated stability tests, and during the execution of daily living activities.

Another important mechanism of the knee joint is the interaction between the tibial and the femoral bones, the tibio-femoral joint. This mechanism, along with the cruciate ligaments, is one of the most important to provide knee joint with its two main functions: stability and mobility. Thus, using the same geometries and same the kinematics acquired and reconstructed for the cruciate ligament model, two different approaches to evaluate the 3D tibio-femoral interaction in living subjects are provided in Chapter 4.

Considering again the cruciate ligaments model described in Chapter 3, the only two aspects, that prevented to obtain a validated subject-specific model, are the lack of the subject-specific elastic modulus and the knowledge of the forces produced from the cruciate ligaments of the selected subject during the kinematical acquisition. In order to overcome these two problems, in Chapter 5, a novel experimental *arthrometer*, a device with the capability to synchronously measure the forces applied to the knee and the joint kinematics, is proposed and developed at a prototype stage.

When all devised methodologies will be improved and integrated, this study will provide the biomechanical and the clinical communities with useful methodologies for the evaluation of the *in-vivo* function and pathology of the knee joint in living subjects, with the capability to perform estimations during the execution of daily living activities. Moreover, the developed methodologies will be useful tools for the development of new prostheses, tools and procedures both in research field and in diagnostic, surgical and rehabilitative fields.

References

AAOS, American Association of Orthopaedic Surgeons, 2004
Available on-line at http://www.aaos.org/Research/stats/patientstats.asp

Chapter 1: Description of Knee Joint

In this chapter, a comprehensive description of the human knee joint is provided in order to better understand the terminology used in next and more specific chapters. First of all, anatomical and articular references are defined with respect to specific clinical and anatomical studies (Gray, 1918; Gray, 1977; Grood and Suntay, 1983). Then, the main structures of the knee joint, such as bones, ligaments and muscles, are deeply described from an anatomical and morphological point of view. A description of the mechanical behaviour is also provided for those anatomical structures considered of major interest in this study. Finally, in order to help the reader, a short survey about the biomechanics of the knee joint is provided paying particular attention to its main functions, the stability and the mobility.

1.1 General Anatomical References

Before specifying the anatomy of the knee joint in detail, in this section the terminology used in the present thesis to define kinematics terms is reported. For descriptive purposes, the body is usually supposed to be in the erect posture, with the arms hanging by the sides and the palms of the hands directed forward (Figure 1.1). The *median plane* is a vertical anterior-posterior (AP) plane, passing through the centre of the trunk, approximately through the sagittal suture of the skull, and hence any plane parallel to it is termed a **sagittal plane.** A vertical plane at orthogonal to the median plane passing through the central part of the coronal suture or through a line parallel to it is known as a **coronal plane**. A plane at right angles to both the median and frontal planes is termed a **transverse plane**. The terms **anterior**, and **posterior**, are used to indicate the relation of parts to the front or back of the body or limbs (*anterior-posterior axis, AP axis*), and the terms **superior**, and **inferior**, to indicate the relative levels of different structures (along the *longitudinal axis, Lg axis*). Structures nearer to or farther from the median plane are referred to as **medial** or **lateral** respectively (along the *medio-lateral axis, ML axis*). In the case of the limbs the words **proximal** and **distal** refer to the relative distance from the attached end of the limb (*along the proximal-distal axis, PD axis*) (Gray, 1918).

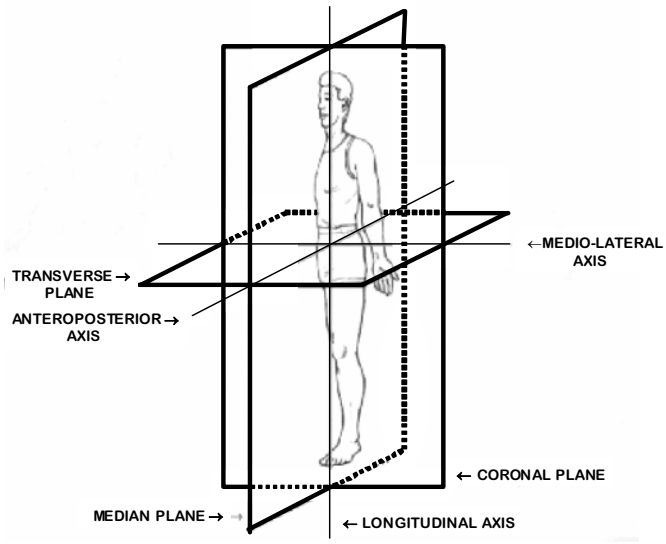

Figure 1.1: Anatomical planes and axis

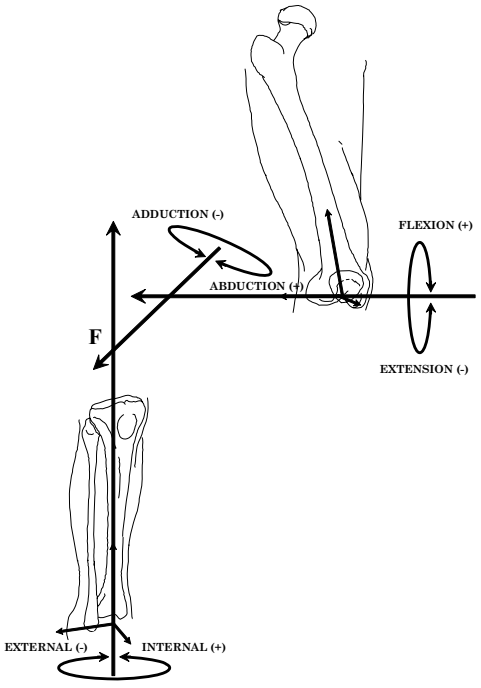

Figure 1.2: Joint angles are defined by rotations occurring about the three joint coordinate axes. Flexion/extension is about the femoral body fixed axes. External/internal tibial rotation is about the tibial fixed axis and ab/adduction is about the floating axis (F).

According to the ISB recommendations (Wu and Cavanagh, 1995), the knee joint coordinate system used in the present thesis allows rotations about axes which can be anatomically meaningful, allowing the preservation of an important linkage with medical terminology. The system used was the one proposed by Grood and Suntay (Grood and Suntay, 1983) (Figure 1.2). Two body fixed axes are established relative to anatomical landmarks, one in each body on opposing sides of the joint: one is the medio/lateral axis of the femur the other is the longitudinal axis of the tibia (Figure 1.2). The third axis, called the floating axis (Figure 1.2, F), is defined as being perpendicular to each of these two body fixed axes. The rotation about the femoral medio/lateral axis is designated as **flexion/extension** (Fl/Ex). The rotation about the tibial longitudinal axis is designated as **external/internal rotation** (Ex/In). The rotation about the floating axis is designated as **ab/adduction** (Ab/Ad).

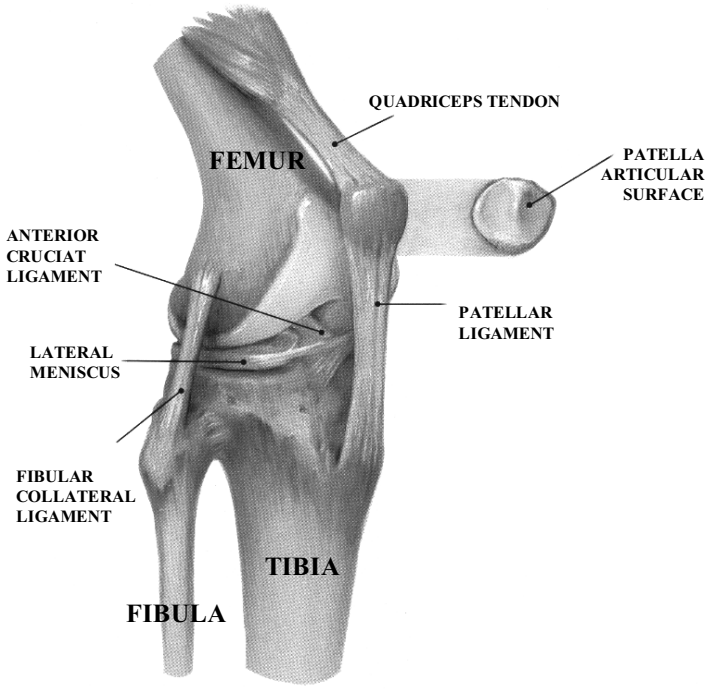

Figure 1.3: Human knee joint

1.2 Anatomy, Morphology, and Mechanics

The human knee is a unique tri-articular joint responsible for the most demanding biomechanical functions of our musculoskeletal system (Figure 1.3). The three distinct contact surfaces are the patello-femoral joint and the medial and lateral tibio-femoral articulations. Although the tibio-femoral articulations involve only two bones, the distal femoral condyles and tibial plateaus articulate in as separate but coordinated manner. These joint movements are further regulated and stabilized dynamically by muscle contractions, and passively by ligamentous and capsular tension. The major part of the detailed description of the human knee anatomy which follows is taken from the Gray's anatomy book (Gray, 1918).

i Bones

The **femur** is the longest and strongest bone in the skeleton. The femur, like other long bones, is divisible into a body (diaphysis) and two extremities (epiphyses). The diaphysis is almost perfectly cylindrical in most of its extent. In the erect posture, it is not vertical, but it inclines gradually downward and medialward, so as to approach the lower part of the contro-lateral femur, with the purpose of bringing the two knee joints near to the line of gravity of the body. This inclination is necessary because the two proximal femurs are separated by a considerable interval, which corresponds to the breadth of the pelvis. Thus, the degree of this inclination varies among subjects, and it is larger in female than in male, on account of the greater breadth of the pelvis. The lower epiphysis, larger than the upper one, is somewhat cuboid in form, but its transverse diameter is larger than its antero-posterior: it consists of two oblong eminences known as the **condyles** (Figure 1.4). The **articular surface** of the lower end of the femur occupies the anterior, inferior, and posterior surfaces of the condyles. Its front part is named the **patellar surface** and articulates with the patella. It presents a median groove which extends downward to the intercondylar fossa and two convexities, the lateral of which is broader, more prominent, and extends farther upward than the medial. The lower and posterior parts of the articular surface constitute the **tibial surfaces** for articulation with the corresponding condyles of the tibia and menisci.

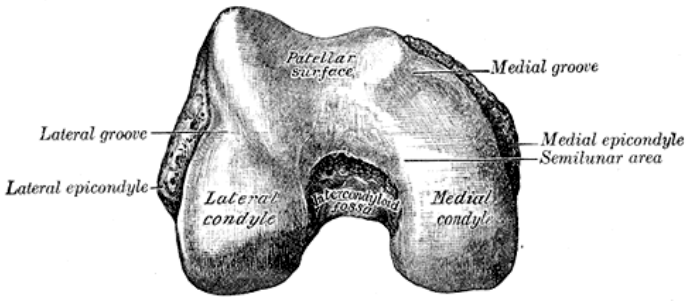

Figure 1.4: Lower extremity of right femur viewed from below (Gray, 1918).

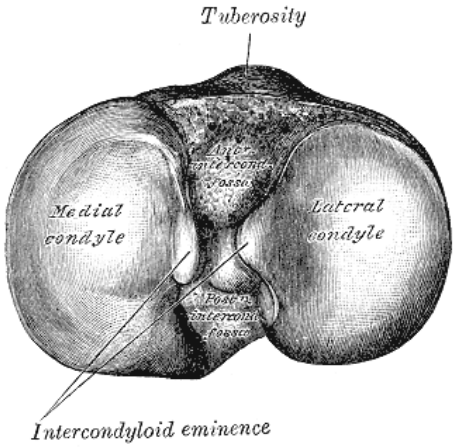

Figure 1.5: Upper surface of right tibia viewed from above (Gray, 1918).

The **tibia** is situated at the medial side of the leg, and, excepting the femur, is the longest bone of the skeleton. It is prismoid in form, expanded above contracted in the lower third, and again enlarged but to a lesser extent below. In male, its direction is vertical, and parallel with the bone of the opposite side, but in the female it has a slightly oblique direction downward and lateralward, to compensate for the greater obliquity of the femur. It has a body and two extremities. The upper extremity is large, and expanded into two eminences, the **medial** and **lateral condyles** (Figure 1.5). The **superior articular surface** presents two smooth articular facets. The medial facet, oval in shape, is slightly concave in the frontal, and in the sagittal plane. The lateral, nearly circular, is concave in the frontal plane, but slightly convex in the sagittal plane, especially at its posterior part, where it is prolonged on to the posterior surface for a short distance. The central portions of these facets

articulate with the condyles of the femur, while their peripheral portions support the menisci of the knee-joint, which here intervene between the two bones.

The **patella** is a flat, triangular bone, situated on the front of the knee-joint (Figure 1.3 and Figure 1.6). It is usually regarded as a sesamoid bone (i.e. a bone embedded within a tendon), developed in the tendon of the Quadriceps femoris, and resembles these bones (1) in being developed in a tendon; (2) in its center of ossification presenting a knotty or tuberculated outline; (3) in being composed mainly of dense cancellous tissue. The primary functional role of the patella is knee extension. In fact, the patella increases the leverage of the Quadriceps femoris muscle group by increasing the angle at which it acts.

ii Joints, Ligaments and Menisci

The bones of the skeleton are joined to one another at different parts of their surfaces, and such connections are termed **Joints** or **Articulations.** The articulations of the human body are divided into three classes: **synarthroses** or immovable, **amphiarthroses** or slightly movable, and **diarthroses** or freely movable. Where the joints are *immovable,* as in the articulations between all the bones of the skull, the adjacent margins of the bones are almost in contact, being separated merely by a thin layer of fibrous membrane, named the **sutural ligament.** In certain regions at the base of the skull this fibrous membrane is replaced by a layer of cartilage. Where *slight movement* combined with great strength is required, the osseous surfaces are united by tough and elastic **fibrocartilages,** as in the joints between the vertebral bodies, and in the interpubic articulation. In the *freely movable* joints the surfaces are completely separated, the bones forming the articulation are expanded for greater convenience of mutual connection, covered by **cartilage** and enveloped by **capsules** of fibrous tissue. The cells lining the interior of the fibrous capsule form an imperfect membrane - the **synovial membrane -** which secretes a lubricating fluid. The joints are strengthened (i.e. restraining unphysiological movements) by strong fibrous bands called **ligaments,** which extend between the bones forming the joint. This latter class includes the greater number of the joints in the body such as

the interphalangeal joints, the joint between the humerus and ulna or the ankle and hip joints.

The knee joint was formerly described as a hinge-joint, but is really of a much more complicated character. It must be regarded as consisting of three articulations in one: two diarthroidal condyloid joints, one between each condyle of the femur and the corresponding meniscus and condyle of the tibia, and a third between the patella and the femur, partly arthrodial, but not completely so, since the articular surfaces are not mutually adapted to each other, so that the movement is not a simple gliding one. The bones of the knee joint are connected together by the following structures.

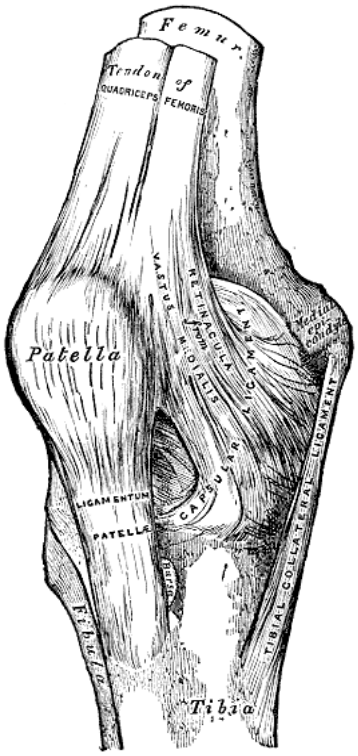

Figure 1.6: Right knee-joint. Anterior view (Gray, 1918).

The **Articular Capsule** (*capsula articularis; capsular ligament*) (Figure 1.6). The articular capsule consists of a thin, but strong, fibrous membrane which is strengthened in almost its entire extent by bands inseparably connected with it. Above and in front, beneath the tendon of the Quadriceps femoris, it is represented only by the synovial membrane. Its chief

strengthening bands are derived from the fascia lata and from the tendons surrounding the joint.

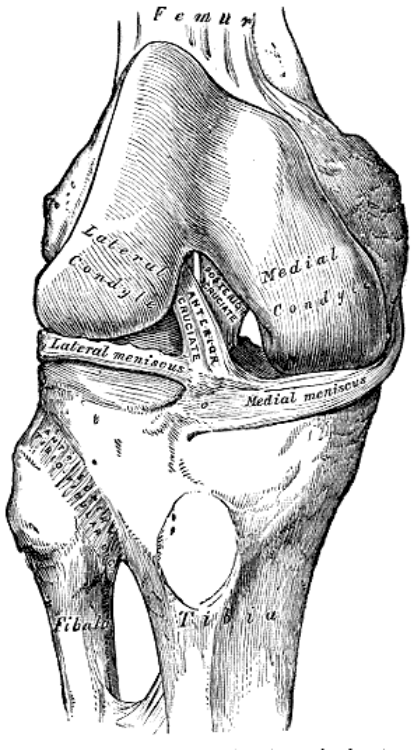

Figure 1.7: Right knee-joint, from the front, showing interior ligaments (Gray, 1918).

The Patellar Ligament (anterior ligament) (Figure 1.6). The patella ligament is the central portion of the common tendon of the Quadriceps femoris, which is continued from the patella to the tuberosity of the tibia. It is a strong, flat, ligamentous band, about 8 cm. in length, attached, above, to the apex and adjoining margins of the patella and the rough depression on its posterior surface, below, to the tuberosity of the tibia. Its superficial fibers are continuous over the front of the patella with those of the tendon of the Quadriceps femoris. The medial and lateral portions of the tendon of the Quadriceps pass down on either side of the patella, to be inserted into the upper extremity of the tibia on either side of the tuberosity.

The **Collateral Ligaments.** The **Medial Collateral Ligament** (MCL, *ligamentum collaterale tibiale, Tibial Collateral Ligament*) (Figure 1.8). The

medial collateral is a broad, flat, membranous band, situated nearer to the back than to the front of the joint. It is attached, *above,* to the medial condyle of the femur immediately below the adductor tubercle, *below,* to the medial condyle and medial surface of the body of the tibia. The **Lateral Collateral Ligament** (LCL, *ligamentum collaterale fibulare; fibular collateral ligament*) (Figure 1.8). The lateral collateral is a strong, rounded, fibrous cord, attached, *above,* to the back part of the lateral condyle of the femur, immediately above the groove for the tendon of the Popliteus, *below,* to the lateral side of the head of the fibula, in front of the styloid process.

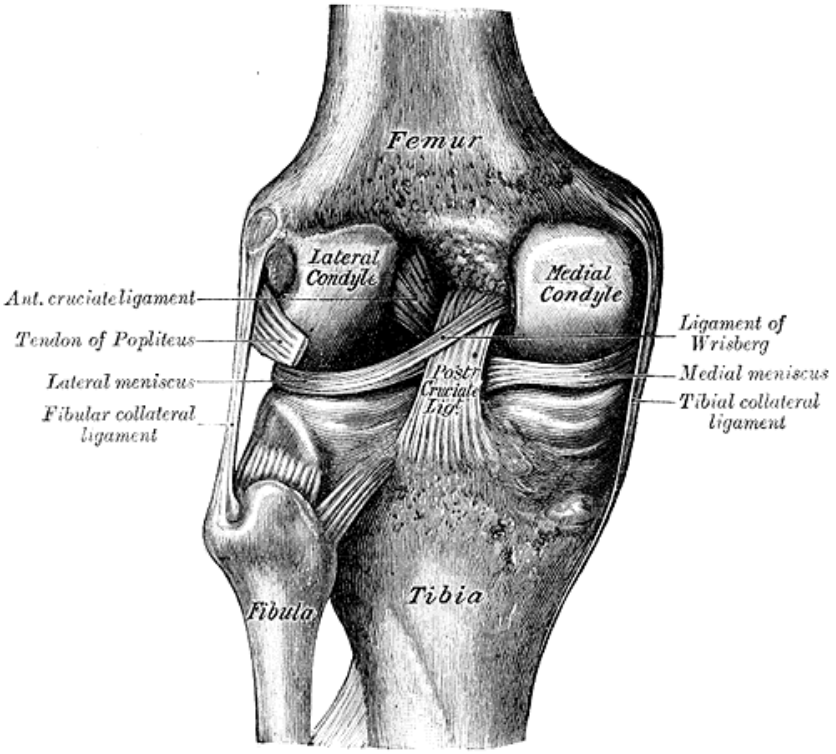

Figure 1.8: Left knee-joint from behind, showing interior ligaments (Gray, 1918).

The **Cruciate Ligaments** (*ligamenta cruciata genu; crucial ligaments*). The cruciate ligaments are of considerable strength, situated in the middle of the joint, nearer to its posterior than to its anterior surface. They are called *cruciate* because they cross each other somewhat like the lines of the letter X, and have received the names **anterior** and **posterior,** from the position of

their attachments to the tibia. The **Anterior Cruciate Ligament** (ACL, *ligamentum cruciatum anterius; external crucial ligament*) (Figure 1.7) is attached to the depression in front of the intercondyloid eminence of the tibia, being blended with the anterior extremity of the lateral meniscus, it passes upward, backward, and lateralward, and is fixed into the medial and back part of the lateral condyle of the femur. The **Posterior Cruciate Ligament** (PCL, *ligamentum cruciatum posterius; internal crucial ligament*) (Figure 1.8) is stronger, but shorter and less oblique in its direction, than the anterior. It is attached to the posterior intercondyloid fossa of the tibia, and to the posterior extremity of the lateral meniscus, and passes upward, forward, and medialward, to be fixed into the lateral and front part of the medial condyle of the femur.

The **Menisci** (*semilunar fibrocartilages*) (Figure 1.9). The menisci are two crescentic lamellæ, which serve to deepen the surfaces of the head of the tibia for articulation with the condyles of the femur and to distributing the compressive loads from the femur to the tibia. The peripheral border of each meniscus is thick, convex, and attached to the inside of the capsule of the joint, the opposite border is thin, concave, and free. The upper surfaces of the menisci are concave, and in contact with the condyles of the femur, their lower surfaces are flat, and rest upon the head of the tibia, both surfaces are smooth, and invested by synovial membrane. Each meniscus covers approximately the peripheral two-thirds of the corresponding articular surface of the tibia. The **medial meniscus** (*meniscus medialis; internal semilunar fibrocartilage*) is nearly semicircular in form, a little elongated from before backward, and broader behind than in front. Its anterior end, thin and pointed, is attached to the anterior intercondyloid fossa of the tibia, in front of the ACL. Its posterior end is fixed to the posterior intercondyloid fossa of the tibia, between the attachments of the lateral meniscus and the PCL. The **lateral meniscus** (*meniscus lateralis; external semilunar fibrocartilage*) is nearly circular and covers a larger portion of the articular surface than the medial one. It is grooved laterally for the tendon of the Popliteus, which separates it from the fibular collateral ligament. Its anterior end is attached in front of the intercondyloid eminence of the tibia, lateral to, and behind, the ACL, with which it blends. The posterior end is attached behind the intercondyloid eminence of the tibia and in front of the posterior end of the medial meniscus. The anterior attachment of the lateral meniscus

is twisted on itself so that its free margin looks backward and upward, its anterior end resting on a sloping shelf of bone on the front of the lateral process of the intercondyloid eminence.

Synovial Membrane. The synovial membrane of the knee-joint is the largest and most extensive in the body. Commencing at the upper border of the patella, it forms a large cul-de-sac beneath the Quadriceps femoris on the lower part of the front of the femur, and frequently communicates with a bursa interposed between the tendon and the front of the femur.

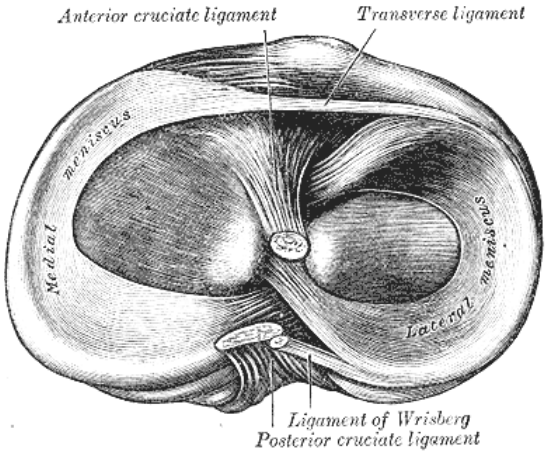

Figure 1.9: Head of right tibia seen from above, showing menisci and attachments of ligaments (Gray, 1918).

iii Structure and Mechanics of Knee Ligaments

As seen, ligaments, lying internal or external to the joint capsule, bind bone to bone and supply passive support and guidance to joints. They function to supplement active stabilizers (i.e. muscles) and bony geometry (Akeson et al., 1984). Well suited for their functional roles, ligaments offer early and increasing resistance to tensile loading over a narrow range of joint motion. This allows joints to move easily within normal limits while causing increased resistance to movement outside this normal range.

Ligaments and tendons are collagenous tissues with their primary building unit being the tropocollagen molecule (Viidik, 1973). Tropocollagen molecules are organized into long crossstriated fibrils that are arranged into bundles to form fibres. Fibres are further grouped into bundles

called fascicles which group together to form the ligament (Figure 1.10). Collagen fibre bundles are arranged in the direction of functional need and act in conjunction with elastic and reticular fibres along with ground substance, which is a composition of glycosaminoglycans and tissue fluid, to give ligaments their mechanical characteristics. In unstressed ligaments, collagen fibres take on a sinusoidal pattern. This pattern is referred to as a "crimp" pattern and is believed to be created by the cross-linking or binding of collagen fibres with elastic and reticular fibres.

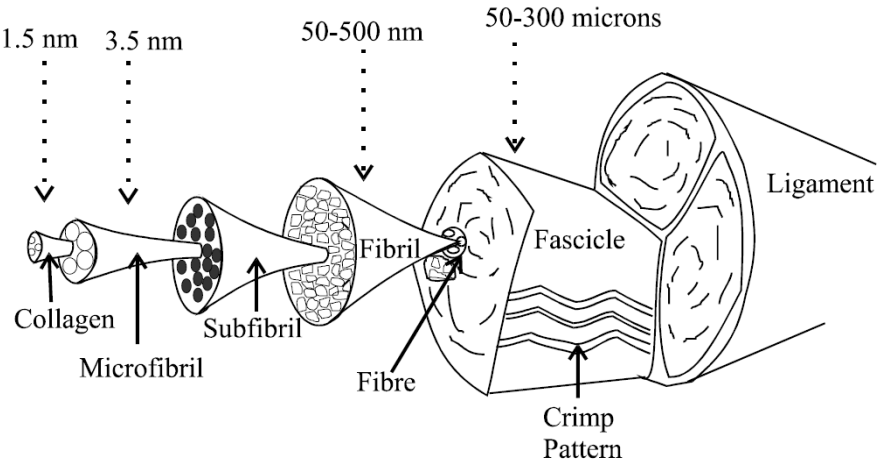

Figure 1.10: Schematic diagram of the hierarchic structure of ligament. The whole ligament is composed of fibre bundles even more small up to reach the basic structural element, which is the tropocollagen molecule.

From a mechanical point of view, ligaments are composite, anisotropic structures exhibiting non-linear time and history-dependent viscoelastic properties. The structural properties of isolated tendons, ligaments, and bone-ligament-bone preparations are normally determined via tensile tests. In such tests, a ligament, tendon, or bone-ligament-bone complex is subjected to a tensile load applied at constant rate. A typical force-elongation curve obtained from a tensile test of bone-ligament-bone preparation is shown in Figure 1.11. The force-elongation curve is initially upwardly concave, but the slope becomes nearly linear in the pre-failure phase of tensile loading. The force-elongation curve represents structural properties of

the ligament. That is, the shape of the curve depends on the geometry of the specimen tested (e.g. tissue length and cross-sectional area).

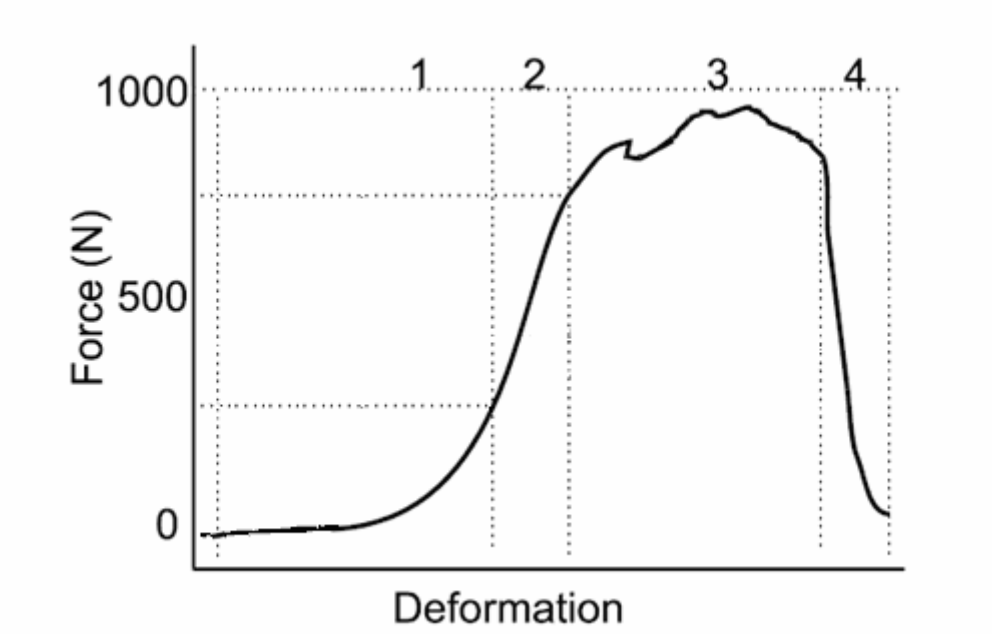

Figure 1.11: Example of a force-elongation curve obtained from bone-ligament-bone specimen. Four regions are commonly used to describe a force-elongation or stress-strain curve. Region 1 is termed the "toe region" and elicits a non-linear increase in load as the tissue elongates. Region 2 represents the linear region of the curve. In Region 3, isolated collagen fibres are disrupted and begin to fail. In Region 4, the ligament completely ruptures.

The material properties of the ligament are expressed in terms of a stress-strain relationship. **Stress** is commonly defined as the force divided by the original specimen cross-sectional area. Whereas, **strain** is defined as the change in length of the specimen relative to its initial length, divided by its initial length. Hence, a tissue's material properties may be obtained from force-elongation data by dividing the recorded force by the original cross-sectional area to give stress, and by dividing the difference between the specimen length and its original length by its original length to give strain. The advantage of constructing a stress-strain diagram is that to a first approximation the stress-strain behaviour is independent of the tissue

dimensions. Stress-strain or force-elongation curves are typically described in terms of four regions. These four regions are illustrated in Figure 1.11. Region 1 is referred to as the "toe region". The non-linear response observed in this region is due to the straightening of the "crimp" pattern resulting in successive recruitment of ligament fibres as they reach their straightened condition (Abrahams, 1967; Diamant et al., 1972). As the strain increases, the "crimp" pattern is lost and further deformation stretches the collagen fibres themselves (Region 2). As the strain is further increased, microstructural damage occurs (Region 3). Further stretching causes progressive fibre disruption and ultimately complete ligament rupture or bony avulsion at an insertion site (Region 4). A hypothetical curve relating the "crimp" pattern and collagen fibre stretch to various portions of a stress-strain curve is illustrated in Figure 1.12

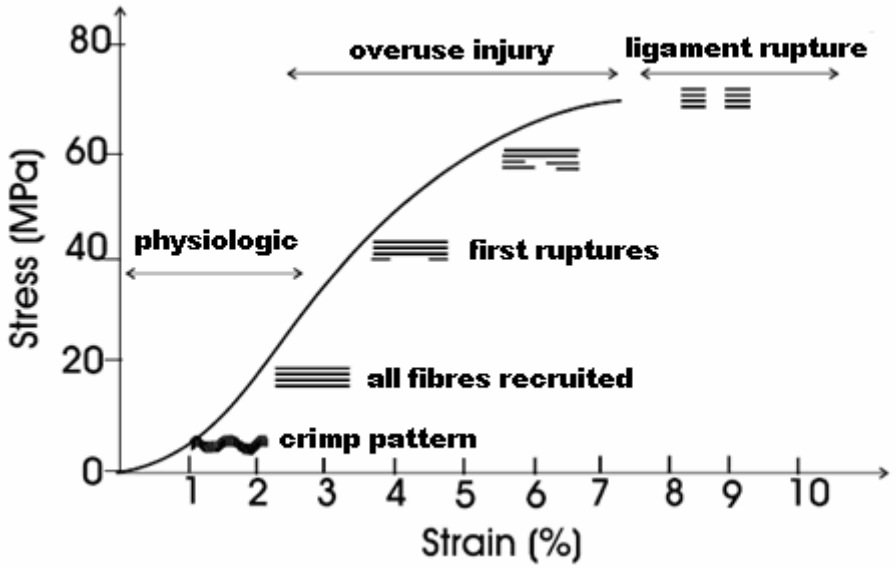

Figure 1.12: Example of stress-strain curve to describe the relationship between changes in the collagen "crimp" pattern, or stretch, and ligament mechanical properties. An increasing of the strain in the ligament at the "toe region" of the curve produces a straightening of the "crimp" pattern. During the linear portion of the curve, the collagen fibres are stretched more and more with the increasing of the strain. As the ligament is further strained isolated ligament fibres begin to rupture and if deformation continues, then complete ligament fail occurs. Modified from (Butler et al., 1978).

Clinically, it is important to know the normal operating conditions of ligaments acting within the body. Such information is needed to relate isolated ligament-bone test data to that of ligaments acting *in-vivo*. A hypothetical force-elongation curve for the human ACL, as postulated by Noyes et al. (1984), is shown in Figure 1.13. Levels of daily activity are shown along the right vertical axis and hypothetical loading levels for the ACL on the left vertical axis. This curve suggests that during daily activities (such as walking or light jogging) the ACL operates along the "toe region" of the force-elongation curve. It is believed that ligaments are not generally loaded above one-fourth of their ultimate tensile load during these daily activities. The early part of Region 2 is considered the upper operating range of the ACL during strenuous activities as might be experienced during fast cutting or pivoting while running. Loading of the ACL beyond Region 2 results in ligament damage and may be incurred during events like clipping in football, a ski accident, or an incorrect landing during a gymnastics floor exercise.

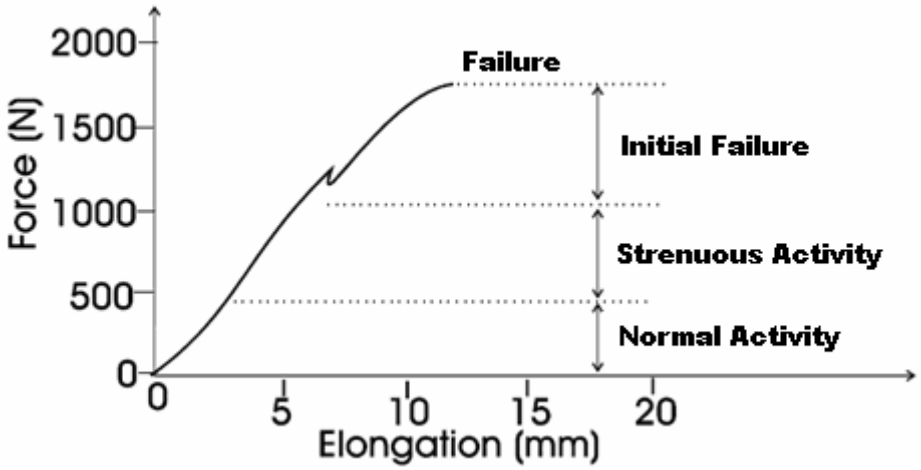

Figure 1.13: A hypothetical force-elongation curve for a human ACL-bone complex is illustrated along with daily activities that correspond to specific loading levels. During routine daily activities such as walking and standing, ligaments are loaded to less than one fourth their ultimate tensile load. During strenuous activities such as fast cutting during intense running, loading levels may enter into region 3 where isolated fibre damage takes place. Modified from (Noyes et al., 1984).

iv Muscles

Skeletal muscles actuate the bones of the body to produce movements at the joints and provide stability by resisting movement across joints. Muscles are active structures which contract themselves, reducing length and providing force, when they are activated by the central nervous system. When standing erect in the attitude of "attention," the weight of the body falls in front of a line carried across the centres of the knee-joints, and therefore tends to produce overextension of the articulations. This, however, is passively prevented by the tension of the anterior cruciate, oblique popliteal, and collateral ligaments. Nevertheless, the equilibrium of a subject is not provided only by passive structures. In fact, the nervous system controls the balance of the subject recruiting muscles with the capability to produce an opposite movement in order to recover the position of equilibrium.

At knee joint, muscles which produce flexion are called 'Flexors', whereas muscles which produce extension are called 'Extensor'. The Extensor muscles are also defined 'Antagonist' of the Flexor ones, and viceversa. Thus, the nervous system can produce motion of the knee joint along different axes, such as flexion-extension and intra-extra axial rotation, controlling the recruitment and the activation of several muscles at the same time. Moreover, the nervous system can also increase the stability of the knee joint, restraining the joint movements due to external loads, by means of the contraction of both Agonist and Antagonist muscles at the same time.

Muscle is composed of many subunits and complex structural arrangements (Figure 1.14). Whole muscle is surrounded by a strong sheath called the epimysium. The gross muscle is divided into a variable number of subunits called fasciculi. Each fasciculus is surrounded by a connective tissue sheath called the perimysium. Fascicles may be further divided into bundles of fibres (or muscle cells) which are surrounded by a sheath called the endomysium (Fung, 1981; Ishikawa, 1983).

The orientation of fibres relative to the orientation of the whole muscle varies among different muscles. Regarding the fibre arrangement, muscle may be classified as fusiform, unipennate, bipennate, triangular, and strap. Fibres attach at both ends to tendon or other connective tissue.

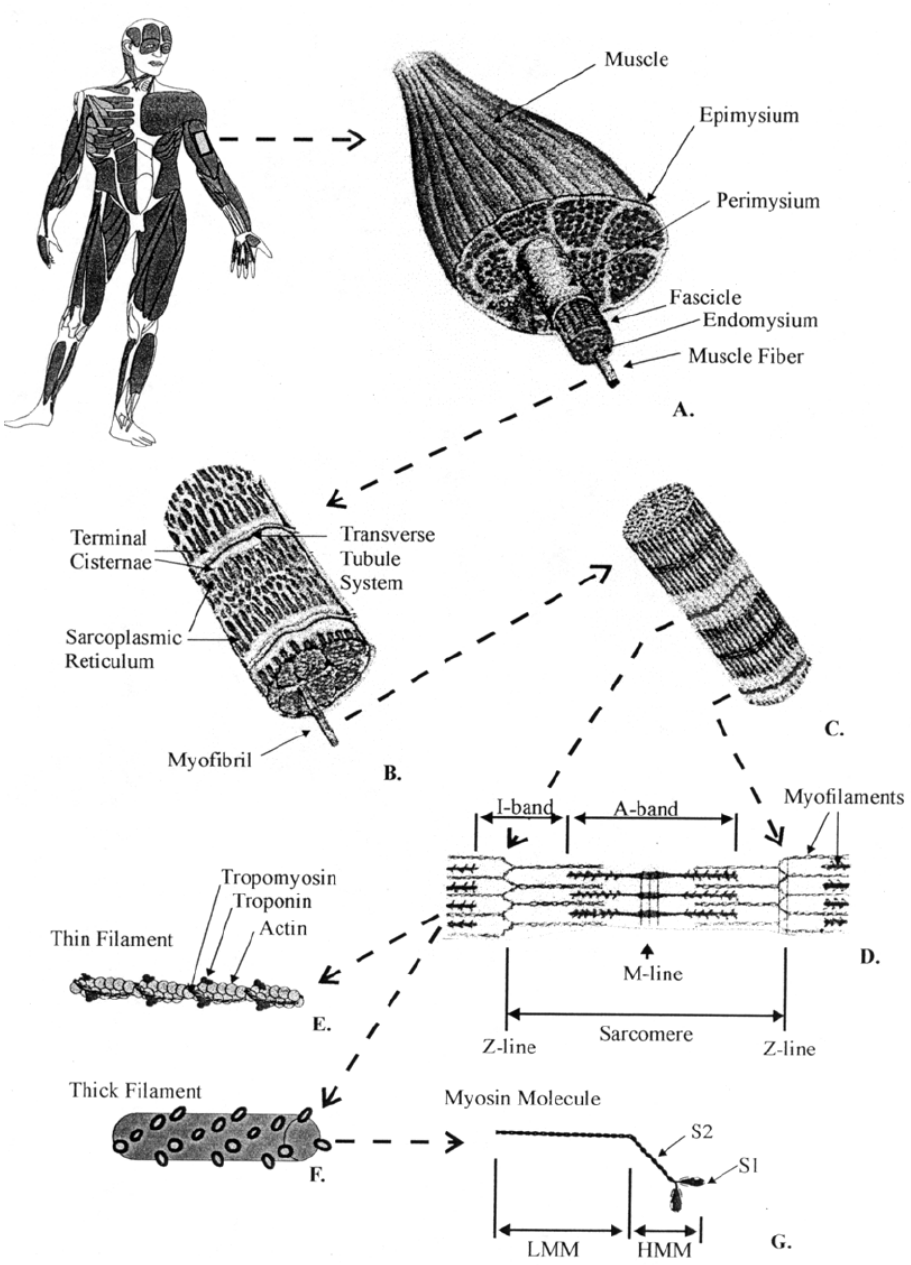

Figure 1.14: Schematic representation of the organizational structure of muscle. The gross muscle is composed of bundles of fascicles that consist of groups of fibres. Fibres can be further divided into myofibrils that contain the myofilaments making up the sarcomeres.

Muscle fibres are multinucleated cells with the nuclei generally located along the cell periphery. The population density of nuclei is estimated to be 50-100 per millimetre of fibre length (Ishikawa, 1983). Muscles have a rich supply of blood vessels. Capillary networks are arranged around each fibre with the capillary density varying around different fibres types (Ishikawa, 1983). A motor unit consists of a single motoneuron and all the fibres it innervates. The number of fibres per motor unit is variable, ranging from just a few in ocular muscles, requiring fine control, to thousands in large limb muscles (Ishikawa, 1983). In intact whole muscle, motor units intermingle throughout the entire muscle cross-sectional area.

Extension of the leg on the thigh is performed by the **Quadriceps femoris** (*Quadriceps extensor*) (Figure 1.15, a). It is subdivided into separate portions, which have received distinctive names. One occupying the middle of the thigh, and connected above with the ilium, is called from its straight course the **Rectus femoris**. The **Rectus femoris** (Figure 1.15, a) is situated in the middle of the front of the thigh, it is fusiform in shape. It arises by two tendons: one, the anterior or straight, from the anterior inferior iliac spine, the other, the posterior or reflected, from a groove above the brim of the acetabulum. The muscle ends in a broad and thick aponeurosis which occupies the lower two-thirds of its posterior surface, and, gradually becoming narrowed into a flattened tendon, is *inserted* into the base of the patella. *Flexion* of the leg is performed by the Biceps femoris, Semitendinosus, and Semimembranosus, assisted by the Gracilis, Sartorius, Gastrocnemius, Popliteus, and Plantaris. The **Biceps femoris** (*Biceps*) (Figure 1.15, b) is situated on the posterior and lateral aspect of the thigh. It has two heads of origin: one, the long head**,** arises from the lower and inner impression on the back part of the tuberosity of the ischium, the other, the short head**,** *arises* from the lateral lip of the linea aspera, extending up almost as high as the insertion of the Glutæus maximus. The **Gastrocnemius** (Figure 1.15, d) is the most superficial muscle, and forms the greater part of the calf. It *arises* by two heads, which are connected to the condyles of the femur by strong, flat tendons. Both heads, also, arise from the subjacent part of the capsule of the knee.

External rotation is effected by the Biceps femoris, and *internal rotation* by the Popliteus, Semitendinosus, and, to a slight extent, the Semimembranosus, the Sartorius, and the Gracilis. The Popliteus comes into

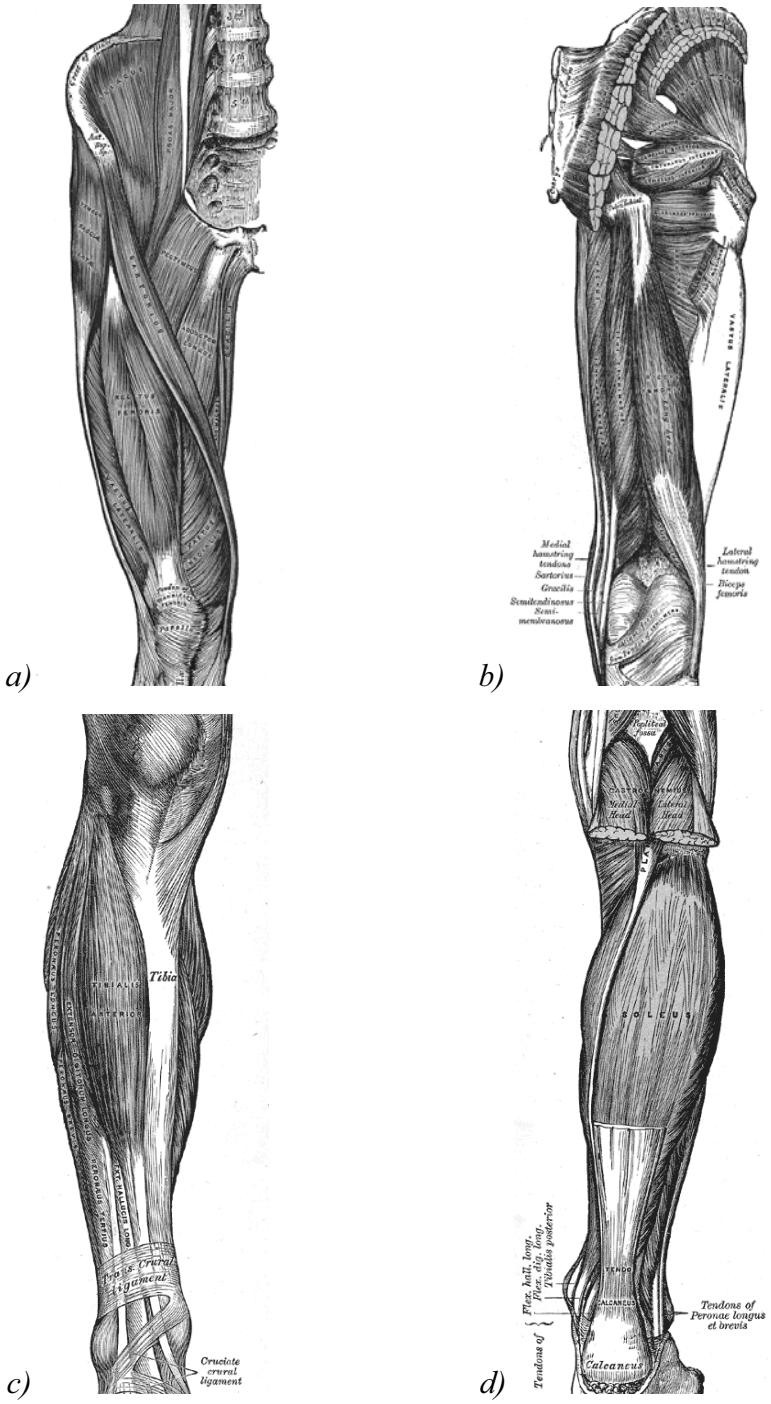

Figure 1.15: Anterior (a, c) and posterior (b, d) views of muscles of a right leg. The thigh is shown in (a, b) and the shank in (c, d) (Gray, 1918).

action especially at the commencement of the movement of flexion of the knee, by its contraction the leg is rotated inward, or, if the tibia be fixed, the thigh is rotated outward, and the knee-joint is unlocked. The **Glutæus medius** (Figure 1.15, b) is a broad, thick, radiating muscle, situated on the outer surface of the pelvis. It arises from the outer surface of the ilium between the iliac crest and posterior gluteal line above, and the anterior gluteal line below, it also arises from the gluteal aponeurosis covering its outer surface. It performs the *abduction* and the *rotation inward/outward* of the thigh together with other muscles. The **Tibialis anterior** (*Tibialis anticus*) (Figure 1.15, c) is situated on the lateral side of the tibia, it is thick and fleshy above, tendinous below. It arises from the lateral condyle and upper half or two-thirds of the lateral surface of the body of the tibia, from the adjoining part of the interosseous membrane. The fibres run vertically downward, and end in a tendon, which is apparent on the anterior surface of the muscle at the lower third of the leg. After passing through the most medial compartments of the transverse and cruciate crural ligaments, it is inserted into the medial and under surface of the first cuneiform bone, and the base of the first metatarsal bone. It performs the *dorsiflexion* of the foot together with other muscles.

1.3 Biomechanics: functional anatomy

Human knee joint provides two apparently contrasting functions: it must be mobile to achieve a large and smooth range of motion, and must be stable to guarantee strong support in activity. The knee joint must allow both flexion and axial rotation to occur while still maintaining stability. The tibio-femoral joint defines the kinematics of flexion, extension and axial rotation while the patello-femoral joint increases the efficiency of the extensor mechanism by enlarging the quadriceps lever arm.

i Mobility

In 1836, Weber (Weber and Weber) described knee motion as a combination of rolling, sliding, and axial rotation of the tibio-femoral joint (Muller, 1938). Nevertheless, as yet there have been few three-dimensional (3D) models described in the literature which incorporate this axial rotation with the rolling and sliding of the joint (Wismans et al., 1980; Feikes, 1999; Wilson et al., 2000; Di Gregorio et al., 2007). At first, the kinematic principles of the knee have been reduced to a two-dimensional midsagittal plane model known as the "cruciate" linkage (Muller, 1938; Kapandji, 1970; Goodfellow and O'Connor, 1978; O'Connor et al., 1989; O'Connor et al., 1990). The four links of this linkage represent the ACL, the PCL, a tibial link between the tibial cruciate insertion sites and a femoral link between the femoral cruciate origin sites (Figure 1.16). If the femoral link is articulated about the fixed tibial link, a graphic representation of knee joint motion can be obtained. Kapandji (Kapandji, 1970) has concluded that "the shape of the femoral condyles are geometrically determined by the lengths of each of the cruciate ligaments, as well as by the ratio of their individual lengths and the arrangements of their insertions". As the knee is flexed from full extension, the point of intersection of the ACL and PCL (i.e. the flexion axis) links moves posteriorly.

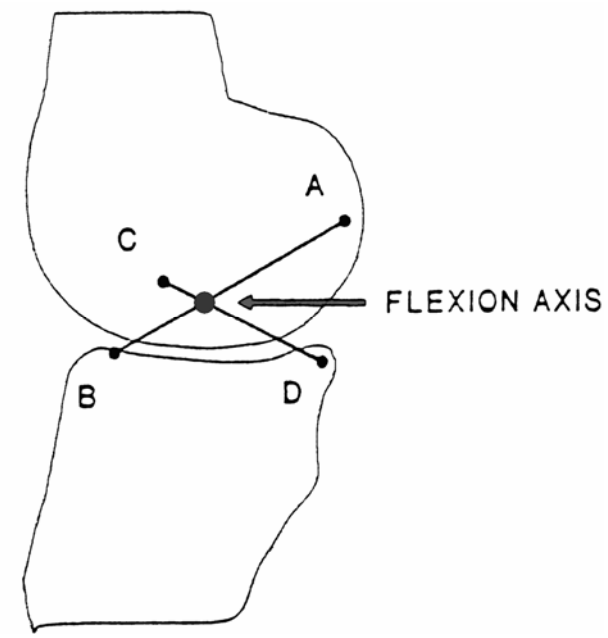

Figure 1.16: The cruciate linkage comprises four links: AB is the neutral fibre of the ACL, CD is the neutral fibre of the PCL, BD is the link between the tibial attachment sites, and CA designates the femoral insertion points. The flexion axis is the point of intersection at each instant between the links AB and CD. (Kapandji, 1970)

A two-dimensional model has been constructed for a situation in which the tibia rotated on a stationary femur and the femur rotated on a stationary tibia (Figure 1.17) (Muller, 1938; O'Connor et al., 1990; O'Connor et al., 1989). These curves developed by plotting the centres of rotation in each situation are called centroids. The tibial centroide approximates a straight line whereas the femoral centroide is elliptical. As the two bones move on each other, they undergo both rolling and sliding. It is obvious that the femur must slide forward on the tibia plateau during flexion (roll-back mechanism): a pure rolling motion would result in the femur falling off the back of the tibia as the knee flexed over 100°. During the early phase of flexion, rolling is the predominant motion (Figure 1.18, A; and Figure 1.19), while flexion continues, sliding tends to predominate (Figure 1.8, B; and Figure 1.19).

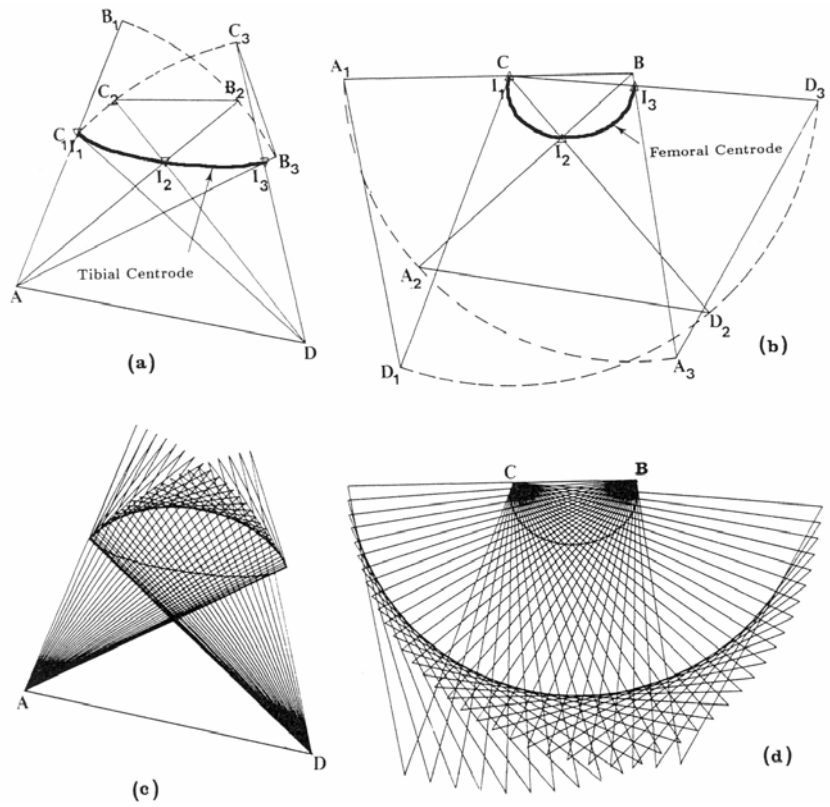

Figure 1.17: The cruciate linkage drawn by the computer with the tibial link fixed, (a) and (c), and with the femoral link fixed, (b) and (d). the relative positions of the links are the same in the pair of diagrams (a) and (b) for each of the corresponding three configurations and in (c) and (d) for each of the corresponding 30 configurations. In (a) and (c), the femoral attachments of the ligaments move on circular arcs about their tibial attachments, and in (b) and (d) the tibial attachments move on circular arcs about the femoral attachments. The curve marked "Tibial centroide" and "Femoral centroide" are the tracks of the flexion axis of the joint on the tibia and femur, respectively, and are drawn through the successive intersections of the cruciates. (O'Connor et al., 1990)

Axial rotation of the tibia relative to the femur is the result of the application of the ground reaction force, the rotation applied by the musculature, and the **screw-home** mechanism. The ligaments and capsular structures act as restraints to this rotation. The musculature of the lower limb serves both as a passive restraint against rotation and to provide the force to cause rotation.

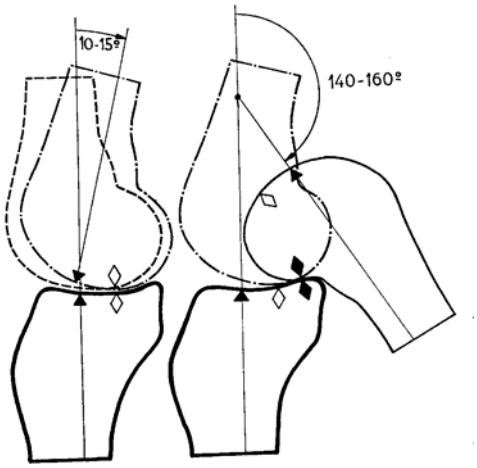

Figure 1.18: From 0 to 10-15°, the motion is predominantly rolling (*A*), from 10-15° to 140-160° sliding (*B*). (Kapandji, 1970)

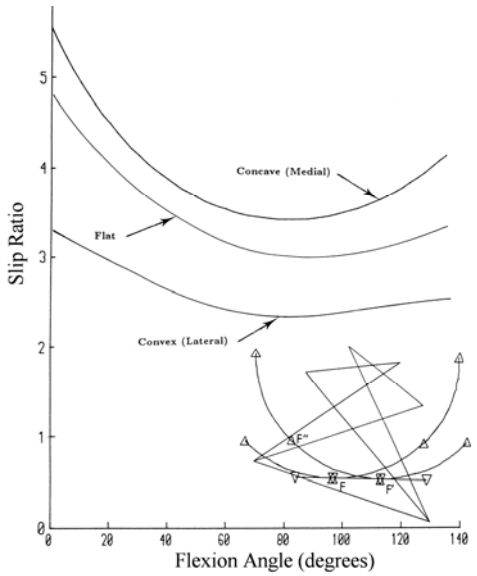

Figure 1.19: The diagram shows the cruciate linkage in two neighboring positions with the corresponding femoral surface touching a flat tibial plateau at F and F'. F'' is the point on the femoral surface which makes contact with F. The slip ration is the distance F'F'' measured along the femur, divided by the distance FF' measured along the tibia. The graphs show the variation with flexion angle for convex, flat and concave tibial plateaus. (O'Connor et al., 1990)

The screw-home mechanism (external rotation of the tibia on the femur) (Figure 1.20) occurs automatically as the knee is extended. In the sagittal plane, the radius of curvature of the medial plateau is different from the lateral plateau. The medial tibial plateau is concave superiorly and the lateral is convex. Therefore, the articulating surfaces of the tibio-femoral joint are not fully conforming. When viewed distally, the lateral femoral condyle is longer than the medial. The unequal lengths and radii of curvature of the two femoral condyles, the shape of the tibial plateaus, and the position of the four primary ligaments force the tibia to rotate externally with extension (Kapandji, 1970).

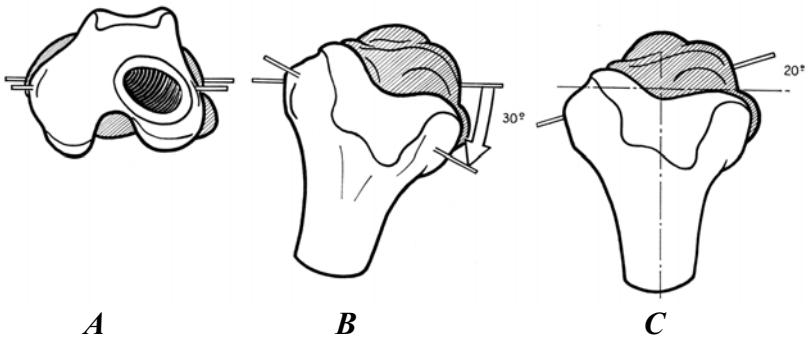

Figure 1.20: The screw-home mechanism: coupled internal rotation of 20° of the tibia on the femur during knee flexion (Kapandji, 1970).

Figure 1.21: Functioning of the menisci: Sliding movements between the femur and the concave upper surface of the menisci allow flexion and extension, sliding movements between the flattened undersurface of the meniscus and the tibial plateau allow rotation and anteroposterior translation of the tibia (Kapandji, 1970)

Lateral radiographs of the knee demonstrate that the articular surfaces of the tibia in the sagittal plane are virtually flat, articulating with the convex femoral condyles only at a point. This appearance is misleading. The dissimilar shapes of the articular surfaces of the two bones are made congruent by the interposed *meniscus*. The important function of the meniscus in distributing compressive load from the femur to the tibia was reported from direct measurements in human and porcine joints in the laboratory (Walker and Erkman, 1975; Shrive et al., 1978). The menisci are integral parts of the tibial articular surface, making it conform to the shape of the femoral condyle as the acetabulum conforms to the head of the femur. Sliding movements between the femur and the concave upper surface of the meniscus allow flexion and extension, sliding movements between the flattened undersurface of the meniscus and the tibial plateau allow rotation and anteroposterior translation of the tibia (Figure 1.21). In fact, sliding movements usually occur simultaneously at both the femoromeniscal and tibiomeniscal joints (Goodfellow and O'Connor, 1994).

ii Stability

Joint Stability is provided by both intrinsic and extrinsic anatomical mechanisms. The intrinsic stability of the knee joint is provided by the four primary ligaments, the capsule, the shape of the bony structures, and the menisci. The ligaments act as tensile check reins which permit motion to occur within limits. The limits of motion are dependent on orientation of these ligaments. The ACL is the primary check against anterior displacement of the tibia relative to the femur, with the PCL being the primary stabilizer preventing posterior displacement. In knee flexion, the superficial MCL is the first defence against external rotation with the ACL acting as a secondary restraint. In knee extension, the ACL and superficial MCL act together as primary stabilizers against external rotation. With the knee flexed, internal rotation is prevented first by the cruciate ligaments and secondly by the LCL. In extension, the ACL is the primary stabilizer and the LCL the secondary (Marshall and Rubin, 1977). The primary and secondary knee stabilizers that resist valgus stresses (opening of the medial side of the knee) are the superficial MCL and the ACL respectively. Varus knee stresses (opening of the lateral side of the knee) are resisted by a combination of knee

structures depending on the angle of knee flexion. The LCL is the primary stabilizer at the mid-range of knee flexion and the PCL at 90 degrees of flexion. At full extension there is no single structure that acts as the primary stabilizer. The intercondylar tubercles are bony structures on the tibial plateau which interlock with the intercondylar notch of the distal femur. Their interference fit provides stability to medial and lateral shear stresses and prevents hyperextension without inhibiting flexion or axial rotation. The tibial plateau in conjunction with the menisci provide channels for the femoral condyles that add stability in flexion and axial rotation without over constraining the joint.

The muscles of the thigh and shank provide extrinsic stability to the knee. The muscles provide both the force to articulate the knee, and the check-rein stability to resist abnormal stresses. The act of extension is achieved trough the quadriceps mechanism transmitted through the patella. The patella acts as a pulley mechanism to increase the efficiency of the extension effort and to direct the action of these quadriceps forces (Pope and Fleming B.C., 1991).

All these mechanisms, relative to the mobility and the stability of the knee joint, have been extensively analysed by means of modelling and experimental tests (Markolf et al., 1976; Goodfellow and O'Connor, 1978; Wismans et al., 1980; O'Connor et al., 1990; Blankevoort et al., 1991; Wilson et al., 1998; Feikes, 1999; Wilson et al., 2000; Komistek et al., 2002; Komistek et al., 2003; Caruntu and Hefzy, 2004; DeFrate et al., 2004; Fantozzi et al., 2004; Komistek et al., 2004; Shelburne et al., 2004; Banks et al., 2005; Dennis et al., 2005; Fregly et al., 2005; Komistek et al., 2005; Mesfar and Shirazi-Adl, 2005; Moglo and Shirazi-Adl, 2005; Fantozzi et al., 2006; Fernandez and Pandy, 2006; Hanson et al., 2006; Li et al., 2006; Di Gregorio et al., 2007; Bertozzi et al., 2007).

1.4 References

Abrahams, M., (1967). Mechanical behaviour of tendon in vitro. A preliminary report. Medical and Biological Engineering and Computing 5**,** 433-443.

Akeson, W. H., Woo, S. L.-Y., Amiel, D., Frank, C. B., (1984). The chemical basis of tissue repair. In: Hunter L.Y., Funk, F. J. (Eds.), Rehabilitation of the Injured Knee. St. Louis: C.V. Mosby Company, pp. 93-104.

Banks, S. A., Fregly, B. J., Boniforti, F., Reinschmidt, C., Romagnoli, S., (2005). Comparing in vivo kinematics of unicondylar and bi-unicondylar knee replacements. Knee Surgery Sports Traumatology Arthroscopy 13**,** 551-556.

Bertozzi, L., Stagni, R., Fantozzi, S., Cappello, A., (2007). Knee model sensitivity to cruciate ligaments parameters: A stability simulation study for a living subject. Journal of Biomechanics 40(S1)**,** 38-44.

Blankevoort, L., Kuiper, J. H., Huiskes, R., Grootenboer, H. J., (1991). Articular contact in a three-dimensional model of the knee. Journal of Biomechanics 24**,** 1019-1031.

Butler, D. L., Grood, E. S., Noyes, F. R., Zernicke, R. F., (1978). Biomechanics of ligaments and tendons. Exercise and Sport Sciences Reviews 6**,** 125-181.

Caruntu, D. I., Hefzy, M. S., (2004). 3-D anatomically based dynamic modeling of the human knee to include tibio-femoral and patello-femoral joints. Journal of Biomedical Engineering 126**,** 44-53.

DeFrate, L. E., Sun, H., Gill, T. J., Rubash, H. E., Li, G., (2004). In vivo tibiofemoral contact analysis using 3D MRI-based knee models. Journal of Biomechanics 37**,** 1499-1504.

Dennis, D. A., Mahfouz, M. R., Komistek, R. D., Hoff, W., (2005). In vivo determination of normal and anterior cruciate ligament-deficient knee kinematics. Journal of Biomechanics 38**,** 241-253.

Di Gregorio, R., Parenti-Castelli, V., O'Connor, J. J., Leardini, A., (2007). Mathematical models of passive motion at the human ankle joint by

equivalent spatial parallel mechanisms. Medical and Biological Engineering and Computing 45**,** 305-313.

Diamant, J., Keller, A., Baer, E., Litt, M., Arridge, R. G., (1972). Collagen; ultrastructure and its relation to mechanical properties as a function of ageing. Proceedings of the Royal Society of London Series b - Biological Sciences 180**,** 293-315.

Fantozzi, S., Catani, F., Ensini, A., Leardini, A., Giannini, S., (2006). Femoral rollback of cruciate-retaining and posterior-stabilized total knee replacements: in vivo fluoroscopic analysis during activities of daily living. Journal of Orthopaedic Research 24**,** 2222-2229.

Fantozzi, S., Leardini, A., Banks, S. A., Marcacci, M., Giannini, S., Catani, F., (2004). Dynamic in-vivo tibio-femoral and bearing motions in mobile bearing knee arthroplasty. Knee Surgery Sports Traumatology Arthroscopy 12**,** 144-151.

Feikes, J. D., (1999). The mobility and the stability of the human knee joint.DPhil, University of Oxford.

Fernandez, J. W., Pandy, M. G., (2006). Integrating modelling and experiments to assess dynamic musculoskeletal function in humans. Experimental Physiology 91**,** 371-382.

Fregly, B. J., Rahman, H. A., Banks, S. A., (2005). Theoretical accuracy of model-based shape matching for measuring natural knee kinematics with single-plane fluoroscopy. Journal of Biomedical Engineering 127**,** 692-699.

Fung, Y. C., (1981). Biomechanics: mechanical properties of living tissues. Springer-Verlag, New York, New York.

Goodfellow, J., O'Connor, J., (1978). The mechanics of the knee and prosthesis design. Journal of Bone and Joint Surgery - British Volume 60-B**,** 358-369.

Goodfellow, J., O'Connor, J., (1994). The role of congruent meniscal bearings in knee arthroplasty. In: Scott, W. N. (Ed.), The knee, Part XIV. Mosby, pp. 1143-1156.

Gray, H., (1918). Anatomy of the Human Body. Crown, Philadelphia.

Gray, H., (1977). Articulation of the lower extremity. In: Pick, T. P., Howden, R. (Eds.), Anatomy, descriptive and surgical. Crown, New York, pp. 274-283.

Grood, E. S., Suntay, W. J., (1983). A joint coordinate system for the clinical description of three- dimensional motions: application to the knee. Journal of Biomedical Engineering 105**,** 136-144.

Hanson, G. R., Suggs, J. F., Freiberg, A. A., Durbhakula, S., Li, G., (2006). Investigation of in vivo 6DOF total knee arthoplasty kinematics using a dual orthogonal fluoroscopic system. Journal of Orthopaedic Research 24**,** 974-981.

Ishikawa, H., (1983). Fine structure of skeletal muscle. Cell and Muscle Motility 4**,** 1-84.

Kapandji, I., (1970). The knee. The physiology of the joints. Curchill Livingstone, New York, pp. 72-135.

Komistek, R. D., Allain, J., Anderson, D. T., Dennis, D. A., Goutallier, D., (2002). In vivo kinematics for subjects with and without an anterior cruciate ligament. Clinical Orthopaedics and Related Research 315-325.

Komistek, R. D., Dennis, D. A., Mahfouz, M., (2003). In vivo fluoroscopic analysis of the normal human knee. Clinical Orthopaedics and Related Research 69-81.

Komistek, R. D., Dennis, D. A., Mahfouz, M. R., Walker, S., Outten, J., (2004). In vivo polyethylene bearing mobility is maintained in posterior stabilized total knee arthroplasty. Clinical Orthopaedics and Related Research 207-213.

Komistek, R. D., Kane, T. R., Mahfouz, M., Ochoa, J. A., Dennis, D. A., (2005). Knee mechanics: a review of past and present techniques to determine in vivo loads. Journal of Biomechanics 38**,** 215-228.

Li, G., Suggs, J., Hanson, G., Durbhakula, S., Johnson, T., Freiberg, A., (2006). Three-dimensional tibiofemoral articular contact kinematics of a cruciate-retaining total knee arthroplasty. Journal of Bone and Joint Surgery - American Volume 88**,** 395-402.

Markolf, K. L., Mensch, J. S., Amstutz, H. C., (1976). Stiffness and laxity of the knee--the contributions of the supporting structures. A quantitative in

vitro study. Journal of Bone and Joint Surgery - American Volume 58**,** 583-594.

Marshall, J. L., Rubin, R. M., (1977). Knee ligament injuries--a diagnostic and therapeutic approach. Orthopedic Clinics of North America 8**,** 641-668.

Mesfar, W., Shirazi-Adl, A., (2005). Biomechanics of the knee joint in flexion under various quadriceps forces. Knee 12**,** 424-434.

Moglo, K. E., Shirazi-Adl, A., (2005). Cruciate coupling and screw-home mechanism in passive knee joint during extension--flexion. Journal of Biomechanics 38**,** 1075-1083.

Muller, W., (1938). Kinematics. The knee: form, function, and ligament reconstruction. Springer - Verlag, New York, pp. 8-28.

Noyes, F. R., Butler, D. L., Grood, E. S., Zernicke, R. F., Hefzy, M. S., (1984). Biomechanical analysis of human ligament grafts used in knee-ligament repairs and reconstructions. Journal of Bone and Joint Surgery - American Volume 66**,** 344-352.

O'Connor, J., Shercliff, T. L., Fitzpatrick, D. P., Bradley, J., Daniel, D. M., Biden, E., Goodfellow, J., (1990). Geometry of the knee. In: Daniel, D. M., Akeson, W. H., O'Connor, J. (Eds.), Knee Ligaments. Structure, Function, Injury, and Repair. Raven Press, New York, pp. 163-199.

O'Connor, J. J., Shercliff, T. L., Biden, E., Goodfellow, J. W., (1989). The geometry of the knee in the sagittal plane. Proceedings of the Institution of Mechanical Engineers Part H - Journal of Engineering in Medicine 203**,** 223-233.

Pope, M. H., Fleming B.C., (1991). Knee Biomechanics and Materials. In: Laskin R.S. (Ed.), Total Knee Replacement. Springer-Verlag, pp. 25-38.

Shelburne, K. B., Pandy, M. G., Anderson, F. C., Torry, M. R., (2004). Pattern of anterior cruciate ligament force in normal walking. Journal of Biomechanics 37**,** 797-805.

Shrive, N. G., O'Connor, J. J., Goodfellow, J. W., (1978). Load-bearing in the knee joint. Clinical Orthopaedics and Related Research 279-287.

Viidik, A., (1973). Functional properties of collagenous tissues. International Review of Connective Tissue Research 6**,** 127-215.

Walker, P. S., Erkman, M. J., (1975). The role of the menisci in force transmission across the knee. Clinical Orthopaedics and Related Research 184-192.

Weber, W., Weber, E., (1991). Mechanics of the Human Walking Apparatus. Springer-Verlag, Berlin and New York (translated from German by Maquet P, Furlong R - from original work in 1836).

Wilson, D. R., Feikes, J. D., O'Connor, J. J., (1998). Ligaments and articular contact guide passive knee flexion. Journal of Biomechanics 31**,** 1127-1136.

Wilson, D. R., Feikes, J. D., Zavatsky, A. B., O'Connor, J. J., (2000). The components of passive knee movement are coupled to flexion angle. Journal of Biomechanics 33**,** 465-473.

Wismans, J., Veldpaus, F., Janssen, J., Huson, A., Struben, P., (1980). A three-dimensional mathematical model of the knee-joint. Journal of Biomechanics 13**,** 677-685.

Wu, G., Cavanagh, P. R., (1995). ISB recommendations for standardization in the reporting of kinematic data. Journal of Biomechanics 28**,** 1257-1261.

Chapter 2: Review of Knee Models

- Bertozzi L., et al. 2008, Digital Humans, The State of the Art Survey. Springer.

Early observations on the biomechanics of the knee joint date back to the first decades of the 19th century (Weber and Weber), while early models were proposed at the beginning of the last century (Strasser H, 1917). More structured theories regarding the biomechanics and the function of the knee joint appeared only in the seventies (Goodfellow and O'Connor, 1978) and in the last three decades plenty of modelling and experimental works have been published about this important articulation for the human musculo-skeletal system. By reviewing the literature of this period, it is possible to recognize several tendencies of thought and different approaches adopted for the knee modelling. The three main tendencies identified in this review are: i) models based on the four-bar linkage mechanism, ii) quasi-static models, and iii) dynamic models.

The largest part of the literature on the knee modelling is comprised into two different kinds of approach, one born by a more physical point of view at the end of the seventies (Goodfellow and O'Connor, 1978) and the other by a more mathematical point of view, with a significant increase of related publication in the eighties and in the nineties (Crowninshield et al., 1976b; Wismans et al., 1980; Andriacchi et al., 1983; Essinger et al., 1989; Blankevoort et al., 1991; Blankevoort and Huiskes, 1996; Mommersteeg et al., 1997; Wilson et al., 1998; Li et al., 1999). The first approach was based on the four-bar linkage mechanism and on the hypothesis that, when no external or muscular forces are applied on knee (passive condition or unloaded state), the passive motion of the knee is guided only by principal passive structures and by the shape of the articular surfaces which are in contact each other along all the range of motion of the joint (Goodfellow and O'Connor, 1978). Whereas, the second approach consisted in writing a set of equations comprising the equilibrium equations of the system along with mathematical representation of the constraints, such as ligaments and articular surfaces interactions. In this second way of modelling the knee, if inertial and viscous components of the system were neglected the model is defined as quasi-static (Crowninshield et al., 1976b; Essinger et al., 1989;

Blankevoort et al., 1991; Blankevoort and Huiskes, 1996; Mommersteeg et al., 1997; Wismans et al., 1980), otherwise as dynamic (Moeinzadeh et al., 1983; Tumer and Engin, 1993; Komistek et al., 1998; Beillas et al., 2004; Caruntu and Hefzy, 2004; Fregly et al., 2005).

In the present chapter, the main tendencies in the modelling of the knee joint and the functions of its principal anatomical structures are presented and critically commented. All the presented approaches resulted very important, effective and widespread for the development and the evolution of new mathematical knee models, which significantly contributed to obtain evaluations even more reliable of the knee functionality in healthy, pathological, and/or prosthesized subjects.

2.1 Kinematical Models

It is long recognized that the passive motion between the tibia and the femur is mainly guided by articular surfaces and the passive structures, particularly by cruciates, collaterals, and other articular passive structures. Strasser (Strasser H, 1917) was probably the first investigator to observe that, during the flexion motion of the knee joint, the cruciate ligaments remain quite isometric, playing a role analogue to the crossed bars of a four-bar linkage mechanism. As cited above, the four-bar linkage mechanism has been used for modelling in the sagittal plane the knee joint. The basic assumption of this approach is that, in the unloaded state, the relative motion between tibia and femur is guided only by cruciate ligaments, which are isometric, and by articular surfaces, which remain in contact each other during the whole range of motion of the joint.

Starting from these assumptions, one of the first significant application obtained exploiting this simple 2D model was the design of an innovative knee prosthesis (Goodfellow and O'Connor, 1978) still of great clinical success (Goodfellow et al., 1987; Goodfellow et al., 1988; Murray et al., 1998; Svard and Price, 2001). Moreover, the four-bar linkage has been also used for the development of other applications, such as the evaluation of the misallocation of the knee prosthesis (Imran and O'Connor, 1996), the calculus of the muscular lever and of the effects produced by external forces (O'Connor et al., 1990), the evaluation of the patello-femoral mechanism (Gill and O'Connor, 1996), the estimation of muscular, ligamentous and

contact forces during activities (Collins and O'Connor, 1991; Lu et al., 1997), the evaluation of the recruitment patterns of the ligament fibres and of the anterior-posterior laxity during drawer test (Zavatsky and O'Connor, 1992b; Zavatsky and O'Connor, 1992a), and the evaluation of the distribution of muscular, ligamentous and contact forces with deformable articular surfaces (Huss et al., 1999; Huss et al., 2000; Imran et al., 2000).

Thus, this 2D kinematic model were of fundamental importance for the development of several following more complex models, because it contributed to clarify different functional aspects of the knee joint, such as the muscular leverage mechanism and its advantage in the production of the articular torque, the protection mechanism of the anatomical structures, even when these are overloaded, and the progressive recruitment mechanism of the fibres needed to better resist to the external loads.

Obviously, 2D version of the model was restricted because of its inability to evaluate potentially significant motions and forces out of the sagittal plane. Indeed, this model was not be able to take into account the tibial axial rotation and the ab-adduction which are, as well known, coupled to the flexion-extension angle. Thus, there was the necessity to improve the model in order to obtain a kinematical model capable to predict the passive movement of the knee in the 3D space.

In order to reach the aim, the theory of spatial equivalent mechanism have been used and several mathematical models based on this theory were developed in the years (Wilson and O'Connor, 1997; Wilson et al., 1998; Feikes et al., 2003; Parenti-Castelli et al., 2004). The theory of the spatial equivalent mechanism states that the mechanical behaviour of the real modelled system can be reproduced by means of passive rigid members (bony segments) connected each other by constraints of different natures (articular surfaces and ligaments).

For example, in one the first attempt to reach this goal (Wilson and O'Connor, 1997) (i.e. the spatial equivalent mechanism called by authors as EMS1 (Parenti-Castelli et al., 2004)), the three ligaments (anterior and posterior cruciates and medial collateral) were considered as rigid bars to account of their isometricity during the passive flexion, and the two articular contacts (on lateral and medial sides) were modelled as rigid frictionless contacts between spheres to planes. In following studies, the same authors developed a couple of mathematical models of the same equivalent

mechanism, called M1 and M2 (Parenti-Castelli et al., 2004), simply expressing mathematically the constraint relative to each contact zone with a serial chain composed by one spherical and two prismatic joints. As it was also reported latterly (Feikes et al., 2003), these mathematical models suffer from two specific limitations: one of these is the discomfort due to the lower manageability of the model and the possibility to fall into singularities of the set of 24 equations, and the second is the impossibility to consider more anatomical geometries of the tibial plateaus instead of two planes.

A subsequent spatial equivalent mechanism (Parenti-Castelli et al., 2004), which considered each contact relation as a rigid frictionless contact between two spheres (ESM-2) (Parenti-Castelli et al., 2004), suggested the implementation of a third mathematical model (M3) to study the knee kinematics (Parenti-Castelli et al., 2004). This model featured a simpler mathematical form comprised by a system of 5 non-linear equations for any given flexion angle and a more anatomical description of the knee joint kinematics because of the use of more anatomical articular surfaces (spheres against planes).

These observations encourage the authors to model the articular contact surfaces shapes progressively even more similar to those of a natural knee. Thus, a new spatial equivalent mechanism (ESM-3) (Parenti-Castelli et al., 2004) was developed by the same authors (Di Gregorio and Parenti-Castelli, 2003) considering each articular surface as a general shape, each described by either scalar equations or parametric forms, and producing a system of 11 or 13 equations, respectively. In the same studies, a new mathematical model (M4) (Parenti-Castelli et al., 2004) was devised in order to study the knee 3D kinematics considering that the tibio-femoral contacts occur between two ellipsoidal (femoral) and two spherical (tibial) surfaces. The authors reported that, as easily predictable, a more precise approximation of the articular surfaces leads to a more accurate model of the knee passive motion.

2.2 Static and Quasi-Static Models

Generally, a system is defined as quasi-static when it follows a succession of equilibrium states. This property is peculiar of systems that reach equilibrium very fast, almost instantaneously, anyhow much faster than their physical parameters vary. In modelling of the knee joint, the quasi-static

hypothesis has been long adopted, because this assumption allows to neglect viscous and inertial contributions of the modelled system, thus significantly simplifying the complexity of the problem. Regarding the knee joint, the equilibrium of the system is calculated, for any given position of the joint, through the balance of all forces and moments acting in the model, such as ligaments and contact forces. Thus, velocity and acceleration of bony segments and viscous properties of ligaments and muscles are neglected.

Several quasi-static models have been proposed in the literature in order to investigate one or more significant aspects for the determination of the complex function of the knee joint, which comes from the synergic contribution of different anatomical structures. For example, some quasi-static models were developed for calculating the contribution, in terms of deformation and force, of each passive structure as a function of joint position (Blankevoort and Huiskes, 1996; Wismans et al., 1980). Moreover, quasi-static models were also developed in order to quantify contact forces and stresses between tibial and femoral articular surfaces (Blankevoort et al., 1991) and others to evaluate the distribution of forces among muscles and ligaments in different loading conditions, such as isometric muscular contractions (Pandy and Shelburne, 1997; Shelburne and Pandy, 1997) or daily living activities like walking (Anderson and Pandy, 2001). Moreover, more complex models, comprising ligamentous structures, contact surfaces, and muscular structures, were also proposed in order to solve more than one of the problems listed above by means of the same model (Fernandez and Pandy, 2006). Nevertheless, these models represent more the whole lower limb model rather than the knee specifically.

The development of knee models, aimed to predict how ligament length depends on flexion angle, has involved measurements of the joint kinematics and of the location of the ligament insertion sites on the bony structures. Considering these data in the model, the joint position is mathematically modified according to the acquired motion, then the distances between the insertion sites are calculated for each flexion angle. This approach allows to evaluate the length of each ligament as the distance between its two insertion sites for each given relative position of the joint.

Nevertheless, the evaluation of deformations and forces in the ligamentous structures during stability tests or daily living activities can be required. In order to solve this problem, given the instantaneous length of the

ligament for a specific position of the knee joint, *reference length* and *stiffness* information are necessary to calculate the deformations and the forces in the ligaments, respectively. In quasi-static knee models, passive structures like ligaments were usually modelled by means of one or more straight lines connecting the insertion sites and producing a force proportional to the deformation. In some models proposed in the literature, each ligament has been modelled by means of only one passive element (single-fibre approach) (Wismans et al., 1980). Whereas in other models, particularly where the objective of the study was particularly focused on the ligaments function, each ligament was modelled by means of more than one straight line in order to take into account the anatomical structure of the ligament (multi-bundle approach) (Andriacchi et al., 1983; Bertozzi et al., 2007; Blankevoort and Huiskes, 1996; Mommersteeg et al., 1997). In those models where the single-fibre approach was adopted, a non-linear mechanical behaviour was usually considered in order to reproduce the non-linear mechanics of the whole ligament, which was experimentally measured and mathematically approximated by means of a quadratic function (Essinger et al., 1989; Moeinzadeh et al., 1983; Wismans et al., 1980) or a linear function joined by a quadratic toe region for small deformations (Blankevoort and Huiskes, 1996; Caruntu and Hefzy, 2004).

In order to anatomically describe and mechanically characterize the behaviour of ligaments and other knee passive structures, several *in-vitro* experimental studies were performed (Butler et al., 1992; Harner et al., 1999; Pioletti et al., 1998; Race and Amis, 1994) testing in tensile conditions the whole ligament and/or part of it, maintaining insertion bony sites too. During these studies, it was also recognized that different fibre-bundles of the same ligament behave differently, such as the anterior and posterior fibre-bundles of the cruciate ligaments. Indeed, in the same ligament, the two fibre-bundles can be together stretched and slacked, and *vice versa*, depending on knee flexion angle. This behaviour is due to the change of the relative orientation between the femoral and the tibial insertion areas during knee flexion, where the length of the anterior and posterior fibre-bundles can be deeply different, with opposite trend too (Momersteeg et al., 1995).

Confirmed by experimental observations, the multi-bundle approach was more and more adopted by researchers, particularly for modelling cruciate ligaments. In this approach, at least two straight lines were used in order to

model anterior and posterior fibre-bundles of each cruciate ligament. In this scenario, some researchers considered mechanical parameters reported in the literature, and so they modelled ligaments in the same manner as the they were experimentally tested (Wismans et al., 1980). On the other hand, some researchers performed studies which included: i) an early experimental part in which measurements of the kinematics, the anatomical geometries and the mechanical properties of anatomical structures were performed, and ii) a following computational part in which predictions, obtained by means of the devised knee model, were compared with the experimental measurements (Blankevoort and Huiskes, 1996; Mommersteeg et al., 1997). By means of this kind of approach, some authors implemented in the model the same values of the mechanical properties published in the literature, thus obtaining a model in which, given the relative position of the bony segments, the deformation and the force of each modelled fibre-bundle was directly calculated. Thus the contribution of each modelled fibre-bundle, in terms of deformation and/or force, was evaluated during the experimental kinematics, such as stability tests (Crowninshield et al., 1976b; Bertozzi et al., 2007), and *in-vivo* acquired activities (Bertozzi et al., 2006). Other authors, instead, used values of the acquired mechanical parameters as reference values, in order to perform an optimization procedure that minimized the difference between the experimental kinematics and the motions predicted by the model (Blankevoort and Huiskes, 1996; Mommersteeg et al., 1997). In this way, the devised knee model was validated calculating the mechanical parameters of the model, *initial strain* and *stiffness* of each modelled spring, which allowed to reproduce the experimentally acquired kinematics of the analyzed cadaveric knee specimen. Nevertheless, since the experimental protocol and the invasiveness of their measurements, this approach allows to validate the model only for the analyzed knee specimen.

Regarding the non-linear mechanical behaviour of each ligament fibre, Mommersteeg et. al (Mommersteeg et al., 1996) modelled the cruciate and collateral ligaments of the knee by means of different numbers of fibre-bundles, e.g. ACL was modelled with 4 and 9 fibres and PCL with 6 and 7 fibres. Authors reported a satisfactory agreement between experimental acquisitions and computer predictions, finding that ligaments with a number of fibres included between 4 to 7 were more suitable to realistically simulate the knee kinematics, ligaments with 3 or less fibres were too sensitive to

geometrical parameters, whereas, ligaments with more than 7 fibres were characterized by an useless mathematical redundancy. Another important aspect of this approach is that, with a higher number of fibres, the ligament mechanics resulted more complex, and so a higher number of parameters had to be defined. Since the difficulty to characterize soft tissues like ligaments, even by means of experimental direct measurements, the definition of an higher number of parameters could result in more experimental error rather than in a more anatomical description. Moreover, this source of error is more significant when the knee model should be specific for a selected living subject. This happens because the specificity of a model requires to measure, or at least to estimate, the highest number of parameters from that selected subject without any direct measurement.

Thus, in order to limit this source of error in subject-specific knee models, Bertozzi et. al (Bertozzi et al., 2007) proposed a quasi-static model of cruciate ligaments, assuming the hypothesis that physiological behaviour of the cruciate ligaments can be reproduced by a model with many linear-fibres (25 fibres for each cruciate), instead of few non-linear fibres as performed in previous studies (Blankevoort et al., 1991; Moglo and Shirazi-Adl, 2005; Wismans et al., 1980). This approach took advantage of a more detailed anatomical description, which can be easily obtained by means of the new technologies in biomedical imaging, with respect to a more mechanical characterization of the whole or part of the modelled structure. Thus, the authors stated that, when this methodology will be fully validated by means of experimental synchronous measurements of forces and kinematics on a series of selected subjects, the devised knee ligaments model will be able to reproduce the complex non-linear mechanical behaviour of the knee ligaments of any healthy, or pathological subject, during the execution of living daily activities too.

Several of the proposed quasi-static knee models aimed to evaluate the biomechanical function (length, deformation, and force) of the ligaments during flexion, or other kinematics, take into account articular contact interaction too (Blankevoort et al., 1991; Wismans et al., 1980). Indeed, in these models, articular contact surfaces were considered along with ligaments in order to calculate relative positions of bony segments, and so to estimate the relative contribution of each modelled anatomical structure.

In the literature, the problem of the contact at the knee joint has been tackled from different points of view and at different levels of complexity. One of the most exploited methods, used to describe the geometrical interactions between articular surfaces, was based on the assumption of contact between rigid bodies. Articular surfaces were usually approximated by means of simple analytical functions, such as polynomials in 2D (Abdel-Rahman and Hefzy, 1993; Moeinzadeh et al., 1983), spheres and planes (Abdel-Rahman and Hefzy, 1998), and polynomial 3D surfaces (Blankevoort et al., 1991; Wismans et al., 1980). Thus, the interaction between articulating surfaces was obtained in the analytical form, and considered as an additional equation to take into account of solving the equilibrium of the system, obtaining, as result, one or more contact points. Nevertheless, if an evaluation of the pressure distribution is necessary to the model, the contact between rigid bodies cannot be assumed yet, and a different method has to be employed to consider the contact between deformable bodies.

In this context, estimation of pressure distribution at the knee joint was analyzed in quasi-static models using different numerical and analytical techniques (Li et al., 1997). Some of these are: the rigid-body-spring-model (RBSM) (Essinger et al., 1989; Kawai, 1980), the finite element method (FEM) (Andriacchi et al., 1983), a simplified elasticity solution (SES) (Bartel et al., 1985) and the modified Hertzian (MH) theory (Eberhardt et al., 1990; Pandy et al., 1998). As reported in the comparison study by Li et. al. (Li et al., 1997), in FEM and MH methods, each articulating surface was covered by an elastic layer, while in RBSM and SES methods, one of the two contacting body was assumed rigid, which indented an elastic concave surface. Li et. al reported that RBSM and FEM methods were able to better predict strain/stress distribution than SES and MH methods, particularly for non-asymmetric loads, and that the RBSM method was relatively simple and effective in predicting joint contact pressure than the other three techniques. This computational efficiency is particularly attractive for the pre-operative planning of reconstructive surgical procedures in orthopaedics. For more details regarding each method, the authors suggest specific mechanical books or specifically each of the published work cited above.

Nevertheless, the two major limitations of RBSM, SES, and MH methods are that: i) the material has to be assumed homogeneous everywhere, and ii) no complex biphasic behaviour can be taken into account. For these reasons,

at present, the FEM method, which was developed in the field of structural mechanics, is one of the most widespread techniques used for evaluating the deformation and the pressure in the cartilage layers of the knee articulating surfaces, and for considering non-homogeneous materials too. However, given its high computational weight, the FEM method was usually employed for static positions of the knee joint, evaluating simple loading conditions, such as anterior-posterior forces (Bendjaballah et al., 1998; Li et al., 1999) and simulated muscular forces (Mesfar and Shirazi-Adl, 2005).

Hence, if the aim of the study is: i) to obtain an evaluation of force, strain, and/or stress distribution inside the cartilaginous layer or parts of prostheses, or ii) to predict kinematics taking into account deformations of these anatomical structures, the FEM method results more appropriated than other approaches. This is even more true because, in the last decades, the FEM code has been implemented in several commercial software-packages and along with the development of more powerful computers, the FEM method became more exploitable by biomechanical researchers.

Several knee models were developed and proposed in the literature for the estimation of the muscular contribution to the knee function for simple motor tasks, such as a single muscle activation (Pandy and Shelburne, 1997; Tumer and Engin, 1993) or the more complex gait-cycle (Anderson and Pandy, 2001). These models were usually based on the inverse dynamic approach applied to *in-vivo* experimental acquisitions, which allows to estimate net loads and moments at the knee joint. From these, through an optimization process based on the minimization of a cost function, forces at each ligament, muscle, and articular contact is estimated. This optimization process is necessary to reduce the indeterminacy of the problem, because the net loads and moments at the knee joint have to be divided amongst all the modelled anatomical structures. The definition of the cost function, to be minimized, refers to different criteria, such as minimum metabolic energy, minimum muscle fatigue, and minimum sense of effort. Nevertheless, all optimization criteria proposed in the literature were often based on hypothetic assumptions, and among these, no one was ever really validated by means of experimental data. This optimization process was considered both in static, taking into account each single position of the knee, and in dynamic conditions, taking into account the whole motor task. Thus, if an isometric contraction of one or more muscles, or a static external force is

applied to the knee system, the static optimization should be exploited (Shelburne and Pandy, 1997), whereas, the dynamic optimization should be considered for dynamic activities, such as maximum-height jumping (Pandy et al., 1990). Nevertheless, during one of the most investigated daily activity (walking), both static and dynamic optimizations were applied to inverse dynamic approach during a whole gait-cycle, resulting practically equivalent (Anderson and Pandy, 2001).

2.3 Dynamic Models

Side by side to quasi-static models, dynamic models of the knee were also developed and proposed in the literature (Abdel-Rahman and Hefzy, 1993; Abdel-Rahman and Hefzy, 1998; Bei and Fregly, 2004; Beillas et al., 2004; Caruntu and Hefzy, 2004; Moeinzadeh et al., 1983; Piazza and Delp, 2001; Tumer and Engin, 1993). The dynamic approach adopted to model the knee joint allowed to calculate position, velocity and acceleration of each considered anatomical structure according to the flexion angle and the loading conditions. Thus, in a dynamic model of the knee joint, dynamic components, like inertia of the bony segments and visco-elasticity of the soft tissues, should be taken into account.

Three-dimensional dynamic modelling of the knee joint can be tackled using two main approaches. The first one is based on the mathematical solution of a system of differential equations (DAEs) obtained by writing the Newton-Euler laws for the mechanical system. This system is difficult to be solved, thus, it is usually simplified (e.g. dropping system index with intermediate variables) and finally, the solution of the problem is obtained by means of the Newton-Raphson iterative technique. Based on a recursive technique, this approach results in more powerful computations, even if it remains complex and computationally heavy. Moreover, all operations, needed for the resolution process, mask the original form of the system formulas and make them difficult to handle or modify. The second approach is based on the D'Alambert's principle, which considers the balance among kinetic and potential energies of the system. Advantages of this method are that the obtained model is more simple and suitable to understand the effects introduced by variations of the parameters. Disadvantages are that the mathematical process of this approach is not as comprehensible by a

physical viewpoint, and that the obtained equations are not optimized for a computational resolution.

A great interest in the dynamic behaviour of the knee joint was expressed by Crowninshield et. al (Crowninshield et al., 1976a; Pope et al., 1976), which, probably for the first time, employed impedance testing techniques applied to this complex and important articulation of the human locomotor system. The authors experimentally measured *in-vivo* the mechanical behaviour of the human knee in dynamic, static and creep conditions, for both healthy and injured knees. The authors reported that the knee behaves dynamically as a Kelvin body (Crowninshield et al., 1976a), and they proposed a complex rheological model of the knee, which was able to describe both static and dynamic behaviour of this articulation (Pope et al., 1976).

Like quasi-static models, different typologies of dynamic models were developed depending on the aim of the study. In order to investigate the dynamic behaviour of the knee joint, early 2D models were proposed adopting a Newton-Euler formulation (Moeinzadeh et al., 1983; Tumer and Engin, 1993). Such models included the ligaments, which were usually characterized by a non-linear elastic behaviour, and the articular surfaces, which interacted with each other through contact between rigid bodies (Abdel-Rahman and Hefzy, 1993). Given the analytical complexity of the problem, in these early attempts, the simulated loading conditions were often simple analytical functions, such as a rectangular pulse and an exponential decaying sinusoidal pulse applied to the tibia (Moeinzadeh et al., 1983), or an impulsive muscular activity of the quadriceps group (Tumer and Engin, 1993). A similar 3D dynamic model was proposed by Abdel-Rahman and Hefzy as evolution of a previous 2D model of the same group. The proposed model consisted in two rigid bony segments, femur and tibia, ligaments (non-linear elastic springs) and articular surfaces, which interacted with each other by means of a frictionless contact between spherical (femur) and planar surfaces (tibia). The model allowed to estimate, under sudden external forcing pulse loads applied to the tibia, the kinematics of the bony segments, according to the restraint function provided by the modelled passive structures. Though very simple analytical shapes, spheres, and planes, were considered as an approximation of the articular surfaces, the models resulted to be too analytically complex and computationally heavy to be solved.

Recently, the same group proposed the last evolution of the model (Caruntu and Hefzy, 2004). The model included deformable contact between anatomical-based articular surfaces, mathematically represented by means of Coons bi-cubic surface patches, and it was employed in order to predict knee extension kinematics due to quadriceps dynamic loading.

Regarding the contact models for evaluating the interactions between the articulating surfaces, the same approaches developed for quasi-static models were also employed in dynamic knee models, e.g. rigid contact (Abdel-Rahman and Hefzy, 1993; Bei and Fregly, 2004), deformable contact of Blankevoort et. al (Blankevoort et al., 1991) based on the elastic foundation theory (Caruntu and Hefzy, 2004; Fregly et al., 2005), and FEM (Beillas et al., 2004). Moreover, if viscous properties of the soft tissues, like ligaments or cartilages, were not considered in the model, the so called "dynamic model" was actually a quasi-static model, along with corrective terms for taking the inertia of bony segments into account. However, since viscous terms relative to ligaments, cartilages, and menisci are almost negligible with respect to their elastic terms, these were usually omitted in dynamic models under physiological loading conditions.

Thus, by exploiting these methods to evaluate the contact in dynamic models of the knee joint, it was possible to perform predictions of the peak and the distribution of the forces and pressures in the cartilage layers, during the execution of daily living activities, such as kicking (Tumer and Engin, 1993), hopping (Beillas et al., 2004), and walking (Bei and Fregly, 2004). A particular interest in the evaluation of pressure peak and distribution on the articular surfaces, during dynamic activities, particularly increased with the development of new technologies for the acquisition of *in-vivo* kinematics, which allowed to acquire experimentally the subject-specific kinematics of a particular living subject. For technological reasons, this kind of applications was early applied to subject who underwent to total knee replacement (TKR) implant (Fregly et al., 2003; Fregly et al., 2005; Piazza and Delp, 2001), and then, with the enhancement of biomedical imaging devices (such as CT, MRI, and fluoroscopy), also in pathological and healthy living subjects.

Three-dimensional, more complex, and anatomically comprehensive models, which included patella bone, ligaments, articular contact, and muscles, were proposed in order to evaluate the dynamic behaviour of the knee taking the quadriceps extensor mechanism into account (Beillas et al.,

2004; Caruntu and Hefzy, 2004; Fernandez and Pandy, 2006; Piazza and Delp, 2001; Tumer and Engin, 1993). Moreover, in the last years, several lower limb models were proposed in order to obtain more comprehensive model for evaluating the dynamic of the knee joint (Fernandez and Pandy, 2006; Shelburne et al., 2004). These models were composed of the geometrical model of the whole femur, tibia and patella, along with the bony kinematics of the pelvis and the foot in order to consider the directions of the muscular actions. In these models, several technologies were usually exploited to obtain subject-specific data experimentally. For example, as proposed by Fernandez et. al (Fernandez and Pandy, 2006), in a first experimental part, the subject would undergo a series of acquisitions: such as nuclear magnetic resonance (NMR), motion capture with electromyography (EMG), ground reaction force (GRF), and X-ray video-fluoroscopy. From NMR data, all the subject-specific geometries of bones, ligaments, and muscles would be reconstructed by means of a segmentation technique. From video-fluoroscopy and bony reconstructed geometries, accurate pose of the bony segments would be reconstructed in the space. Then, in a rigid body model of the whole lower limb, muscles forces would be estimated using data from the EMG, the GRF and the reconstructed bony kinematics. Finally, in a FEM model of the knee, the dynamic contact pressure would be estimated during the acquired motor task performed by the selected subject.

Nevertheless, these models need plenty of information to be geometrically modelled and mechanically characterized in an accurate manner, and so they would be based on an anatomical database of a specific cadaveric specimen, or on an average geometrical model of the anatomical structures associated with scaling methods for adapting the general femur to the selected subject (Fernandez and Pandy, 2006), or again, they would be based on a collection of geometrical and mechanical parameters derived from different and non-homogeneous sources (Piazza and Delp, 2001).

2.4 Proposal for Innovative Approaches

As comprehensively reported above, the problem of knee modelling has been tackled from different points of view and at different levels of complexity. Several 2D knee models were proposed in the literature (Goodfellow and O'Connor, 1978; Moeinzadeh et al., 1983; Zavatsky and O'Connor, 1992b; Zavatsky and O'Connor, 1992a). The aim of these models was usually to investigate, under simple loading conditions, the function of the knee ligaments in the sagittal plane (Shelburne and Pandy, 1997; Zavatsky and O'Connor, 1993). 3D mathematical and finite elements models were also developed (Blankevoort et al., 1991; Blankevoort and Huiskes, 1996; Fernandez and Pandy, 2006; Li et al., 1999; Moglo and Shirazi-Adl, 2005; Mommersteeg et al., 1997; Wismans et al., 1980). These more complex models allowed to consider also anatomical articular surfaces, contact forces, articular deformations, different passive structures, like ligaments, capsule, and menisci, and active structures like muscles. On the other hand, because of their computational weight, these complex models can hardly be applied in a physiological context. Moreover, if a subject-specific model of a selected healthy subject has to be developed, a more complex model and its higher number of parameters, necessary for the characterization of its mechanical behaviour, can be principally a disadvantage. In fact, even if the model is properly designed for a specific application, its potential can be nullified by the errors resulting from an inappropriate and/or inaccurate definition of the parameters. These errors are often due to disagreement in the origin of the parameters and inputs, obtained from different and non-homogeneous sources (Li et al., 1999; Piazza and Delp, 2001; Fernandez and Pandy, 2006).

In order to limit this kind of errors, the foundations of the present work is to model the knee joint and its single anatomical structures as subject-specific as possible, with particular attention paid to the anatomical geometries and the bony kinematics. In fact, with the evolution of the medical and the diagnostic imaging technologies, such as MRIs and video-fluoroscopy, now these data can be acquired and reconstructed by a selected living and healthy subject with little invasiveness, due to the little X-ray dose of the video-fluoroscopy. In this way, avoiding direct and invasive measurements, it is possible to investigate the function and/or the pathology

of an anatomical structure of interest during its actual physiological and/or pathological condition.

The proposed method was based on the *inverse approach*, which allows to calculate and/or estimate deformations and forces of passive structures as consequence of the imposed bony motion. Thus, since the acquired subject-specific bony kinematics was a reliable data that it is possible to obtain from the subject, the amount of the deformation in its passive anatomical structures, such as cruciate and collateral ligaments, capsule and articular cartilage, can be simply estimated as consequence of the relative position of the bony segments in which the structure inserted. Moreover, considering the mechanical properties too, estimations of the forces produced by these structures can be performed.

i Model of Cruciate Ligaments

In the first part of this work (Chapter 3), a subject-specific model of the human cruciate ligaments of a healthy living subject was developed. The model was aimed to perform estimations of the forces produced by the cruciate ligaments both during simulated stability tests and during the execution of daily living activities. The reached amount of the subject-specificity of the model was as high as possible. In fact, only the elastic modulus parameter of the cruciate ligaments was considered from the literature, but a novel experimental method to overcome this limit of the model was designed and proposed in the Chapter 5. Moreover, another peculiarity of the developed model of the cruciate ligaments was that the model had to be characterized from the smaller number of parameters, so to limit the number of estimations to perform on the subject. For example, the main hypothesis of the proposed study was that the physiological behaviour of the whole ligament can be reproduced by using many linear-fibres (25 fibres), instead of only one or few non-linear fibres (Wismans et al., 1980; Blankevoort et al., 1991; Mommersteeg et al., 1997; Moglo and Shirazi-Adl, 2005). This hypothesis was supported by the theory of the Quasi-linear viscoelasticity by Fung (1994), in which the non-linear behaviour of a complex structure, such as the cruciates, can be obtained by a hierarchical recruitment of linear fibres, due to their geometrical relationship and the relative kinematics of their origin and insertion. Thus, this approach can be

used to reproduce the non-linearity of the cruciate ligaments using elastic and linear elements arranged and characterized according to the experimental data acquired on the selected subject, leaving the reproduction of the non-linearity (as demonstrated by Fung) to their relative geometrical distribution and hierarchical recruitment. Moreover, if non-linear fibres were considered, additional parameters had to be defined and quantified for the specific application. The literature about the experimental characterization of the mechanical parameters of the cruciate ligaments showed that this characterization was extremely critical. Thus, additional parameters could increase the complexity and introduce further experimental inaccuracies, without improving the reliability of the model.

ii Model of Tibio-Femoral Contact

In the second part of the study (Chapter 4), the tibio-femoral articular contact was evaluated using a similar approach used for the cruciate ligament model. Also in this case, the foundation of the model was the use of the bony geometries and kinematics acquired and reconstructed from the selected subject. The contact between the two bony geometries, tibia and femur, was considered as the consequence of the imposed kinematics. Nevertheless, as better explained in Chapter 4, in this context the word 'contact' assumed an incorrect meaning. In fact, a material contact between two bodies never occurred. Thus, since the reconstructed bony geometries, on which the bony kinematics were imposed, were exactly the geometries of the bones, meant as the more mineralized part of the bones, then the two bony geometries never interacted each other during the acquired kinematics because of the actual presence of the cartilages and the menisci between the tibia and the femur.

The modelling of the tibio-femoral 'contact' was approached as already proposed in the literature (DeFrate et al., 2004; Corazza et al., 2005) but considering *in-vivo* and physiological bony kinematics. Thus, for each considered frame of the acquired kinematics, the articular contact was estimated calculating the *proximity* between the femur and the tibia and then considering the distances lower than a threshold properly defined in order to consider the thickness of cartilages and menisci.

2.5 References

Abdel-Rahman, E., Hefzy, M. S., (1993). A two-dimensional dynamic anatomical model of the human knee joint. Journal of Biomedical Engineering 115**,** 357-365.

Abdel-Rahman, E. M., Hefzy, M. S., (1998). Three-dimensional dynamic behaviour of the human knee joint under impact loading. Medical Engineering and Physics 20**,** 276-290.

Anderson, F. C., Pandy, M. G., (2001). Static and dynamic optimization solutions for gait are practically equivalent. Journal of Biomechanics 34**,** 153-161.

Andriacchi, T. P., Mikosz, R. P., Hampton, S. J., Galante, J. O., (1983). Model studies of the stiffness characteristics of the human knee joint. Journal of Biomechanics 16**,** 23-29.

Bartel, D. L., Burstein, A. H., Toda, M. D., Edwards, D. L., (1985). The effect of conformity and plastic thickness on contact stresses in metal-backed plastic implants. Journal of Biomedical Engineering 107**,** 193-199.

Bei, Y., Fregly, B. J., (2004). Multibody dynamic simulation of knee contact mechanics. Medical Engineering and Physics 26**,** 777-789.

Beillas, P., Papaioannou, G., Tashman, S., Yang, K. H., (2004). A new method to investigate in vivo knee behavior using a finite element model of the lower limb. Journal of Biomechanics 37**,** 1019-1030.

Bendjaballah, M. Z., Shirazi-Adl, A., Zukor, D. J., (1998). Biomechanical response of the passive human knee joint under anterior-posterior forces. Clinical Biomechanics 13**,** 625-633.

Bertozzi, L., Stagni, R., Fantozzi, S., Cappello, A., (2006). Investigation of the Biomechanic Function of Cruciate Ligaments Using Kinematics and Geometries from a Living Subject During Step Up/Down Motor Task. Spring Verlag Lectures Note in Computer Science 3994**,** 831-838.

Bertozzi, L., Stagni, R., Fantozzi, S., Cappello, A., (2007). Knee model sensitivity to cruciate ligaments parameters: A stability simulation study for a living subject. Journal of Biomechanics 40(S1)**,** 38-44.

Blankevoort, L., Huiskes, R., (1996). Validation of a three-dimensional model of the knee. Journal of Biomechanics 29**,** 955-961.

Blankevoort, L., Kuiper, J. H., Huiskes, R., Grootenboer, H. J., (1991). Articular contact in a three-dimensional model of the knee. Journal of Biomechanics 24**,** 1019-1031.

Butler, D. L., Guan, Y., Kay, M. D., Cummings, J. F., Feder, S. M., Levy, M. S., (1992). Location-dependent variations in the material properties of the anterior cruciate ligament. Journal of Biomechanics 25**,** 511-518.

Caruntu, D. I., Hefzy, M. S., (2004). 3-D anatomically based dynamic modeling of the human knee to include tibio-femoral and patello-femoral joints. Journal of Biomedical Engineering 126**,** 44-53.

Collins, J. J., O'Connor, J. J., (1991). Muscle-ligament interactions at the knee during walking. Proceedings of the Institution of Mechanical Engineers Part H - Journal of Engineering in Medicine 205**,** 11-18.

Corazza, F., Stagni, R., Castelli, V. P., Leardini, A., (2005). Articular contact at the tibiotalar joint in passive flexion. Journal of Biomechanics 38**,** 1205-1212.

Crowninshield, R., Pope, M. H., Johnson, R., Miller, R., (1976a). The impedance of the human knee. Journal of Biomechanics 9**,** 529-535.

Crowninshield, R., Pope, M. H., Johnson, R. J., (1976b). An analytical model of the knee. Journal of Biomechanics 9**,** 397-405.

DeFrate, L. E., Sun, H., Gill, T. J., Rubash, H. E., Li, G., (2004). In vivo tibiofemoral contact analysis using 3D MRI-based knee models. Journal of Biomechanics 37**,** 1499-1504.

Di Gregorio, R., Parenti-Castelli, V., (2003). A spatial mechanism with higher pairs for modelling the human knee joint. Journal of Biomedical Engineering 125**,** 232-237.

Eberhardt, A. W., Keer, L. M., Lewis, J. L., Vithoontien, V., (1990). An analytical model of joint contact. Journal of Biomedical Engineering 112**,** 407-413.

Essinger, J. R., Leyvraz, P. F., Heegard, J. H., Robertson, D. D., (1989). A mathematical model for the evaluation of the behaviour during flexion of condylar-type knee prostheses. Journal of Biomechanics 22**,** 1229-1241.

Feikes, J. D., O'Connor, J. J., Zavatsky, A. B., (2003). A constraint-based approach to modelling the mobility of the human knee joint. Journal of Biomechanics 36**,** 125-129.

Fernandez, J. W., Pandy, M. G., (2006). Integrating modelling and experiments to assess dynamic musculoskeletal function in humans. Experimental Physiology 91**,** 371-382.

Fregly, B. J., Bei, Y., Sylvester, M. E., (2003). Experimental evaluation of an elastic foundation model to predict contact pressures in knee replacements. Journal of Biomechanics 36**,** 1659-1668.

Fregly, B. J., Rahman, H. A., Banks, S. A., (2005). Theoretical accuracy of model-based shape matching for measuring natural knee kinematics with single-plane fluoroscopy. Journal of Biomedical Engineering 127**,** 692-699.

Fung, Y. C., (1994). A first course in continuum mechanics. Englewood Cliffs, N.J., Prentice-Hall, Inc..

Gill, H. S., O'Connor, J. J., (1996). Biarticulating two-dimensional computer model of the human patellofemoral joint. Clinical Biomechanics 11**,** 81-89.

Goodfellow, J., O'Connor, J., (1978). The mechanics of the knee and prosthesis design. Journal of Bone and Joint Surgery - British Volume 60-B**,** 358-369.

Goodfellow, J. W., Kershaw, C. J., Benson, M. K., O'Connor, J. J., (1988). The Oxford Knee for unicompartmental osteoarthritis. The first 103 cases. Journal of Bone and Joint Surgery - British Volume 70**,** 692-701.

Goodfellow, J. W., Tibrewal, S. B., Sherman, K. P., O'Connor, J. J., (1987). Unicompartmental Oxford Meniscal knee arthroplasty. Journal of Arthroplasty 2**,** 1-9.

Harner, C. D., Baek, G. H., Vogrin, T. M., Carlin, G. J., Kashiwaguchi, S., Woo, S. L., (1999). Quantitative analysis of human cruciate ligament insertions. Arthroscopy 15**,** 741-749.

Huss, R. A., Holstein, H., O'Connor, J. J., (1999). The effect of cartilage deformation on the laxity of the knee joint. Proceedings of the Institution of Mechanical Engineers Part H - Journal of Engineering in Medicine 213**,** 19-32.

Huss, R. A., Holstein, H., O'Connor, J. J., (2000). A mathematical model of forces in the knee under isometric quadriceps contractions. Clinical Biomechanics 15**,** 112-122.

Imran, A., Huss, R. A., Holstein, H., O'Connor, J. J., (2000). The variation in the orientations and moment arms of the knee extensor and flexor muscle tendons with increasing muscle force: a mathematical analysis. Proceedings of the Institution of Mechanical Engineers Part H - Journal of Engineering in Medicine 214**,** 277-286.

Imran, A., O'Connor, J. J., (1996). Computer simulation of surgical malplacement of an unconstrained unicompartimental knee prosthesis with cruciates intact. British Orthopaedics Research Society, Brighton.

Kawai, T., (1980). Some consideration on the finite element method. International Journal for Numerical Methods in Engineering 16**,** 81-120.

Komistek, R. D., Stiehl, J. B., Dennis, D. A., Paxson, R. D., Soutas-Little, R. W., (1998). Mathematical model of the lower extremity joint reaction forces using Kane's method of dynamics. Journal of Biomechanics 31**,** 185-189.

Li, G., Gil, J., Kanamori, A., Woo, S. L., (1999). A validated three-dimensional computational model of a human knee joint. Journal of Biomedical Engineering 121**,** 657-662.

Li, G., Sakamoto, M., Chao, E. Y., (1997). A comparison of different methods in predicting static pressure distribution in articulating joints. Journal of Biomechanics 30**,** 635-638.

Lu, T. W., Taylor, S. J., O'Connor, J. J., Walker, P. S., (1997). Influence of muscle activity on the forces in the femur: an in vivo study. Journal of Biomechanics 30**,** 1101-1106.

Mesfar, W., Shirazi-Adl, A., (2005). Biomechanics of the knee joint in flexion under various quadriceps forces. Knee 12**,** 424-434.

Moeinzadeh, M. H., Engin, A. E., Akkas, N., (1983). Two-dimensional dynamic modelling of human knee joint. Journal of Biomechanics 16**,** 253-264.

Moglo, K. E., Shirazi-Adl, A., (2005). Cruciate coupling and screw-home mechanism in passive knee joint during extension--flexion. Journal of Biomechanics 38**,** 1075-1083.

Momersteeg, T. J., Blankevoort, L., Huiskes, R., Kooloos, J. G., Kauer, J. M., Hendriks, J. C., (1995). The effect of variable relative insertion orientation of human knee bone-ligament-bone complexes on the tensile stiffness. Journal of Biomechanics 28**,** 745-752.

Mommersteeg, T. J., Blankevoort, L., Huiskes, R., Kooloos, J. G., Kauer, J. M., (1996). Characterization of the mechanical behavior of human knee ligaments: a numerical-experimental approach. Journal of Biomechanics 29**,** 151-160.

Mommersteeg, T. J., Huiskes, R., Blankevoort, L., Kooloos, J. G., Kauer, J. M., (1997). An inverse dynamics modeling approach to determine the restraining function of human knee ligament bundles. Journal of Biomechanics 30**,** 139-146.

Murray, D. W., Goodfellow, J. W., O'Connor, J. J., (1998). The Oxford medial unicompartmental arthroplasty: a ten-year survival study. Journal of Bone and Joint Surgery - British Volume 80**,** 983-989.

O'Connor, J. J., Shercliff, T., FitzPatrick, D., Biden, E., Goodfellow, J., (1990). Mechanics of the Knee Ligaments: Structure, Function, Injury, and Repair. Raven Press, New York 201-238.

Pandy, M. G., Sasaki, K., Kim, S., (1998). A Three-Dimensional Musculoskeletal Model of the Human Knee Joint. Part 1: Theoretical Construct. Computer Methods in Biomechanics and Biomedical Engineering 1**,** 87-108.

Pandy, M. G., Shelburne, K. B., (1997). Dependence of cruciate-ligament loading on muscle forces and external load. Journal of Biomechanics 30**,** 1015-1024.

Pandy, M. G., Zajac, F. E., Sim, E., Levine, W. S., (1990). An optimal control model for maximum-height human jumping. Journal of Biomechanics 23**,** 1185-1198.

Parenti-Castelli, V., Leardini, A., Di, G. R., O'Connor, J. J., (2004). On the Modeling of Passive Motion of the Human Knee Joint by Means of Equivalent Planar and Spatial Parallel Mechanisms. Autonomous Robots 16**,** 219-232.

Piazza, S. J., Delp, S. L., (2001). Three-dimensional dynamic simulation of total knee replacement motion during a step-up task. Journal of Biomedical Engineering 123**,** 599-606.

Pioletti, D. P., Rakotomanana, L. R., Benvenuti, J. F., Leyvraz, P. F., (1998). Viscoelastic constitutive law in large deformations: application to human knee ligaments and tendons. Journal of Biomechanics 31**,** 753-757.

Pope, M. H., Crowninshield, R., Miller, R., Johnson, R., (1976). The static and dynamic behavior of the human knee in vivo. Journal of Biomechanics 9**,** 449-452.

Race, A., Amis, A. A., (1994). The mechanical properties of the two bundles of the human posterior cruciate ligament. Journal of Biomechanics 27**,** 13-24.

Shelburne, K. B., Pandy, M. G., (1997). A musculoskeletal model of the knee for evaluating ligament forces during isometric contractions. Journal of Biomechanics 30**,** 163-176.

Shelburne, K. B., Pandy, M. G., Anderson, F. C., Torry, M. R., (2004). Pattern of anterior cruciate ligament force in normal walking. Journal of Biomechanics 37**,** 797-805.

Strasser H, (1917). Lehrbuch der Muskel und Gelenkmechanik. Springer, Berlin.

Svard, U. C., Price, A. J., (2001). Oxford medial unicompartmental knee arthroplasty. A survival analysis of an independent series. Journal of Bone and Joint Surgery - British Volume 83**,** 191-194.

Tumer, S. T., Engin, A. E., (1993). Three-body segment dynamic model of the human knee. Journal of Biomedical Engineering 115**,** 350-356.

Weber, W., Weber, E., (1991). Mechanics of the Human Walking Apparatus. Springer-Verlag, Berlin and New York (translated from German by Maquet P, Furlong R - from original work in 1836).

Wilson, D. R., Feikes, J. D., O'Connor, J. J., (1998). Ligaments and articular contact guide passive knee flexion. Journal of Biomechanics 31**,** 1127-1136.

Wilson, D. R., O'Connor, J. J., (1997). A three-dimensional geometric model of the knee for the study of joint forces in gait. Gait & Posture 5**,** 108-115.

Wismans, J., Veldpaus, F., Janssen, J., Huson, A., Struben, P., (1980). A three-dimensional mathematical model of the knee-joint. Journal of Biomechanics 13**,** 677-685.

Zavatsky, A. B., O'Connor, J. J., (1992a). A model of human knee ligaments in the sagittal plane. Part 1: Response to passive flexion. Proceedings of the Institution of Mechanical Engineers Part H - Journal of Engineering in Medicine 206**,** 125-134.

Zavatsky, A. B., O'Connor, J. J., (1992b). A model of human knee ligaments in the sagittal plane. Part 2: Fibre recruitment under load. Proceedings of the Institution of Mechanical Engineers Part H - Journal of Engineering in Medicine 206**,** 135-145.

Zavatsky, A. B., O'Connor, J. J., (1993). Ligament forces at the knee during isometric quadriceps contractions. Proceedings of the Institution of Mechanical Engineers Part H - Journal of Engineering in Medicine 207**,** 7-18.

Chapter 3: Model of Cruciate Ligaments

- Stagni R., et.al. 2005, WIT Trans. Biomed. Health, 8, 381-399. In proc. Biomed. 2005.
- Bertozzi L., et.al. 2005, In Press in Gait & Posture. In proc. SIAMOC 2005.
- Bertozzi L., et.al. 2005, Oral Presentation. EMBEC 2005.
- Bertozzi L., et.al. 2006, Springer-Verlag LNCS, 3994, 831-838. In proc. ICCS 2006.
- Bertozzi L., et.al. 2006, Oral Presentation Knee2006.
- Bertozzi L., et.al. 2006, Journal of Biomechanics 39(1) S69-S70. In Proc. 5th W.C.B.
- Bertozzi L., et.al. 2006, Gait & Posture 24(1) S31-S32. In proc. SIAMOC 2006.
- Bertozzi L., et.al. 2007, Journal of Biomechanics 40 (1) S38-S44.
- Bertozzi L., et.al. 2008, Digital Humans, The State of the Art Survey. Springer.
- Bertozzi L., et.al. 2008, Journal of Applied Biomechanics. In Press.

In this chapter, a 3D quasi-static model of the human cruciate ligaments was proposed and developed in order to estimate, in a living subject, the forces at the cruciate ligaments during the execution of daily activities.

As described in Chapter 1, the mechanics of the ligaments is quite complex because of its inner hierarchic structure. Scientists have usually modelled each ligament using one or few elements with a mechanical behaviour as similar as possible to the mechanical behaviour of the whole ligament (Wismans et al., 1980; Blankevoort et al., 1991a; Blankevoort and Huiskes, 1996; Li et al., 1999; Moglo and Shirazi-Adl, 2005). Nevertheless, using the theory of the Quasi-linear viscoelasticity by Fung (1994), as reported in Chapter 2, a first approximation of the non-linear behaviour of a complex structure, such as the cruciates, can be obtained by a hierarchical recruitment of linear fibres, due to their geometrical relationship and the relative kinematics of their origin and insertion.

The developed model was based on specific data from a living selected subject. In particular, the subject-specific geometries (of bones and of cruciates) and the bony kinematics were the foundation of the devised cruciate ligaments model. Thus, each cruciate ligament was modelled arranging 25 linear and elastic elements on the subject-specific geometries in order to leave, as demonstrated by Fung (1994), the reproduction of the non-linearity of the whole ligament to the geometrical distribution and hierarchical recruitment of all fibres of each cruciate.

Considering that the force expressed by a passive structures like the cruciate ligament is mainly due to the relative position of its insertions on the bony structures, the length of each ligament can be calculated knowing just the bony geometries and kinematics along with the geometry and the position of the insertion of the cruciates on the bony structures. But, in order to be able to estimate the elongation and the force of each ligament, geometrical and mechanical parameters of the cruciates need to be defined. Thus, in the devised model, methods to estimate the geometrical parameters from the selected subject, such as the reference length and the cross-sectional area, were proposed and implemented. The elastic modulus was considered from the literature and the sensitivity of the model with respect to all parameters was also analysed. Finally, using the developed methodology along with additional non-invasive measurements, a new experimental method to estimate the elastic modulus from the same subject was also proposed.

All the results obtained during this study and presented in this chapter were submitted for publication and many of these were published in conferences and journals (Stagni et al., 2005; Bertozzi et al., 2005; Bertozzi et al., 2006c; Bertozzi et al., 2006a; Bertozzi et al., 2006b; Bertozzi et al., 2007b; Bertozzi et al., 2007a; Bertozzi et al., 2007c; Bertozzi et al., 2008).

3.1 Materials and Methods

i Selected Subject and Experimental Acquisitions

A young Caucasian male (height 1.68 m, weight 62 kg, and age 30 years), free from musculo-skeletal affections, gave his informed consent to undergo a NMR scan and video-fluoroscopy acquisitions. Then, the subject underwent an high resolution NMR scan of his right knee by means of a 1.5T Gemsow scanner (*GE Medical Systems, Milwaukee, Wisconsin*), see details of the scanning procedure in Table 3.1. During the NMR acquisition the subject was lying down on the NMR couch with the considered knee at the full extension. This relative position between the tibia and femur was considered as position “without body weight”, because the gravity force was perpendicular to the PD axis of the subject.

Scanning sequence	Spin Echo (T1 weighted)
Number of slices	54
Pixel spacing	0.037 x 0.037 (cm x cm)
Scanned region length (across the knee)	15.9 (cm)
Slice thickness	2.5 (mm)
Slice spacing	3 (mm)

Table 3.1: Parameters of the NMR scanning-procedure

In order to record the bony kinematics, the same subject underwent several video-fluoroscopic acquisitions using a video-fluoroscope (*SBS 1600, Philips Medical System, Nederland B.V.*) at 10 images per second. During the movements, the considered knee was kept inside the fluoroscopic field of view. A qualified operator imposed a slow passive-flexion movement to the knee under analysis, which lasted about one second and a half covering the range from full extension to about 100 degrees of flexion. Moreover, the same subject was acquired during the execution two repetitions of step up/down motor task and nine repetitions of the chair rising/sitting motor tasks.

ii Reconstruction of Subject-Specific Data

In order to reconstruct the **bony geometries** of the femur and the tibia, the subject-specific NMR dataset was exploited. In fact, for each NMR image, the outer contour of each anatomical structure of interest was detected and outlined with a manual 2D segmentation technique using the software Amira (*Indeed - Visual Concepts GmbH, Berlin, Germany*). The resulting stacks of segmented images were interpolated generating external surfaces of the distal femur, of the proximal tibia, and of the Anterior and the Posterior Cruciate Ligaments (ACL and PCL respectively) (Figure 3.1) (Stagni et al., 2004).

Regarding the reconstruction of the **bony kinematics**, instead, both the bony geometries and the fluoroscopic images were needed. Thus, the accurate 3D pose of the femur and tibia was reconstructed using an automatic iterative-procedure frame by frame. The reconstruction was based on the tangency condition between the fluoroscope projection-lines and the surface of the bony geometries. The accuracy of the reconstruction process

was assessed in prosthesized knees to be better than 1.5 degrees and 1.5 mm for relative rotations and translations, respectively (Zuffi et al., 1999). In fluoroscopic images of natural knees, the contour of the cortical bone generally results less defined with respect to the contour produced by the metallic components of a knee implant. Nevertheless, the low sampling rate of the fluoroscopic acquisitions (10fps) used in this work, allowed to obtain images sufficiently contrasted to clearly identify and define the projections of the knee bones. Moreover, in the process of the reconstruction of the bony kinematics, the use of MRI-based with respect to more accurate CT-based geometries generated errors similar of the theoretically accuracy of the technique, which were both near to about 2 mm for translations and about 1.5 degrees for rotations (Fregly et al., 2005; Moro-oka et al., 2007).

iii Geometrical Aspects of the Model

In order to subject-specifically model the **cruciate ligaments**, more elaborations to the acquired NMR dataset were needed. In fact, using Amira, 3D anatomical-insertion areas of the cruciate ligaments were estimated as prints of the cruciate-ligaments geometries on the external bony surfaces. Each anatomical-insertion area was described with a 3D cloud of points (Figure 3.1) which were called anatomical-insertion points.

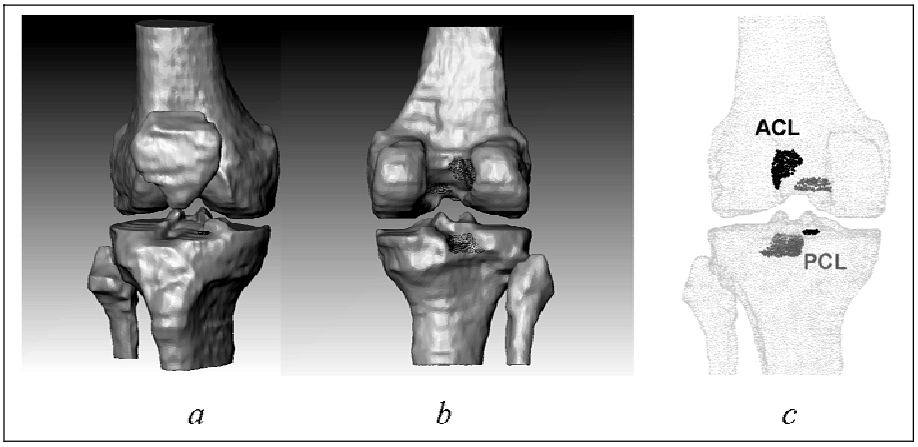

Figure 3.1: Anterior (*a*) and posterior view (*b*) of the bony segments reconstructed by NMR. Ligament insertion areas (*dotted regions*) on the femur and the tibia (*c*) from an anterior viewpoint. From Bertozzi et. al (Bertozzi et al., 2006c).

From each anatomical-insertion area, composed by N equally weighted points, the inertia tensor I was calculated according to the Equation (4.1) (Goldstein et al., 2002), where m_i was equal to one for all points.

$$I = \sum_{i=1}^{N} m_i \begin{bmatrix} \left(y_i^2 + z_i^2\right) & -x_i y_i & -x_i z_i \\ -x_i y_i & \left(x_i^2 + z_i^2\right) & -y_i z_i \\ -x_i z_i & -y_i z_i & \left(x_i^2 + y_i^2\right) \end{bmatrix} \tag{4.1}$$

Since the moment of inertia tensor is real and symmetric, it is possible to find a Cartesian coordinate system in which it is diagonal, having the form of the Equation (4.2)

$$I = \begin{bmatrix} I_1 & 0 & 0 \\ 0 & I_2 & 0 \\ 0 & 0 & I_3 \end{bmatrix} \tag{4.2}$$

where the coordinate axes are called the principal axes and the constants I_1, I_2 and I_3 are called the principal moments of inertia and, usually, these are increasingly arranged $I_1 \leq I_2 \leq I_3$.

Then, the anatomical-insertion points were projected on the plane passing through the first and the second principal axes (Corazza et al., 2005). On this local plane, the projected anatomical-insertion points were outlined automatically with a quadratic equation. Ellipses were obtained for all anatomical-insertion areas. For each ellipse, 25 planar modelled-insertion points were defined on the elliptical area: 1 in the centre of the ellipse, 12 uniformly distributed on the contour of the evaluated ellipse and 12 uniformly distributed along the contour of an ellipse having the same centre and semi-axes half of the previous ones. Finally, 3D modelled-insertion points have been defined fitting the 25 planar modelled-insertion points on each 3D anatomical-insertion area using the *thin plate splines* method (TPS) (Bookstein, 1989) (Figure 3.2).

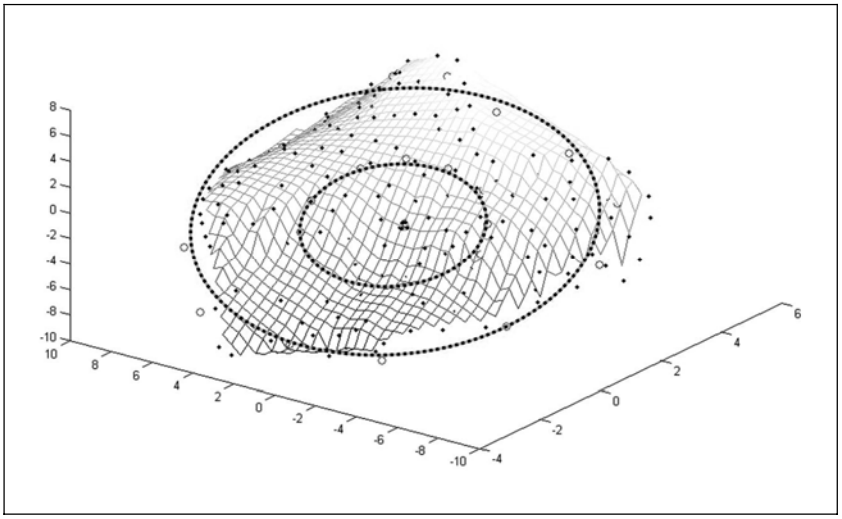

Figure 3.2: Example of an anatomical insertion area with the 25, insertion points, fitted in 3D by TPS method, and the two elliptical contours. From (Bertozzi et al., 2006c)

The procedure used to join the femoral-insertion points with the tibial ones took the anatomical twisting of the fibres into account. Coherently with the physiological external twist of the ACL, the tibial-insertion area of this ligament was rotated externally by 90° with respect to the femoral one. In other words, the fibre connected to the most anterior-insertion point laying on the femoral insertion-area, joined the most lateral-insertion point on the tibial insertion-area (Figure 3.3). On the contrary, the tibial-insertion area of the PCL was rotated internally by 90° with respect the femoral one (Figure 3.3). Untwisted version of the model (i.e. considering for each cruciate ligament a coherent fibre bundle) was also evaluated, but the obtained results were quite far from the physiology (Bertozzi et al., 2005; Stagni et al., 2005).

According to the anatomical description of the cruciate-ligaments insertions provided by Harner (1999), each fibre *j* was assigned to belong to one of the two fibre bundles depending to the position of its 3D modelled-insertion points onto the femoral and tibial anatomical-insertion areas.

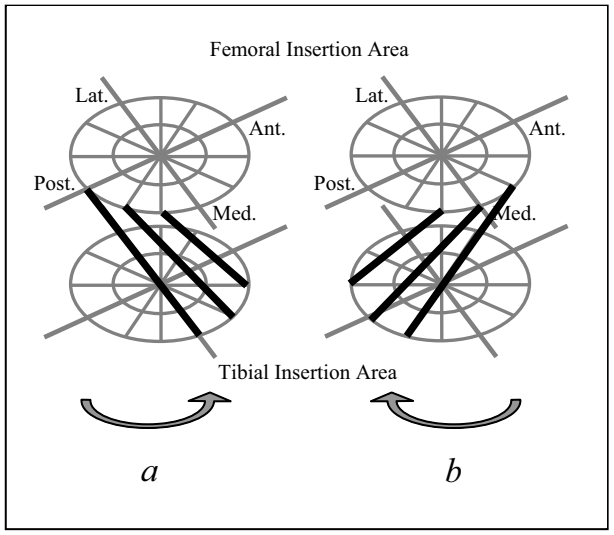

Figure 3.3: Ordering pattern relative to the Anterior Cruciate Ligament (*a*) and the Posterior Cruciate Ligament (*b*).

iv Mechanics of Ligaments and Definition of Parameters

As already reported, each cruciate was modelled by means of 25 fibres, which were arranged on the subject-specific bony geometries following the description given in the previous paragraph.

Each fibre was modelled using a linear and elastic spring and characterized by means of the Hooke's law (first part of Equation 4.3). Thus, expressing the force F_j and the extension Δl_j in the in function of the stress σ_j and the strain ε_j, the stiffness coefficient K_j of each fibre j was estimated from the cross-sectional area A_j, the reference length l_{0j}, and the elastic modulus E_j.

$$K_j = \frac{F_j}{\Delta l_j} = \frac{\sigma_j A_j}{\varepsilon_j l_{0j}} = \frac{E_j \cdot A_j}{l_{0j}} \tag{4.3}$$

The force vector of each fibre j was calculated according to the Equation (4.4):

$$\begin{cases} \vec{F}_j = -K_j \left(\left\| \vec{l}_j \right\| - l_{0j} \right) \dfrac{\vec{l}_j}{\left\| \vec{l}_j \right\|} & \left\| \vec{l}_j \right\| - l_{0j} \geq 0 \\ \vec{F}_j = 0 & \left\| \vec{l}_j \right\| - l_{0j} < 0 \end{cases} \tag{4.4}$$

where the vector $\vec{l}_j$ connected at each frame, the two modelled-insertion points of each fibre *j* from the tibia to the femur.

The **reference length** l_{0j} of each fibre *j* was defined according to hypothesis proposed by Goodfellow and O'Connor (1978), which states that the reference length of the cruciate ligaments, meant as the length at which it becomes to produce force, is equal to the maximal length reached by each ligament during the passive flexion path in physiological conditions. Thus, applied to the whole intact ligament, it could be possible estimate the amount of elongation (i.e. the length) at which the ligament passes from the toe region (Region 1) to linear region (Region 2), see the force-elongation curve shown in Figure 1.11 (Chapter 1). Applying this method to each fibre, it is possible estimate the reference length (the length threshold between Region 1 and 2) at which each fibre is recruited. Thus, each single fibre is recruited at different amounts of elongation, producing the toe region, whereas the linear behaviour is reached only when all fibres are recruited.

A qualitative indication of the values obtained for the reference length of all fibres was provided in terms of mean value and the standard deviation, which were equal to 39.7 ± 2.9 mm for the ACL and 45.8 ± 5 mm for the PCL.

The **cross-sectional area** A_j of each fibre *j* was estimated as the mean value between the femoral and the tibial insertion sub-areas relative to the fibre *j*. Each sub-area was calculated from the NMR dataset as proportional value to the square of the distance of the modelled-insertion point from its adjacent ones after the TPS deformation. The sum of all cross-sectional areas A_j of each cruciate ligament was approximately 110 mm^2 for the ACL and 157 mm^2 and the PCL.

Finally, since an estimation of the **elastic modulus** was not available from the selected subject, because of the invasiveness of direct measurements, mean values and standard deviations were taken from the literature (Butler et al., 1992; Race and Amis, 1994; Zavatsky and O'Connor,

1992a; Zavatsky and O'Connor, 1992b). A *first set* of values comprised data coming from experimental works. The elastic modulus values were 284 ± 140 MPa and 155 ± 120 MPa for the anterior and the posterior fibres bundle of the ACL respectively, and 248 ± 119 MPa and 145 ± 69 MPa for the anterior and the posterior fibres bundle of the PCL respectively (Butler et al., 1992; Race and Amis, 1994). From this first set of values, the mean values were considered for all fibres of the relative fibre bundle during almost all the performed simulations and the standard deviations were considered only for the sensitivity analysis with respect to the elastic modulus. A *second set* of values was also considered in order to evaluate the effects introduced from the use of the simpler definition of this critical parameter in physiological conditions. This simpler definition consisted in considering the same value, of the elastic modulus for all the fibres of both cruciate ligaments, instead of different values for fibres belonging to different fibre bundles and ligaments. In fact, during these simulations, the elastic modulus was defined first as described in relative sensitivity analyses, and then considering the elastic modulus of all the fibres of both cruciates equal to a constant value of 175 MPa, which was derived from works by Zavatsky and O'Connor (1992a; 1992b) according to experimental data relative to the first set of values (Butler et al., 1992; Race and Amis, 1994).

v Simulations

Early simulations performed in this study were aimed to evaluate the mechanical behaviour of the devised model for translations along anterior-posterior axis and rotations about proximal-distal axis of the anatomical reference coordinate-system of the tibia (Grood and Suntay, 1983). Thus, for each mechanical parameter of the cruciate ligaments, a sensitivity analysis was performed simulating both anterior/posterior tibial translations (**drawer test**) and internal/external rotations of the tibia (**axial stability test**).

The **first** sensitivity analysis was performed with respect to the reference length varying the *in-vivo* estimated value of l_{0j} in the range of ± 5% with 1% step. During this sensitivity analysis, the elastic modulus was considered equal to 175 MPa for all fibres of both cruciates, and the cross-sectional area was equal to the in-vivo estimated value for each fibre. The **second** sensitivity analysis was performed with respect the elastic modulus,

considering each possible combination among the mean value and plus and minus one standard deviation of the values reported in the literature (Butler et al., 1992; Race and Amis, 1994). During this sensitivity analysis, both the reference length and the cross-sectional area were considered from the in-vivo estimated values for each fibre. The **third** sensitivity analysis was performed with respect to the cross-sectional area parameter, considering variations from 100% to 10% of the in-vivo estimated values with 10% step. During this sensitivity analysis, the reference length of each fibre was equal to the *in-vivo* estimated value, and the considered elastic modulus were the mean values reported in the literature.

Regarding the simulations of the drawer test, for each position along the passive flexion path, the pose of the femur was fixed in the global reference system and a total translation of 20 mm (Markolf et al., 1976; Piziali and Rastegar, 1977) was imposed to the tibia along the anterior-posterior tibial direction by steps of 0.1 mm. Other translations and any rotations were not allowed. The A/P component of the forces was estimated in order to calculate some parameters (Markolf et al., 1976; Markolf et al., 1978): laxity, anterior, posterior, and neutral stiffness, considered in several other studies concerning knee modelling (Wismans et al., 1980; Blankevoort et al., 1991b; Mommersteeg et al., 1996; Bendjaballah et al., 1998). Laxity has been defined as the tibial translation necessary to reach a specified level of A/P force, ± 100 N or ± 200 N (Markolf et al., 1978). Whereas, anterior and posterior stiffness were defined as the slope of the tangents to the A/P force restraint curve versus the A/P tibial displacement at ± 100 N (Markolf et al., 1976). The predicted mechanical parameters (i.e. laxity, anterior and posterior stiffness) were compared with experimental measurements reported in the literature (Markolf et al., 1976; Markolf et al., 1978; Markolf et al., 1981; Markolf et al., 1984; Shoemaker and Markolf, 1985).

Regarding the simulations of the axial stability test, for each position along the passive flexion path, a rotation of the tibia with respect to femur was imposed around the proximal-distal axis of the anatomical tibial reference system. A 90° of internal/external rotation was divided into 360 steps, starting from 45° of internal rotation to 45° of external rotation. All other degrees of freedom were locked. During these simulations, internal/external tibial torques were calculated around the proximal/distal axis of the anatomical reference system of the tibia.

Once the mechanical behaviour of the model was evaluated during the drawer and the axial stability tests, the devised cruciate ligaments model was employed in the evaluation of the biomechanic function provided by the cruciate ligaments during the execution of two daily activity, which were the **step up/down** and the **chair rising/sitting** motor tasks. The mechanical parameters considered during these simulations were: the *in-vivo* estimated reference length, the 100% NMR cross-setional area and the mean values of the elastic modulus, differently for each fibre bundle.

Moreover, during the execution of the step up/down motor task, a different definition of the elastic modulus parameter was also analysed in order to evaluate the effects introduced from the use of the simpler definition of this critical parameter in physiological conditions. As reported above, the simpler definition consisted in considering the same value of the elastic modulus, equal to 175 MPa, for all the fibres of both cruciate ligaments.

For each relative position between femur and tibia, which were calculated by means of the 3D fluoroscopy technique applied to the experimental measurements, the three components of the forces, anterior-posterior (A/P), proximal-distal (P/D) and medial-lateral (M/L) projections, and the magnitude of each fibre were calculated and exported for both cruciate ligaments.

The mechanical system, composed of the bones and the cruciate ligaments models, was implemented in ADAMS/View 2005 (MSC.Software Corporation 2 MacArthur Place Santa Ana,CA 92707 USA). All the post-processing was performed using the software Matlab 7 (The MathWorks, Inc, MA 01760-2098).

3.2 Results

i Drawer Test

As predictable, from the sensitivity analysis with respect to the **reference length**, underestimations of the reference length (-5%) produced larger A/P forces because of a faster recruitment of the fibres, whereas, overestimations of the reference length (+5%) produced smaller forces. As shown in Figure 3.4, estimations of the Laxity parameter were obtained and compared with the experimental results reported in the literature (Markolf et al., 1978; Markolf et al., 1981). At 20° of flexion, all variations of the reference length

produced Laxity values within the experimental range. At the full extension and at 90° of flexion, only overestimations of the reference length bigger than 1% produced Laxity values out of the experimental range. Thus, the devised model estimated Laxity in accordance with the literature when the reference length was obtained from the passive-flexion path of the selected subject. Predictions of anterior and posterior stiffness were less sensitive to variations of the reference length parameter and they were often close to the experimental mean values (Markolf et al., 1976; Markolf et al., 1978; Markolf et al., 1984).

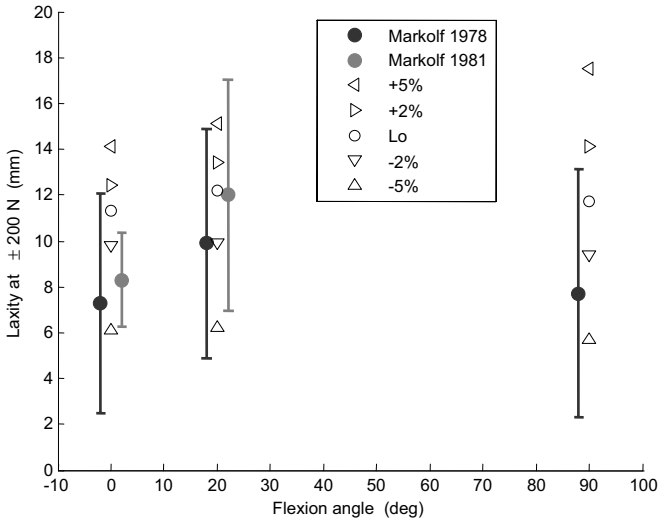

Figure 3.4: **Laxity** calculated at ±200N at different flexion angle and superimposed with the experimental data reported by Markolf et al. in 1978 and 1981. Mean values (*full dots*) plus and minus two standard deviations (*vertical bars*) were shown for experimental results.

Regarding the sensitivity analysis with respect to the **elastic modulus**, predictions of anterior and posterior stiffness were more sensitive than laxity ones. The anterior stiffness, see Figure 3.5, reached values quite similar to the experimental results at 90° of flexion, whereas at the full extension, the mean value of the predicted anterior stiffness was approximately three times bigger than the experimental means. At 20° of flexion, estimations were about twice as much. The smallest variability was obtained at 45° of flexion, and referring to it, at 20° and at 90° of flexion the variability was more than

twice as much, whereas at full extension was about six times bigger (Markolf et al., 1978; Markolf et al., 1984). Predictions of posterior stiffness, see Figure 3.6, were very similar to the experimental measurements (Markolf et al., 1978; Markolf et al., 1984). At full extension, the estimated mean value of the posterior stiffness was at the upper bound of the experimental 95% confidence interval, whereas at 20° of flexion, estimations were approximately twice as much as the experimental results. The trend of variability of the posterior stiffness was opposite of that of the anterior one. The smallest variability was obtained at full extension and at 90° of flexion. A little larger variability was obtained at 20° of flexion and the largest one was calculated at 45° of flexion.

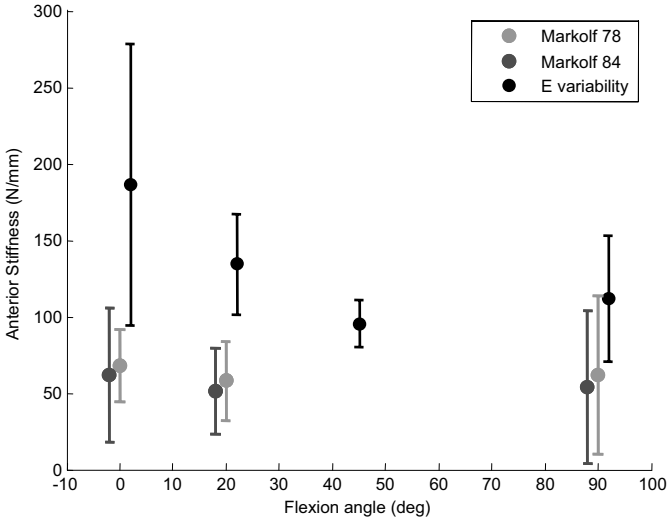

Figure 3.5: **Anterior Stiffness** calculated at different flexion angle and superimposed with the experimental data reported by Markolf et al. in 1978 and 1984. Mean values (*dots*) plus and minus two standard deviations (*vertical bars*) were shown in figure.

As already state, the Laxity parameter was less sensitive to variations of the elastic modulus. In fact, estimations of the Laxity obtained at ±200 N were 10.5 ± 0.4 mm at 20° of flexion and 5.7 ± 0.6 mm at 90°, which were quite close to the experimental measurements of 9.6 ± 2.1 and 7.4 ± 1.9 mm, respectively (Markolf et al., 1984), whereas at full extension, the estimated

Laxity, 12.1 ± 0.5 mm, was a slightly bigger than the experimental one, 7.7 ± 2.3 mm (Markolf et al., 1984).

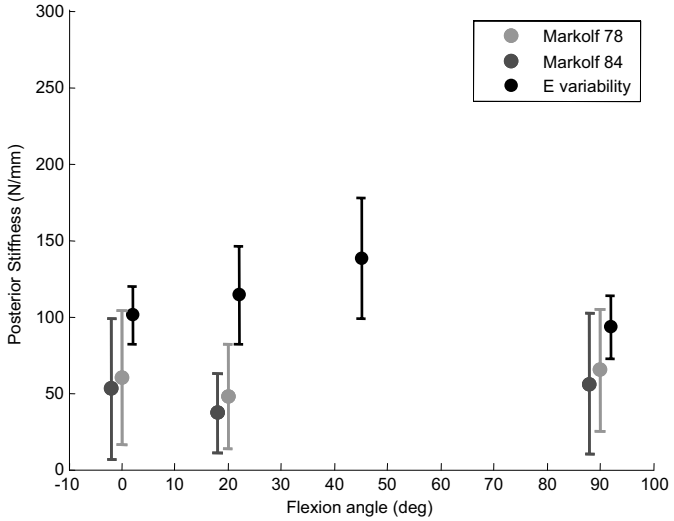

Figure 3.6: **Posterior Stiffness** calculated at different flexion angle and superimposed with the experimental data reported by Markolf et al. in 1978 and 1984. Mean values (*dots*) plus and minus two standard deviations (*vertical bars*) were shown in figure.

Regarding the sensitivity analysis of the model with respect to the **cross-sectional area**, see Figure 3.7, predictions of laxity, calculated at ±100 N of A/P forces, followed the experimental behaviour only beyond 20° of flexion. At the full extension, an overestimation of the parameter was recognized. Prediction of laxity, obtained considering 30% of the in-vivo cross-sectional area, was the closest to the experimental results (Markolf et al., 1978; Markolf et al., 1981; Shoemaker and Markolf, 1985). Smaller values of the cross-sectional area produced significantly larger estimations of the laxity, whereas larger values produced estimations negligibly smaller. The neutral stiffness parameter was very sensitive to flexion angle variations. However, for the firsts 45° degrees of flexion, all the simulated conditions produced results within the experimental range along with a very small sensitivity in the first 30° of flexion (Markolf et al., 1976; Markolf et al., 1981). Whereas, over 45° of flexion, predictions of the neutral stiffness were more and more distant from each other, demonstrating that the sensitivity of this parameter

significantly increased beyond the 45° of flexion. Nevertheless, the 20-30% cross-sectional area condition produced a very good fitting of the experimental measurements at every flexion angle. A similar behaviour was observed for the posterior stiffness, and also in this case, the predictions obtained with the 20-40% of the cross-sectional area were very close to the experimental mean values (Markolf et al., 1981; Markolf et al., 1984). Predictions of the anterior stiffness parameter were not so sensitive with respect to the flexion angle, and predictions, obtained with the 20-30% of the cross-sectional area, produced results very close to the experimental measurements (Markolf et al., 1981; Markolf et al., 1984).

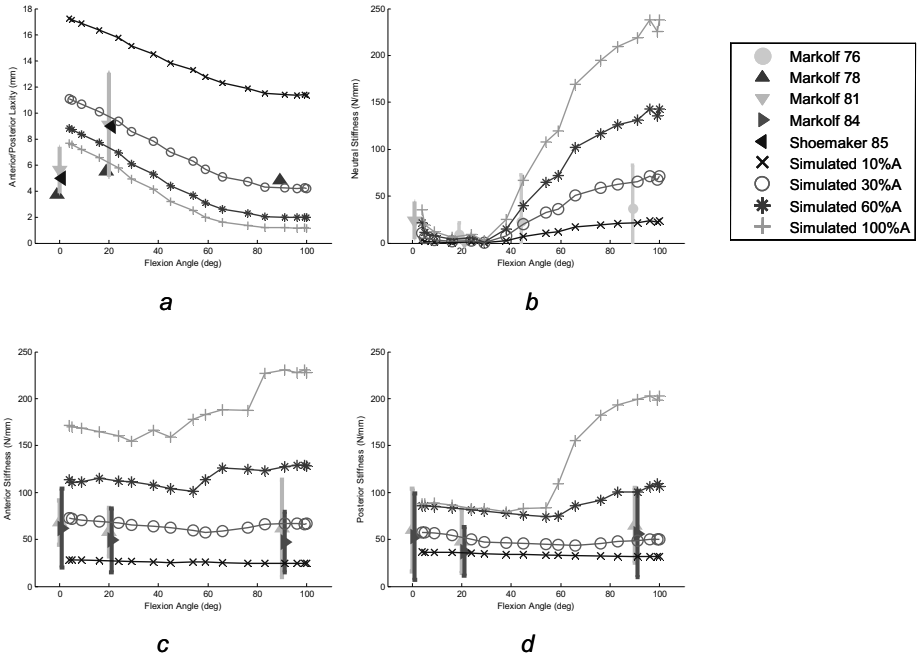

Figure 3.7: Laxity calculated at ±100N (a), Neutral Stiffness (b), Anterior Stiffness (c) and Posterior Stiffness (d) calculated considering 30% (o), 60% (*) and 100% (+) of the in-vivo estimated cross-sectional area value versus flexion angle. Predictions compared with the experimental measurements reported by Markolf et. al (Markolf et al., 1976; Markolf et al., 1978; Markolf et al., 1981; Markolf et al., 1984; Shoemaker and Markolf, 1985).

ii Axial Test

During the simulations of the internal/external axial rotations, no significant torques were obtained for external rotations, at each flexion angle for each of the three sensitivity analyses. Moreover, exception made for the full extension, no ACL contribution was ever recognized. The axial torques, obtained during the three sensitivity analyses, showed always the same global behaviour, see Figure 3.8. At full extension, the ACL produced an internal torque from 0° to 10° of internal rotation, which became an external torque from 10° to about 20° of internal rotation. This curve extended also in the first 20° of external rotation providing negligible torques. Anyway, this contribution of the ACL was negligible both for internal and for external rotations.

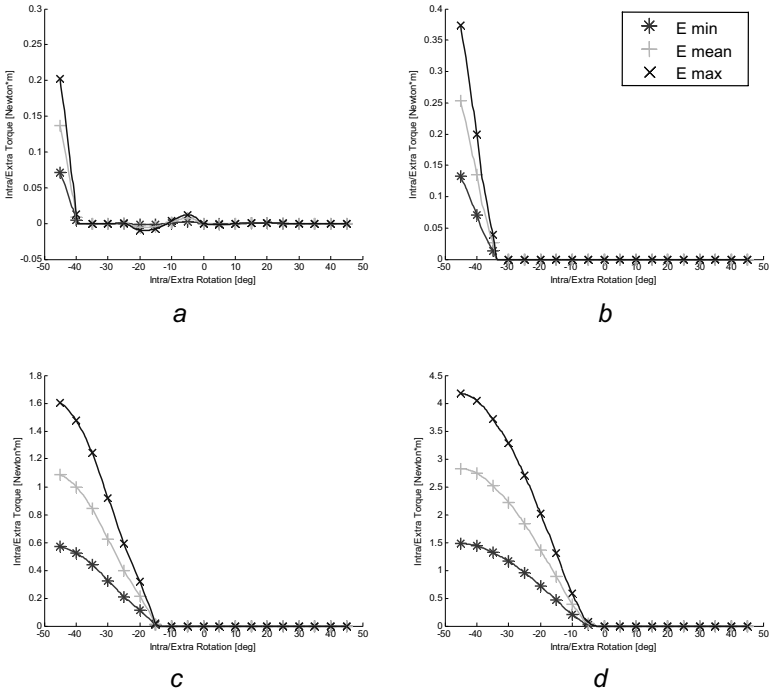

Figure 3.8: Internal/external tibial torque versus internal/external axial rotation drawn at 0° (*a*), 10° (*b*), 25° (*c*) and 45° (*d*) of flexion. Three curves were plotted considering different elastic modulus values: mean value (+), mean value minus one standard deviation (*) and mean value plus one standard deviation (x) (Butler et al., 1992; Race and Amis, 1994).

Considering the contribution of the PCL, at full extension, it began to produce internal torque only over the 40° of internal rotation (a totally un-physiological torsion). At about 10° of flexion, the contribution of the ACL disappeared and the PCL was recruited already at about 30° of internal rotation. At about 25° of flexion, the PCL was recruited at 15° of internal rotation and its contribution was almost linear until 30° of internal rotation, then it appeared like a quadratic curve. At 45° and at 90° of flexion, this behaviour was similar: the PCL was already recruited at only a few degrees of internal rotation and at the boundaries of the curves an almost quadratic behaviour was observed.

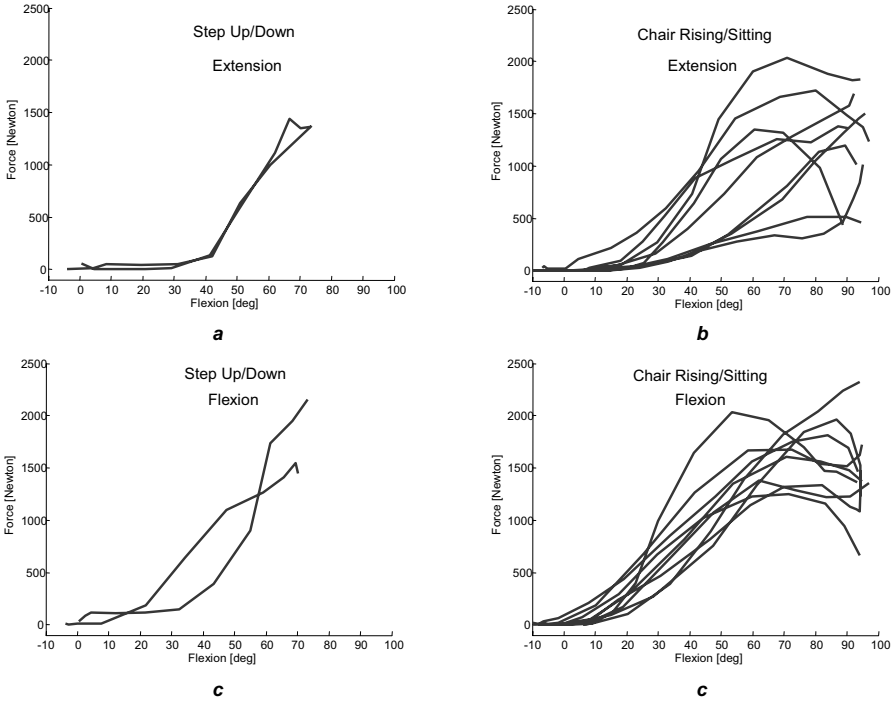

Figure 3.9: Anterior/posterior component forces provided by PCL versus the knee flexion angle: two repetitions of extension (A) and flexion (C) motions during step up/down motor task, nine repetitions of extension (B) and flexion (D) motions during chair rising/sitting motor task.

iii Daily Living Activities

Regarding the forces calculated during the simulations of the **chair rising/sitting** motor task, the global qualitative behaviour of the PCL was very similar along the three anatomical directions, in particular considering the extension movements. In the A/P (Figure 3.9-*b,d*) and in the P/D components, similar and larger forces, respectively, were always reached than those reached along the M/L direction. The mechanical contribution of the posterior cruciate ligament, during both extension and flexion motions, showed small force from full extension to 10°-20° of flexion. Increasing the flexion angle, forces increased almost linearly until a force plateau at about 50°-70° of flexion was reached. In some repetitions of the chair rising/sitting motor task, a little decrease of force was observed for higher flexion angles. In the A/P and in the P/D components, a larger variability was recognized during extension motions (Figure 3.9-*b*) with respect to the flexion motions (Figure 3.9-*d*). A similar variability was obtained in the M/L force component of the posterior cruciate ligament. During the chair rising/sitting motor task, negligible forces were obtained for the ACL, for both extension and flexion motions and along any anatomical directions.

Regarding the forces calculated during the simulations of the **step up/down** motor task, the global qualitative behaviour of the PCL was very similar along the three anatomical directions, in particular considering the extension movements. In the A/P (Figure 3.9-*a,c*) and in the M/L components, similar and larger forces, respectively, were always reached than those reached in the P/D direction. In fact, in the A/P and the M/L direction, the maximum forces reached were three times bigger than those reached in the P/D direction during the extension movements, and over five times bigger during the flexion movements. In the extension movements (Figure 3.9-*a*) the mechanical contribution of the posterior cruciate ligament was very small from the full extension to about 30°-40° of flexion. Then a rapid and quite linear increase of its contribution was observed until the maximum force was reached at about 70° of flexion. The behaviour of the two flexion movements (Figure 3.9-*c*) was different with respect to each other, in particular along the P/D direction. As during the extension movements, also in this case, very little forces were expressed from the full extension to about 20°-40° of flexion. Over this flexion angle, both two

curves showed an increasing of their contribution until reaching maximum forces larger than those calculated in the extension movements. Regarding the ACL the results obtained, also during simulations of the step up/down motor task null forces were always obtained, along every anatomical directions.

Moreover, considering the forces of the PCL obtained using the two different definitions of the elastic modulus, the global behaviour did not change and very little differences were obtained. In fact, as visible in Figure 3.10, the distance between the two estimations increased with the flexion angle, reaching its maximum value, about 180 N (7.2 %), during a flexion movement at the maximum flexion angle.

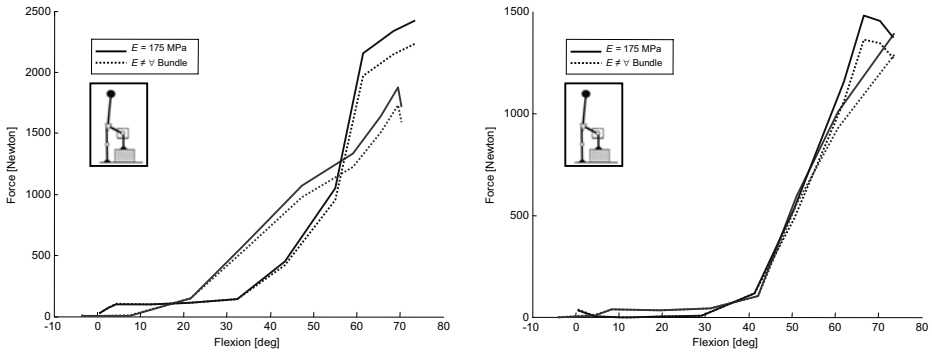

Figure 3.10: Medial/lateral component forces provided by the posterior cruciate ligament versus the knee flexion angle: two repetitions of extension (*left*) and flexion (*right*) motions during step up/down motor task evaluated using the two definitions of the Elastic Modulus parameter.

3.3 Discussion

In the present work, a quasi-static model of the cruciate ligaments was implemented using bony geometries and kinematic data acquired from a selected living and healthy subject. Each cruciate ligament was modelled taking the anatomical twist of the fibres into account. In the first part of the study, the sensitivity of the model with respect to the mechanical parameters of the cruciate ligaments was evaluated simulating the drawer test (A/P tibial translations), and then simulating the axial stability test (I/E tibial rotations).

Three sensitivity analyses were performed with respect to: the reference length, the elastic modulus, and the cross-sectional area of each fibre of both cruciate ligaments. In the second part of the study, the devised model was employed to evaluate the cruciate ligaments force during the execution of daily living activities performed by the same selected subject, such as the step up/down and the chair rising/sitting motor tasks.

Considering the sensitivity analyses, as predictable, the mechanical effects introduced by variations of the reference length parameter influenced more the laxity parameter than the anterior and the posterior stiffness, on the other hand, variations of the elastic modulus influenced more the prediction of the anterior and the posterior stiffness than the laxity. In general, the laxity fitted the experimental results reported in the literature very well (Figure 3.4), and variations of ±5 % of the *in-vivo* estimated reference length produced prediction of the laxity often inside of the experimental range (Markolf et al., 1978; Markolf et al., 1981). Regarding the sensitivity of the model to the elastic modulus variations, see Figure 3.5 and Figure 3.6, the comparison between the predicted and the experimental laxity was very good, in particular at large flexion angles. The anterior and the posterior stiffness were usually larger than the experimental measurements. In particular, at the full extension, the anterior stiffness was almost three times larger than the experimental measurements. These overestimations were associated to an overestimation of the cross-sectional area parameter, according to anatomical observations (Harner et al., 1999). In fact, regarding the sensitivity analysis with respect to the cross-sectional area, the percentage of the *in-vivo* estimated value of cross-sectional area, which produced best fittings with the literature (Markolf et al., 1976; Markolf et al., 1978; Markolf et al., 1981; Markolf et al., 1984; Shoemaker and Markolf, 1985), resulted to be included in the range from 20% to 40% (Figure 3.7). Thus, accordingly to Harner (Harner et al., 1999), which reported that the mid-substance cross-sectional area of the cruciates should be at least three times lower than the ligament insertion area, the 30% of the *in-vivo* cross-sectional area, which was estimated as the mean value between the two insertion areas, resulted to be considered as a reliable estimation of the actual value which should be considered as cruciate ligament parameter.

Regarding the simulations of the axial stability test, example in Figure 3.8, the three sensitivity analyses (reference length, elastic modulus and

cross-sectional area) reported no significant information, exception made for the fact that, it was verified that cruciate ligaments provided no torques for external rotations, which tended to untwist themselves. It was also observed that, at the full extension, a significant overlapping of the ligament fibres of the two cruciates appeared at about 20-25° of internal rotation. Since the wrapping of the ligament fibres was not considered in the model, the estimation of the tibial axial torque for larger internal rotations could not be considered reliable. However, this limit for internal rotation was recognized as compatible with the active rotation ranges reported in the literature for daily living activities (Kandel and Kapandji, 1988), for the analysis of which the proposed model was devised, limiting its computational weight.

Considering the simulations of the two considered living activities, the total inactivity of the anterior cruciate ligament was probably due to the typology of the two movements that tended to slack the anterior cruciate and to stretch the posterior cruciate ligament (Zavatsky and O'Connor, 1993). Regarding the contribution of posterior cruciate ligament during the step up/down motor task, the greater repeatability obtained in the step up movement (Figure 3.9 and Figure 3.10) was probably due to a major activity of the muscles for controlling the movement. These had a goal to perform the movement against the gravity force and their concentric contractions were more controlled by the nervous system. On the other hand, the step down phase was a movement in accordance with the gravity force, and thus the eccentric contraction of the muscles was less controlled, and a minor repeatability is obtained (Figure 3.9 and Figure 3.10). Moreover, the largest anatomical force components were obtained along the A/P and the M/L directions, where the largest contribution to the stabilization function of the knee joint was necessary. On the contrary, regarding the chair rising/sitting motor task, smaller M/L components of the posterior cruciate ligament force were calculated than those obtained during the step up/down motor task. This can be explained considering the characteristics of the motor task, which was performed using both the two legs, and thus a smaller stabilization contribution, in particular in the M/L direction, was required to the posterior cruciate ligament. The greater variability, obtained in the chair rising movement (Figure 3.9), was probably due to the fact that the subject, to overcome the force of gravity, used a rapid movement of the trunk versus the anterior direction, in order to obtain an inertial component helpful for

beginning the movement, but generating a less control of the muscular activity against the gravity by nervous system. Thus, in both the considered motor tasks, predictions according to physiology are obtained. In fact, in this kind of motor task, the stabilizing role of the anterior cruciate ligament was always substituted by the muscular activity, whereas the posterior cruciate ligament contributed to stabilize the knee joint more and more with the increasing flexion angle, in particular at about 60°-70° degrees of flexion, position in which the mechanism spine-cam of knee prostheses is usually recruited.

3.4 Conclusions

In the literature of the knee modelling, several approaches at different level of complexity were developed. Early 2D models of the knee joint were principally aimed to the evaluation of the knee kinematics and to the function of anatomical structures, such as ligaments, in the sagittal plane (Goodfellow and O'Connor, 1978; Moeinzadeh et al., 1983; Shelburne and Pandy, 1997; Zavatsky and O'Connor, 1992b; Zavatsky and O'Connor, 1992a; Zavatsky and O'Connor, 1993). Nevertheless, these models were restricted because of their inability to investigate motions and forces potentially significant which occur out of the sagittal plane, such as internal/external and ab/adduction rotations. Thus, 3D, more complex, and anatomically comprehensive models of the knee joint were also proposed in the literature (Blankevoort et al., 1991b; Fernandez and Pandy, 2006; Moglo and Shirazi-Adl, 2005; Mommersteeg et al., 1997; Wismans et al., 1980). Nevertheless, the development of more complex models produced the necessity of a large number of parameters in order to anatomically describe and mechanically characterize the model in a reliable manner. Thus, researchers considered these parameters from both experimental measurements and from data reported in the literature. This approach resulted useful in order to understand qualitatively the function of several anatomical structures, also during the daily living activities (Piazza and Delp, 2001). Nevertheless, even if a model is designed properly for a specific application, its potential can be invalidated by the errors due to inaccurate parameter definitions. Indeed, this kind of error is often due to disagreement in the origin of the parameters and inputs, considered from

different and non-homogeneous sources. In order to limit this kind of errors, the authors proposed in the case study a methodology to model the cruciate ligaments of a human healthy subject, which permit to evaluate forces in the cruciates during the execution of daily living activities.

Thus, a 3D quasi-static model of the cruciate ligaments of the human knee joint was developed, assuming as foundations of the proposed methodology the measurements of the subject-specific anatomical geometries and of the in-vivo kinematic data. Special attention was paid to the geometrical and the mechanical parameters of the cruciate ligaments. The cross-sectional area and the reference length were estimated by means of subject-specific nuclear magnetic resonance (NMR) and 3D video-fluoroscopy, respectively. Moreover, in this study, the problem of the measurement or the estimation of the elastic modulus of the cruciate ligaments was proposed. Indeed, the elastic modulus of the soft tissues, like cruciate ligaments, is a critical parameter to evaluate, even by means of direct in-vitro measurements. Thus, since a subject-specific elastic modulus evaluation could not be obtained in in-vivo conditions, experimental measurements reported in the literature were considered to set the parameters of the model (Butler et al., 1992; Race and Amis, 1994). Finally, the mechanical behaviour of the devised model was evaluated during the simulation of the drawer test (A/P tibial translations) and the axial stability test (I/E tibial rotations). Moreover, the model was employed in order to predict the forces of the cruciate ligaments during the execution of two daily living activities, performed by the same selected healthy subject.

This work was intended as evaluation of the reliability of the devised methodology, including both experimental measurements and data processing. Although the devised model was simpler than other models presented in the literature (Blankevoort et al., 1991b; Moglo and Shirazi-Adl, 2005; Mommersteeg et al., 1997; Wismans et al., 1980), good comparison with the experimental data reported in the literature and physiologically meaningful predictions were obtained. Indeed, if we consider the difficulty to characterize soft tissues, as demonstrated by the dispersion of the experimental data reported in the literature, a more complex model would not necessarily imply more precise estimations. In this way, the hypothesis, which stated to use linear-elastic mechanical-properties for each ligament fibre, seems to be not so wrong. Even more true, if the target of the

study is to investigate a living subject without any invasive mechanical-measurement.

In conclusion, some of the future developments of this research, see relative chapter, consist in the acquisitions of a set of living subjects in order to increase the reliability of the proposed methodology. In addition, all the selected subjects will be acquired with a new mechanical apparatus (*arthrometer*) appositely designed in order to: i) record synchronously forces and torques imposed manually to the tibia, by means of a 6-axis load cell, and the bony kinematics, by means of the video-fluoroscopy; ii) estimate the elastic modulus on a living subject. The first point will give us the ability to validate the proposed model exploiting experimental measurements which comes all from the same living subject, whereas the second point will give the model the actual subject-specificity.

3.5 References

Bendjaballah, M. Z., Shirazi-Adl, A., Zukor, D. J., (1998). Biomechanical response of the passive human knee joint under anterior-posterior forces. Clin.Biomech.(Bristol., Avon.) 13**,** 625-633.

Bertozzi, L., Stagni, R., Fantozzi, S., Cappello, A., (2006a). Estimation of knee cruciate loads during living activities: Step up/down and chair rising/sitting motor tasks. Gait & Posture 24**,** S31-S32.

Bertozzi, L., Stagni, R., Fantozzi, S., Cappello, A., (2006b). Evaluation of the elastic modulus variations in a subject-specific knee model using the drawer test. Journal of Biomechanics 39(s1)**,** s69-s70.

Bertozzi, L., Stagni, R., Fantozzi, S., Cappello, A., (2007a). Evaluation of a cruciate-ligament model: sensitivity to the parameters during drawer-test simulation. Journal of Applied Biomechanics In Press..

Bertozzi, L., Stagni, R., Fantozzi, S., Cappello, A., (2007c). Knee model sensitivity to cruciate ligaments parameters: a stability simulation study for a living subject. Journal of Biomechanics 40(S1)**,** 38-44.

Bertozzi, L., Stagni, R., Fantozzi, S., Cappello, A., (2008). Biomechanical Modeling with In-Vivo Data. In: Cai, Y. (Ed.), Digital Humans, The State of the Art Survey. Springer.

Bertozzi, L., Stagni, R., Fantozzi, S., Cappello, A., (2007b). Knee model sensitivity to cruciate ligaments parameters: A stability simulation study for a living subject. Journal of Biomechanics 40(S1)**,** 38-44.

Bertozzi, L., Stagni, R., Fantozzi, S., Cappello, A., (2006c). Investigation of the Biomechanic Function of Cruciate Ligaments Using Kinematics and Geometries from a Living Subject During Step Up/Down Motor Task. Spring Verlag Lectures Note in Computer Science 3994**,** 831-838.

Bertozzi, L., Stagni, R., Fantozzi, S., Lannocca, M., Cappello, A., (2005). A 3D quasi-static model to investigate biomechanic function of the knee cruciate ligaments using subject specific geometry and kinematic data.

Blankevoort, L., Huiskes, R., (1996). Validation of a three-dimensional model of the knee. Journal of Biomechanics 29**,** 955-961.

Blankevoort, L., Huiskes, R., de, L. A., (1991a). Recruitment of knee joint ligaments. Journal of Biomechanical Engineering 113**,** 94-103.

Blankevoort, L., Kuiper, J. H., Huiskes, R., Grootenboer, H. J., (1991b). Articular contact in a three-dimensional model of the knee. J.Biomech. 24**,** 1019-1031.

Bookstein, F. L., (1989). Principal Warps: Thin-Plate Splines and the Decomposition of Deformations. IEEE Transactions on Pattern Analysis and Machine Intelligence 11**,** 567-585.

Butler, D. L., Guan, Y., Kay, M. D., Cummings, J. F., Feder, S. M., Levy, M. S., (1992). Location-dependent variations in the material properties of the anterior cruciate ligament. Journal of Biomechanics 25**,** 511-518.

Corazza, F., Stagni, R., Castelli, V. P., Leardini, A., (2005). Articular contact at the tibiotalar joint in passive flexion. Journal of Biomechanics 38**,** 1205-1212.

Fernandez, J. W., Pandy, M. G., (2006). Integrating modelling and experiments to assess dynamic musculoskeletal function in humans. Experimental Physiology 91**,** 371-382.

Fregly, B. J., Rahman, H. A., Banks, S. A., (2005). Theoretical accuracy of model-based shape matching for measuring natural knee kinematics with single-plane fluoroscopy. Journal of Biomechanical Engineering 127**,** 692-699.

Fung, Y. C., (1994). A first course in continuum mechanics. Englewood Cliffs, N.J., Prentice-Hall, Inc..

Goldstein, H., Poole, C. P., Safko, J. L., (2002). Classical Mechanics. Addison Wesley.

Goodfellow, J., O'Connor, J., (1978). The mechanics of the knee and prosthesis design. Journal of Bone and Joint Surgery - British Volume 60-B**,** 358-369.

Grood, E. S., Suntay, W. J., (1983). A joint coordinate system for the clinical description of three-dimensional motions: application to the knee. Journal of Biomedical Engineering 105**,** 136-144.

Harner, C. D., Baek, G. H., Vogrin, T. M., Carlin, G. J., Kashiwaguchi, S., Woo, S. L., (1999). Quantitative analysis of human cruciate ligament insertions. Arthroscopy 15**,** 741-749.

Kandel, M. J., Kapandji, I. A., (1988). The Physiology of the Joints: Lower Limb, Volume 2. Churchill Livingstone.

Li, G., Gil, J., Kanamori, A., Woo, S. L., (1999). A validated three-dimensional computational model of a human knee joint. Journal of Biomechanical Engineering 121**,** 657-662.

Markolf, K. L., Bargar, W. L., Shoemaker, S. C., Amstutz, H. C., (1981). The role of joint load in knee stability. Journal of Bone and Joint Surgery - American Volume 63**,** 570-585.

Markolf, K. L., Graff-Radford, A., Amstutz, H. C., (1978). In vivo knee stability. A quantitative assessment using an instrumented clinical testing apparatus. Journal of Bone and Joint Surgery - American Volume 60**,** 664-674.

Markolf, K. L., Kochan, A., Amstutz, H. C., (1984). Measurement of knee stiffness and laxity in patients with documented absence of the anterior cruciate ligament. Journal of Bone and Joint Surgery - American Volume 66**,** 242-252.

Markolf, K. L., Mensch, J. S., Amstutz, H. C., (1976). Stiffness and laxity of the knee--the contributions of the supporting structures. A quantitative in vitro study. Journal of Bone and Joint Surgery - American Volume 58**,** 583-594.

Moeinzadeh, M. H., Engin, A. E., Akkas, N., (1983). Two-dimensional dynamic modelling of human knee joint. Journal of Biomechanics 16**,** 253-264.

Moglo, K. E., Shirazi-Adl, A., (2005). Cruciate coupling and screw-home mechanism in passive knee joint during extension--flexion. Journal of Biomechanics 38**,** 1075-1083.

Mommersteeg, T. J., Huiskes, R., Blankevoort, L., Kooloos, J. G., Kauer, J. M., (1997). An inverse dynamics modeling approach to determine the restraining function of human knee ligament bundles. Journal of Biomechanics 30**,** 139-146.

Mommersteeg, T. J., Huiskes, R., Blankevoort, L., Kooloos, J. G., Kauer, J. M., Maathuis, P. G., (1996). A global verification study of a quasi-static knee model with multi-bundle ligaments. Journal of Biomechanics 29**,** 1659-1664.

Moro-oka, T. A., Hamai, S., Miura, H., Shimoto, T., Higaki, H., Fregly, B. J., Iwamoto, Y., Banks, S. A., (2007). Can magnetic resonance imaging-derived bone models be used for accurate motion measurement with single-plane three-dimensional shape registration? Journal of Orthopaedic Research 25**,** 867-872.

Piazza, S. J., Delp, S. L., (2001). Three-dimensional dynamic simulation of total knee replacement motion during a step-up task. Journal of Biomedical Engineering 123**,** 599-606.

Piziali, R. L., Rastegar, J. C., (1977). Measurement of the nonlinear, coupled stiffness characteristics of the human knee. Journal of Biomechanics 10**,** 45-51.

Race, A., Amis, A. A., (1994). The mechanical properties of the two bundles of the human posterior cruciate ligament. Journal of Biomechanics 27**,** 13-24.

Shelburne, K. B., Pandy, M. G., (1997). A musculoskeletal model of the knee for evaluating ligament forces during isometric contractions. Journal of Biomechanics 30**,** 163-176.

Shoemaker, S. C., Markolf, K. L., (1985). Effects of joint load on the stiffness and laxity of ligament-deficient knees. An in vitro study of the anterior cruciate and medial collateral ligaments. Journal of Bone and Joint Surgery - American Volume 67**,** 136-146.

Stagni, R., Fantozzi, S., Davinelli, M., Lannocca, M., (2004). Comparison of knee cruciate ligaments models using kinematics from a living subject during chair rising-sitting. Spring Verlag Lectures Note in Computer Science 3036**,** 1073-1080.

Stagni, R., Fantozzi, S., Lannocca, M., Bertozzi, L., Cappello, A., (2005). Estimation of knee ligaments loads using the modelling approach applied on in-vivo accurate kinematics and morphology of a young subject. WIT Transactions on Biomedicine and Health 8**,** 391-399.

Wismans, J., Veldpaus, F., Janssen, J., Huson, A., Struben, P., (1980). A three-dimensional mathematical model of the knee-joint. Journal of Biomechanics 13**,** 677-685.

Zavatsky, A. B., O'Connor, J. J., (1993). Ligament forces at the knee during isometric quadriceps contractions. Proceedings of the Institution of Mechanical Engineers - Part H 207**,** 7-18.

Zavatsky, A. B., O'Connor, J. J., (1992a). A model of human knee ligaments in the sagittal plane. Part 1: Response to passive flexion. Proceedings of the Institution of Mechanical Engineers - Part H 206**,** 125-134.

Zavatsky, A. B., O'Connor, J. J., (1992b). A model of human knee ligaments in the sagittal plane. Part 2: Fibre recruitment under load. Proceedings of the Institution of Mechanical Engineers - Part H 206**,** 135-145.

Zuffi, S., Leardini, A., Catani, F., Fantozzi, S., Cappello, A., (1999). A model-based method for the reconstruction of total knee replacement kinematics. IEEE Transactions on Medical Imaging 18**,** 981-991.

Chapter 4: Model of Tibio-Femoral Contact

- Casaletto A., et. al. 2007, Tesi di Laurea Spec. in Ing. Biomedica, Cesena.
- Bertozzi L., et.al. 2007, In Proc. SIAMOC 2007.

In this chapter, the problem of the evaluation of the tibio-femoral contact was addressed using two different approaches. The first one employed the *thin plate splines* tool (TPS) to mathematically describe the articular surfaces of the femur, whereas the second one used the Distance Transform to represent, in the nearby space, the proximity from each tibial plateau. Both these approaches were implemented using subject-specific data experimentally acquired from a selected healthy subject.

Before presenting how this problem was handled, an important observation has to be done. As already stated, in this chapter, the problem of the tibio-femoral contact was approached. Nevertheless, viewing as the problem was dealt with the term 'contact' could be misleading. In fact, as already reported in Chapter 2 (paragraph 2.4.ii), in both devised approaches, an actual material contact, meant as a null distance between the surfaces of two bodies (i.e. femoral and tibial articulating surfaces), never occurred. This resulted from modelling the articular contact as passive contribution obtained by the bony geometries (i.e. not cartilaginous) moved accordingly of the subject-specific bony kinematics.

The two devised approaches were based on the use of specific data from a living selected subject and since the input of the model were the bony geometries and kinematics, the 'contact' was defined as the condition which occur when two objects, in this case the femur and the tibia, were closer than a threshold distance. Thus, in all this chapter, the evaluation of the tibio-femoral 'contact' was performed by means of the calculus of the **proximity** between the geometries of the femur and the tibia posed in the space according to the specific kinematics acquired from the subject. Once the proximity between the femur and the tibia was calculated, indicator values of the contact point and of the contact area were estimated. These indicators were then analyzed in function of different values of the threshold length, of the density of the TPS grid, and of experimental conditions, such as with and without the body weight.

4.1 Materials and Methods

i Subject, Experimental Acquisitions, Data Reconstruction

The selected subject to evaluate the tibio-femoral contact was the same described in the chapter focused on the modelling on the cruciate ligaments. Briefly, the selected subject was acquired both with the NMR and the video-fluoroscopy. Using the software Amira, the 3D geometries of the distal femur and the proximal tibia were reconstructed from the NMR images. Whereas, the bony kinematics were reconstructed using an iterative procedure which exploited both geometrical models of the bony geometries and the video-fluoroscopic images acquired during the execution of daily living activities performed by the same selected subject.

4.2 Thin Plate Splines for Static Evaluations of Proximity

The TPS tool was originally introduced into medical image analysis by Bookstein (Bookstein F.L., 1989). It was then applied in several fields, such as automatic multimodality image fusion (Meyer et al., 1997), tissue deformations (Amini et al., 1998), joint surface modeling (Boyd et al., 1999), and ventricular motion reconstruction (Suter and Chen, 2000).

In this study, the TPS method was used as mathematical tool for interpolating the experimental data which represent the articular surfaces (Boyd et al., 1999). This allowed to exploit the analytical features of the mathematical description of the surfaces in the evaluation of the tibio-femoral contact in the living subject (Bookstein F.L., 1989; Boyd et al., 1999; Corazza et al., 2005).

i Preliminary Elaborations of the Experimental Data

The 3D geometries of the femur and the tibia, already used for the reconstruction of the bony kinematics and the modeling of the cruciate ligaments, were elaborated in order to reduce the number of the points to be considered. Since the TPS method produces artifacts if applied to a set bigger than 2000 experimental points (Boyd et al., 1999), this reduction of the number of points was needed since the original bony geometries produced by Amira were composed by more than 60000 and 90000 vertexes for the femur and the tibia-fibula, respectively. The method used to

performed this reduction was to select the points of the original geometries which lay at the quotes relative to NMR images, one every 3 mm along the proximal-distal axis of the NMR reference system. Actually, the selected the points were included inside a little stripe defined from the value of each quote plus and minus a threshold of 0.25 mm. Then, the more proximal points of the femur, the more distal points of the tibia and all points of the fibula were deleted in order to further reduce the number of the experimental points to be considered with the TPS method. Finally, as input to the TPS method were selected about 140 and about 200 points to describe the lateral and medial condyle of the femur, respectively, and about 150 and about 345 points to describe the lateral and medial plateau of the tibia, respectively.

From the selected points of each tibial plateau, the moment of inertia and its principal axes were calculated as described in Eq. (4.1) and Eq. (4.2). The approximating plane of each tibial plateau was defined from the minimum and the medium principal axes of the moment of inertia. The Root Mean Square Error (RMSE) obtained by the approximation of the experimental tibial points with the tibial planes was equal to 1.2 mm for the lateral side and 1.7 mm for the medial one.

ii Using TPS to Describe Bony Surfaces

From the selected points of each of the two femoral condyles, the moment of inertia was calculated as follows:

$$I = \sum_{i=1}^{N} m_i \begin{bmatrix} \left(y_i^2 + z_i^2\right) & -x_i y_i & -x_i z_i \\ -x_i y_i & \left(x_i^2 + z_i^2\right) & -y_i z_i \\ -x_i z_i & -y_i z_i & \left(x_i^2 + y_i^2\right) \end{bmatrix} \tag{4.1}$$

where the experimental points were equally weighted. Since the moment of inertia tensor is real and symmetric, it is possible to find a Cartesian coordinate system in which it is diagonal, having the form

$$I = \begin{bmatrix} I_1 & 0 & 0 \\ 0 & I_2 & 0 \\ 0 & 0 & I_3 \end{bmatrix} \tag{4.2}$$

where the coordinate axes are called the *principal axes* and the constants I_1, I_2 and I_3 are called the *principal moments of inertia* and increasingly

arranged $I_1 \le I_2 \le I_3$. The first and the second principal axes (i.e. those relative to I_1 and I_2) were considered in order to define the x and y axes, respectively, of the local reference system. The points were then projected on the xy plane and the rectangular region R was defined in order to bound all these projected points, see Figure 4.1. The region D, which is the shape including all the projected points on the xy plane, was defined by means of the use of the convex hull algorithm (Barber et al., 1996). The region R was divided into a M x M grid of Δx x Δy rectangular elements with nodes coordinates $(\overline{x}_i, \overline{y}_i)$ where the values of Δx and Δy were defined several times in order to evaluate the sensitivity of the model to the parameter M, which was considered from 20 to 100 with step 20.

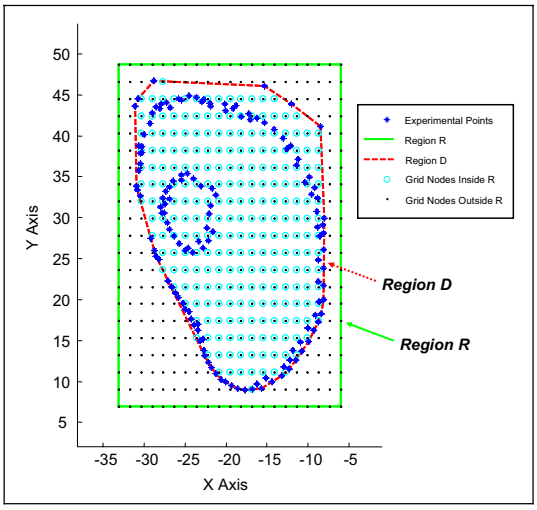

Figure 4.1: Experimental points of the lateral condyle projected on the xy plane (*blu asterisks*). The region R (*green rectangle*), region D (*red dashed line*), grid nodes inside and outside the region D (*azure circles* and *little black dots*, respectively) are depicted.

For each of the two femoral condyle, described from a could of points with coordinates (x_i, y_i), a Thin Plate Spline (TPS) representation was calculated (Figure 4.2) considering the following form.

$$z = S(x, y) = \sum_{i=1}^{n} C_i f_i(x_i, y_i) + C_{n+1} + C_{n+2} x + C_{n+3} y \tag{4.3}$$

where n is the number of the experimental points, (x_i, y_i) are their relevant projections on the xy plane, C_i are the coefficients of the surface, and the

functions f_i are translations of radial function $r^2 \ln(r)$ to the data sites (x_i, y_i). Thus,

$$\Phi(r) = f_i(x, y) = r_i^2 \ln(r_i + \varepsilon) \tag{4.4}$$

where ε is a positive infinitesimal value and with

$$r_i^2 = (x - x_i)^2 + (y - y_i)^2 \tag{4.5}$$

Without the quantity ε, f_i would be indeterminate at (x_i, y_i). This makes the f_i functions and their first partial derivatives continuous, but the second partial derivatives are discontinuous at the data sites (x_i, y_i).

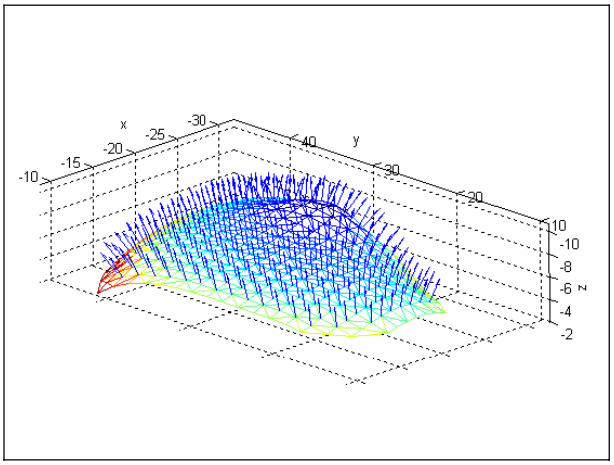

Figure 4.2: Final form of the TSP of the lateral condyle (*colored mesh*) with outgoing normals calculated at grid nodes (*blue arrows*).

As reported by Boyd (Boyd et al., 1999), the *n+3* coefficients in the function S are only partially determined by the n interpolation conditions $z_i = S(x_i, y_i)$, $i = 1, \ldots, n$. Thus, an additional polynomial precision condition is that if the points (x_i, y_i, z_i) lie on a plane, then $S(x, y)$ reduces to the equation of the plane by virtue of the vanishing of the coefficients C_i, $i = 1, \ldots, n$. It is convenient to use matrix notation to describe $S(x, y)$ and the method for determining its coefficients

$$S(x, y) = \mathbf{f}\mathbf{c}^T \tag{4.6}$$

where $\mathbf{f} = [f_1(x, y), \ldots, f_n(x, y), 1, x, y]$ and $\mathbf{c} = [C_1, \ldots, C_{n+3}]$.
The interpolation and the polynomial precision condition imply that the coefficient vector **c** is a solution of the following (n+3) X (n+3) linear system, conveniently written in block form as

$$\begin{bmatrix} \mathbf{A} & \mathbf{B} \\ \mathbf{B}^T & \mathbf{0} \end{bmatrix} \begin{bmatrix} \mathbf{c}_1 \\ \mathbf{c}_2 \end{bmatrix} = \begin{bmatrix} \mathbf{z} \\ \mathbf{0} \end{bmatrix} \tag{4.7}$$

The entries in $\boldsymbol{A}$ are $a_{ij} = f_i\left(x_j, y_j\right)$, $i \neq j; a_{ii} = 0$; $i, j = 1,...,n$. This matrix is in fact symmetric. As mentioned earlier, $\boldsymbol{A}$, which is created from radial function $\Phi(r)$, has to be such that the matrix in Eq. (4.7) is invertible. The other vectors and matrices have the forms

$$\begin{aligned} \mathbf{B}^T &= \begin{bmatrix} 1 & 1 & 1 & \cdots & 1 \\ x_1 & x_2 & x_3 & \cdots & x_n \\ y_1 & y_2 & y_3 & \cdots & y_n \end{bmatrix} \\ \mathbf{c}_1^T &= \left[C_1, C_2, C_3, \ldots, C_n\right] \\ \mathbf{c}_2^T &= \left[C_{n+1}, C_{n+2}, C_{n+3}\right] \\ \mathbf{z} &= \left[z_1, z_2, z_3, \ldots, z_n\right]^T \end{aligned} \tag{4.8}$$

The first block equation $A\mathbf{c}_1 + B\mathbf{c}_2 = \mathbf{z}$ represents the interpolation conditions, and the second one, $B^T\mathbf{c}_1 = 0$ is the polynomial precision condition. The coefficients in **c** can be determined from this system by using any linear equation solver. These solvers use techniques that may be more efficient than matrix inversion. Formally, the solution may be written

$$\mathbf{c} = \begin{bmatrix} \mathbf{A} & \mathbf{B} \\ \mathbf{B}^T & \mathbf{0} \end{bmatrix}^{-1} \begin{bmatrix} \mathbf{z} \\ \mathbf{0} \end{bmatrix}. \tag{4.9}$$

The determination of surface normals and curvature requires the first and second partial derivates of the function *S* in Eq. (4.6). The coefficient vector **c** of Eq. (4.6) has already been obtained by solving the system in Eq. (4.7); therefore only partial derivates of the functions *f*, in the vector **f** need to be calculated. The first partial derivates are calculated as follows:

$$\frac{\partial}{\partial x} S(x, y) = \left[f_1^x \;\; f_2^x \;\; f_3^x \;\cdots\; f_n^x \;\; 0 \;\; 1 \;\; 0 \right] \mathbf{c}^T \qquad \text{and}$$

$$f_i^x = \frac{\partial f}{\partial x} = \left(x - x_i\right) \ln\left(r_i^2\right) + \left(x - x_i\right) \tag{4.10}$$

A similar calculation yields $\partial S/\partial y$ and f_i^y.

The second partial derivates are:

$$\frac{\partial^2}{\partial x^2} S(x, y) = \left[f_1^{xx} \;\; f_2^{xx} \;\; f_3^{xx} \;\cdots\; f_n^{xx} \;\; 0 \;\; 0 \;\; 0 \right] \mathbf{c}^T \qquad \text{and}$$

$$f_i^{xx} = \frac{\partial^2 f}{\partial x^2} = \frac{2\left(x - x_i\right)^2}{r_i^2} + \ln\left(r_i^2\right) + \left(x - x_i\right) + 1 \tag{4.11}$$

And similarly for $\partial^2 S/\partial y^2$ and f_i^{yy}. Finally,

$$\frac{\partial^2}{\partial x \partial y} S\left(x, y\right) = \left[f_1^{xy} \;\; f_2^{xy} \;\; f_3^{xy} \;\cdots\; f_n^{xy} \;\; 0 \;\; 0 \;\; 0 \right] \mathbf{c}^T \qquad \text{and}$$

$$f_i^{xy} = \frac{\partial^2 f}{\partial x \partial y} = \frac{2\left(x - x_i\right)\left(y + y_i\right)}{r_i^2}. \tag{4.12}$$

Thus, the unit vectors t_x and t_y tangent to the TPS surface in a generic point $\left(x, y, S\left(x, y\right)\right)$, which belongs to the surface, are consequently:

$$t_x = \frac{\left[1 \;\; 0 \;\; \partial S/\partial x\right]^T}{\left\| \left[1 \;\; 0 \;\; \partial S/\partial x\right]^T \right\|} \qquad \text{and} \qquad t_y = \frac{\left[0 \;\; 1 \;\; \partial S/\partial y\right]^T}{\left\| \left[0 \;\; 1 \;\; \partial S/\partial y\right]^T \right\|} \tag{4.13}$$

And the normal unit vector n is

$$n = t_x \wedge t_y \tag{4.14}$$

For each value of the parameter *M*, a number of points of the approximating surface along with the associated surface normals (Figure 4.2) were calculated in S at the grid nodes $\left(\overline{x}_i, \overline{y}_i\right)$ belonging to the region D.

iii Distance between Surfaces and Contact Area Estimations

For each of the two couples of surfaces, the distance from each TPS approximated node of the femoral condyle and the relative tibial plateau was analytically calculated intersecting the outgoing normal from the TPS in that point with the plane approximating the tibial plateau. The minimum distance D_{min}, both for the lateral and the medial side, was found. Thus, the evaluation of the contact zone was obtained as the region in which the distances are smaller than $D_{min} + D_{th}$; where D_{th} is a distance threshold value. In order to evaluate the sensitivity of the contact model with respect to the D_{th} parameter, this was varied several times considering the distance range from 0.2 mm to 4 mm with a variable step. Finally, the contact area on each femur TPS was defined and calculated as follows:

$$A_{cont} = \int_{Fem} n \, dx \, dy = \sum_j^m n_j \, dx \, dy \tag{4.15}$$

Moreover, the contact area on each tibial plane was conventionally defined as the area of the convex hull (Barber et al., 1996) of the points generated from the intersections between the normals of a TPS and the relative plane (Figure 4.3).

Thus, for the selected subject, the devised model for the tibio-femoral contact evaluation was used both to perform sensitivity analyses with respect to the parameters of the model and to evaluate the contact in physiological conditions.

In the firsts evaluation of the model, the body weight was "ideally" neglected considering the position assumed by the subject during the NMR scan. This position was used in order to perform the sensitivity analyses with respect to the model parameters, in particular the M parameter (density of the TPS grid nodes) and the D_{th} parameter (contact distance threshold). As already described, the M parameter was varied from 20 to 100 with step 20. Whereas, the parameter D_{min} was varied from 0.2 mm up to 4 mm with a variable step, precisely for values equals to 0.2 mm, 0.5 mm, 1 mm, 1.5 mm, 2 mm, 2.5 mm, 3 mm, and 4 mm, see example at the Figure 4.4.

The devised model was also used to evaluate the tibio-femoral contact area when the specific knee was loaded by the selected subject with its full body weight. In particular, three positions at the full extension were considered during the execution of the step up/down motor task so as perform an evaluation of the tibio-femoral contact area during living activities. The value of the parameter M, chosen for these evaluations, was equal to 100, whereas the value of the threshold which define the contact zone ($D_{min} + D_{th}$) was equal to the value of the D_{min}(NMR) obtained in conditions without body weight, that was equal to 4.6 mm for the lateral side and the 5 mm for the medial side. Assuming that during the NMR scan the articular surfaces of the tibio-femoral joint were in contact but not loaded, these values of D_{min}(NMR) could be considered as estimations of the cartilage thicknesses, of the femur and the tibia, for that specific knee flexion angle (full extension).

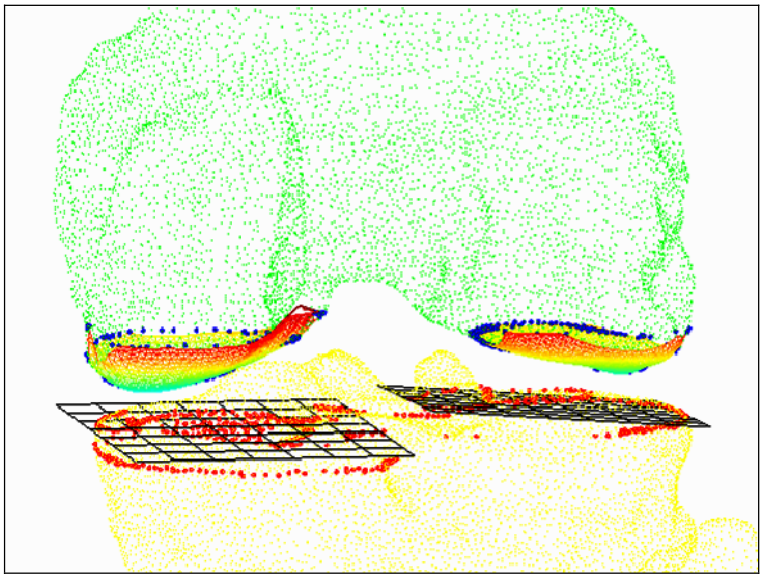

Figure 4.3: Femoral and tibial original geometries (*little green and yellow dots, respectively*). The selected femoral points and the relative femoral TPS (*blue points and meshes*) for the lateral and the medial side (*left and right*). The selected tibial points and the relative tibial planes (*red points and planar grids*).

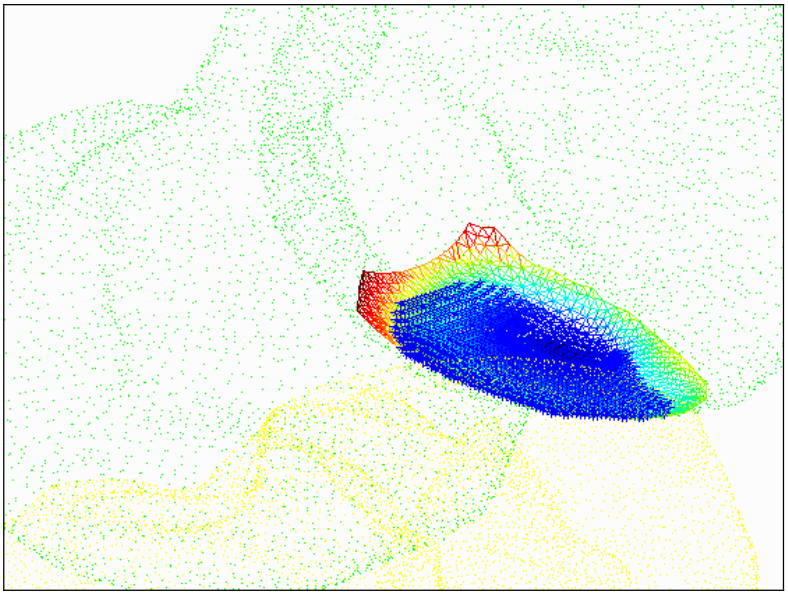

Figure 4.4: Bottom-rear sight of the lateral TPS (*colored mesh*) and estimated contact area (*blue region*) obtained without body weight with D_{th} = 3 mm and $M = 40$.

iv Results for Static Positions With and Without Body Weight

Regarding the two sensitivity analyses with respect to the M and the D_{th} parameters, the contact areas on the femoral TPS and on the tibial plane were calculated varying these two parameters. Considering the sensitivity of the model with respect to the D_{th} parameter, it was expected that the estimations of the contact area resulted bigger with the increasing of the D_{th} parameter because of the higher level of recruitment of the TPS normals which took part to the contact estimation. In fact, it was obtained that the estimation of the femoral and tibial contact areas increased almost linearly with the increasing of the D_{th} parameter for values higher than 1.5 mm for the lateral side (Figure 4.5) and for values higher than 0.2 mm for the medial one (Figure 4.6). Moreover, the same behavior was obtained for the percentage of the normals which took part to the contact with respect to the total number of TPS nodes, see Figure 4.5 and Figure 4.6, obtaining that with D_{th} = 4 mm more than the 90% of the normals took part to the contact in the lateral side and about 60% in the medial one. The estimations of the femoral contact area were always smaller than those of the tibial ones. Considering the sensitivity of the model with respect to the M parameter, the higher variability in the calculus of the femoral contact area was obtained considering the smaller value of the parameter ($M=20$), both in the lateral and in the medial side, Figure 4.7. Increasing the value of the M parameter, the estimations of the contact area seemed to tend at an asymptotic value for value of M bigger than 60 for the lateral side. Whereas, the increasing of the M value, in the medial side, produced a little decreasing of the variability but without a clear tendency as that one obtained in the lateral side, Figure 4.7.

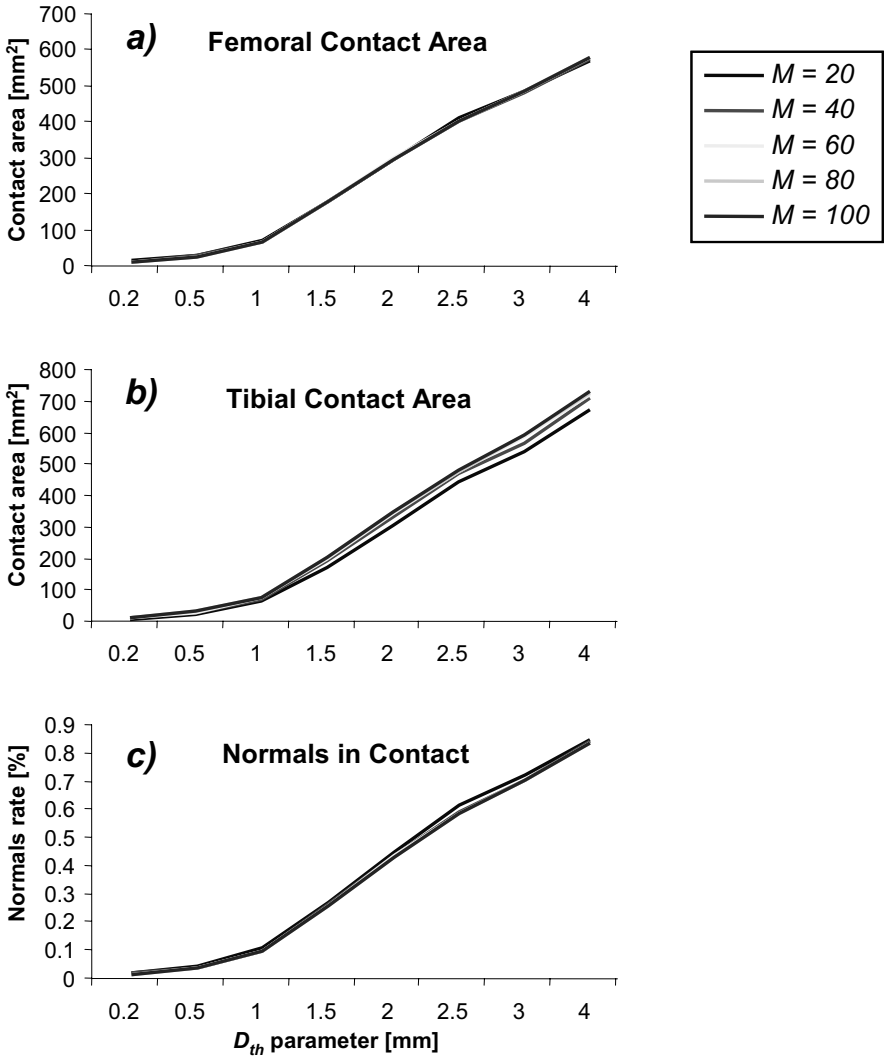

Figure 4.5: Estimations of the femoral (*a*) and the tibial (*b*) contact areas on the **lateral** side in function of the D_{th} parameter. Percentage, on the total number, of the normals outgoing from the femoral TPS which take part of the contact zone (*c*). Curves obtained with different values of the *M* parameter are shown.

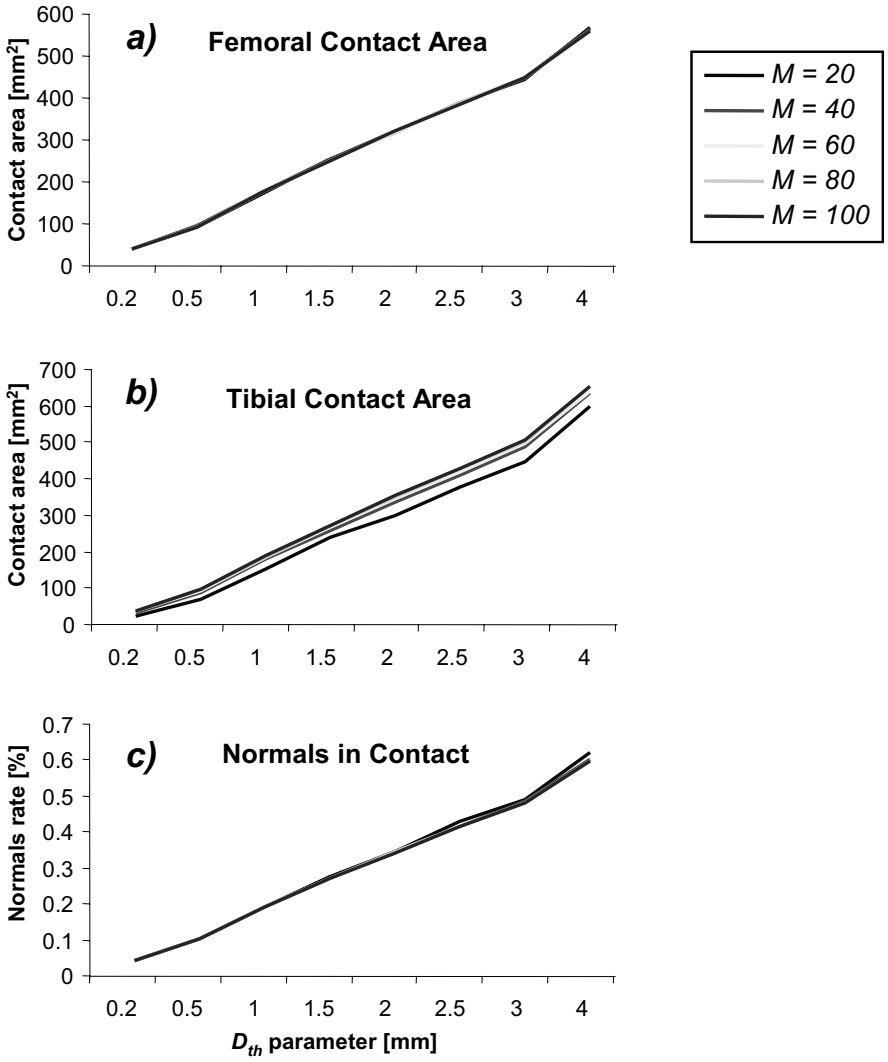

Figure 4.6: Estimations of the femoral (*a*) and the tibial (*b*) contact areas on the **medial** side in function of the D_{th} parameter. Percentage, on the total number, of the normals outgoing from the femoral TPS which take part of the contact zone (*c*). Curves obtained with different values of the *M* parameter are shown.

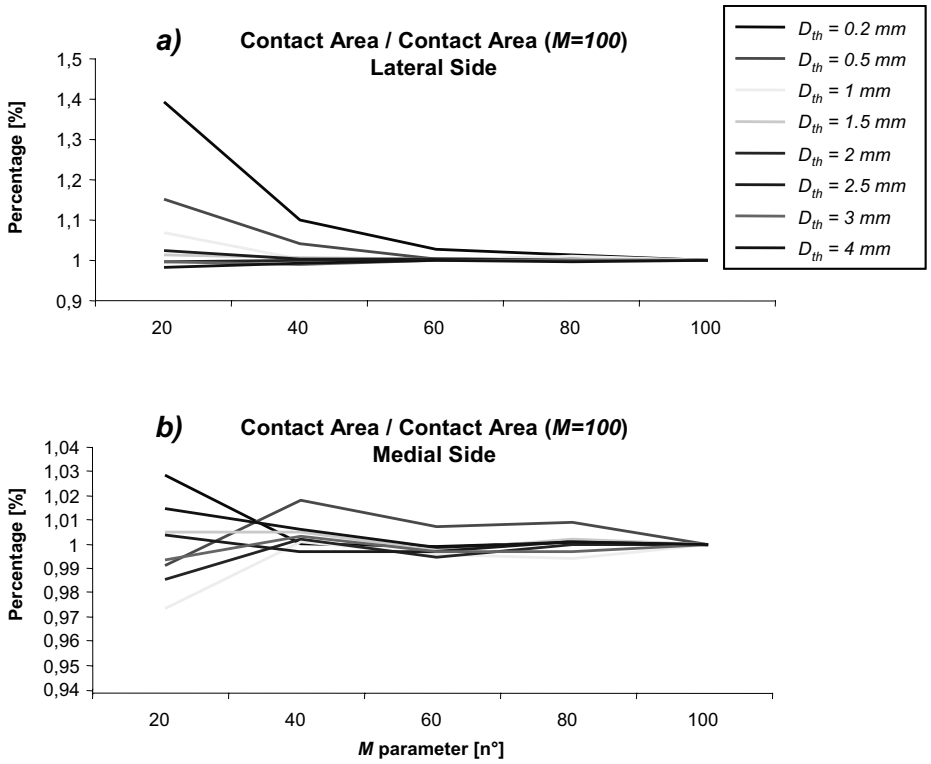

Figure 4.7: Femoral contact area in function of the *M* parameter normalized with respect to the femoral contact area obtained with $M = 100$ on the lateral (*a*) and the medial (*b*) side. Curves obtained with different values of the D_{th} parameter are shown.

Regarding the use of the model evaluating the tibio-femoral contact in physiological conditions, three static relative positions between femur and tibia (Frame 1, 2, and 3) were considered from the subject-specific kinematics of the step up/down motor task. In these positions, the proximity between the femoral TPS and the tibial plane was calculated in all grid nodes of the TPS, both for the lateral and the medial side. Thus, the contact zone was defined as the region where the distance between the two surfaces were smaller than the D_{min}(NMR) obtained during the NMR scan. As seen also in the sensitivity analyses of the model, it was obtained that the femoral contact areas were always bigger than the tibial contact areas. Moreover, it was recognized that the repeatability of the estimations of the lateral contact was

higher than that of the medial ones, Table 4.1. The Frame 2 produced the smaller values in all estimations made. Whereas, Frame 1 and Frame 3 produced values very similar in the lateral side, but quite different to each other in the medial side. In fact, the standard deviation calculated for the contact areas on the lateral side, both the femoral and the tibial one, was about the 10% of the relative mean value, whereas in the medial side, each the standard deviation was about the 20% of the relative mean value, Table 4.1.

mm^2	Frame 1	Frame 2	Frame 3	Mean ± Std
Lat. Fem.	265.5	222.9	269.4	252.6 ± 25.8
Lat. Tib.	297.8	249.3	302.2	283.1 ± 26.8
Med. Fem.	218.4	166.6	259.7	214.9 ± 46.6
Med. Tib.	232.3	176.9	279.7	229.6 ± 51.4

Table 4.1: Contact areas estimations, with mean values and standard deviations, obtained for the three positions of the knee loaded at the full extension.

v Discussion

A subject-specific model to evaluate the tibio-femoral contact was developed and implemented on a selected subject. It was based on specific experimental acquisitions performed by means of imaging technologies, such as NMR and vide-fluoroscopy. The peculiarity adopted in this model for the evaluation of the articular contact at the knee was the description of the femoral condyles surfaces by means of the TPS method (*thin plate spline*), which is a mathematical tool already used in this and other research fields. The sensitivity of the model to two parameters and its capability to be suitably adopted in physiological conditions was evaluated.

As seen in results, it was obtained that the estimated femoral contact area increased almost linearly with the increasing of the D_{th} parameter, and how this behavior was less sensitive to variations of the M parameter. The contact areas calculated on the tibial planes were always bigger of the respective femoral ones. This was due to the convexity of the femoral condyles, which, moving away from the minimum distance point, produced normals even less perpendicular to the tibial plane and so this difference between the values of

the femoral and tibial contact area became even more big with the increasing of the D_{th} parameter. Considering the femoral contact areas, the lateral one resulted to be more sensitive to values smaller than 60 and 1 mm for the M and the D_{th} parameter, respectively, whereas the medial one was more sensitive for values smaller than 40 for the M parameter, without a particular tendency provided by the D_{th} parameter.

Thus, the implemented model resulted to be suitable for the aim to be devised. The TPS method, which was used to interpolate the experimental data of the femoral condyles and to provide an analytical representation of these, showed the advantage to be capable to consider experimental data spatially disordered, and so to can suitably use the experimental data acquired on a specific subject, on the contrary of other mathematical methods such as NURBS. Nevertheless, the TPS method featured the disadvantage to hardly manage high number of experimental data. As reported by Boyd (Boyd et al., 1999), TPS can produce artifacts if more than 2000 data points are used for the interpolation conditions described above. For this particular problem, the subject-specific bony geometries, reconstructed from the NMR dataset by means of the software AMIRA, needed to be reduced in the number of points. In this process of reduction, it was important to chose the right points in order to be able to describe, with a smaller number of points, the original geometry without modifying it. As explained above, this process was based on the selection of only the points which lay at the quotes relative to the quotes of the NMR images along the proximal-distal axis of the NMR reference system. The amount of the points to be considered was manually chosen in order to avoid any artifact or discontinuity in the final form of each femoral TPS.

Since TPS method is based on the minimum energy deformation of a thin plate, it represents a surface by means of a function like $z = S(x, y)$, and this prevents to describe a surface too much curved such as the entire surface of a femoral condyle, meant as the surface which takes part to the contact from the full extension to the full flexion. Thus, only the part of femoral condyles, which it was known to be in contact with the tibia at the full extension, was described by means of the TPS method. If the tibio-femoral contact at other flexion angles of the knee would to be evaluated, it would be necessary to select the experimental points and perform new calculus of the TPS forms for each considered position of the knee joint.

In the devised model, the procedure consisted in the interpolation of the two femoral condyles by means of the TPS method and of the two tibial plateaus by means of two simple planes. Hypothesizing each tibial plateau with a simple plane is certainly a great limitation for the model. Nevertheless, this choice was made for two particular reasons. The first reason was that no further variables wanted to introduced in the model in order to have more control of the parameters during the sensitivity analyses, whereas the second one was that in this way it was possible to perform an analytical calculus of the intersection points between the outgoing normals of the femoral TPS and the linear mathematical representation (plane) of each tibial plateau. This allowed to evaluate the sensitivity of the contact model to the parameters of each femoral TPS maintaining constant (as a fixed reference) the mathematical description of the relative tibial plateau.

In future improvements of the devised model, both the femoral and tibial articular surfaces will be represented by means of the TPS method. Thus, describing the bony geometries more anatomically, an higher level of specificity of the model will be reached. Given the non-linearity of the TPS form, differently by the developed model this procedure will require the solution of a non-linear system by means of a minimization process, in order to calculate the interaction points between the outgoing normals of the femoral TPS with the tibial TPS.

4.3 3D Distance Maps for Quasi-Static Evaluations of Proximity

As reported in the previous paragraph, since the TPS tool is based on the minimum energy deformation of a infinite thin plate, it represents a surface in the form $z=S(x,y)$ and this inhibits to describe surfaces with high curvature. Thus, one limit of the TPS tool in this approach is that it can hardly describe a whole femoral condyle, meant as the surface which takes part to the zone from the full extension to the full flexion. If the tibio-femoral contact at other flexion angles of the knee would to be evaluated by means of this approach, it would be necessary to select the experimental points and perform new calculus of the TPS forms for each considered position of the knee joint. Otherwise, it would be possible describe the whole condyle by means of just 2, 3 or more TPS forms (e.g. one for the contact at full extension, one at 45 degrees and one at 90 degrees of flexion) and mediating among these different TPS forms in function of the flexion angle. Nevertheless, it is clear to understand that this kind of approach, adopted to make evaluations during the execution of daily living activities, could be disadvantageous, especially in an high range of movement joint like the knee. Thus, in order to deal with this kind of problems and limitations, a fully different approach was implemented.

The new devised approach was based on the use of Euclidean Distance Transforms, which permitted to overcome the problem due to the different poses of the femoral surface with respect to the tibial one during the execution of living motor tasks. In fact, since the use of the distance map permits a very quick evaluation of the distance of all femoral points of each condyle with respect to the relative tibial plateau, the repetition of this process for each position assumed by the subject during the execution of the select motor task did not resulted too much heavy. Moreover, this approach featured the capability to manage over-sampled geometries like those reconstructed by the NMR dataset with the software AMIRA.

A 3D Distance Map is a particular Distance Transform. Distance transforms were first proposed by Rosenfeld and Pfalz (Rosenfeld and

Pfaltz, 1968), who developed a rapid algorithm for their evaluation. The original algorithm computed a 'city block' distance, and Danielsson (Danielsson, 1980) developed an algorithm for two-dimensional Euclidean distance functions. This algorithm was then extended to three dimensions by Mohr and Bajcsy in 1983 (Mohr and Bajcsy, 1983). Subsequently, Borgefors (Borgefors, 1984) classified theories and methods for arbitrary dimension distance functions, and Rangnemalm (Ragnemalm, 1993) developed a method for evaluating the sufficiency of algorithms for Euclidean distance calculation. Distance functions have been used for many image processing operations such as computing the skeleton, morphological dilation and contraction, construction of shortest paths between points, shape factor computation, and multi-dimensional alignment of objects (Kozinska et al., 1997; Lavallee and Szeliski, 1995; Zuffi et al., 1999).

In this study, the used 3D Distance Map was calculated as simple Euclidean Distance Transform without using any optimized algorithm. This choice was adopted in order to preliminarily evaluate this kind of approach to the problem of the tibio-femoral contact in living subjects. In future developments, optimized algorithms and smart data structures will be certainly considered in order to limit storage size and so calculation time.

i 3D Distance Map: Construction and How It Works

A distance map is a data structure. If three-dimensional, this data structure represents a spatial domain (volume) which includes the considered object. The whole volume is spatially divided, with a constant or a variable resolution, in order to generate a regular or irregular grid of nodes. The knowledge held by this data structure is simply the distances from the considered object of each node of the grid. Thus, using the distance map of an object, the distance of a generic point, inside its spatial domain from the surface of the object, can be quickly computed by a trilinear interpolation of the eight map nodes closest to the point.

Generally, in order to calculate the Distance Map of an object, it is necessary to define a volume, which is the spatial domain of the distance map, so as it includes the whole or just the part of interest of the considered object and preferably so as it includes the points to be evaluated too. We used the word 'preferably' because this specification is not obligatory. In

fact, a discussion about how to evaluate the distance from the considered object of a point outside the domain will be provided. Then, it is necessary to spatially divide the domain in order to create the grid of nodes. If the use of the distance map wants to be efficient, the definition of the position of the nodes has to be cleverly done in order to can usefully use the advantages which the usage of the distance map can give. For example, if it is known the correlation between the spatial coordinates of the nodes and the indexes which represents the nodes position inside of the data structure, the individuation of the eight map nodes closest to point results simply immediate just by the coordinate of the point. Finally, the distance of the point from the object can be estimated by means of the interpolation of the distances previously stored in the eight nodes around the point. Different kind of interpolations can be used, but if the resolution of the distance map is sufficiently high, then a simple linear interpolation is recommended also in order to not further increase the computational weight of the model.

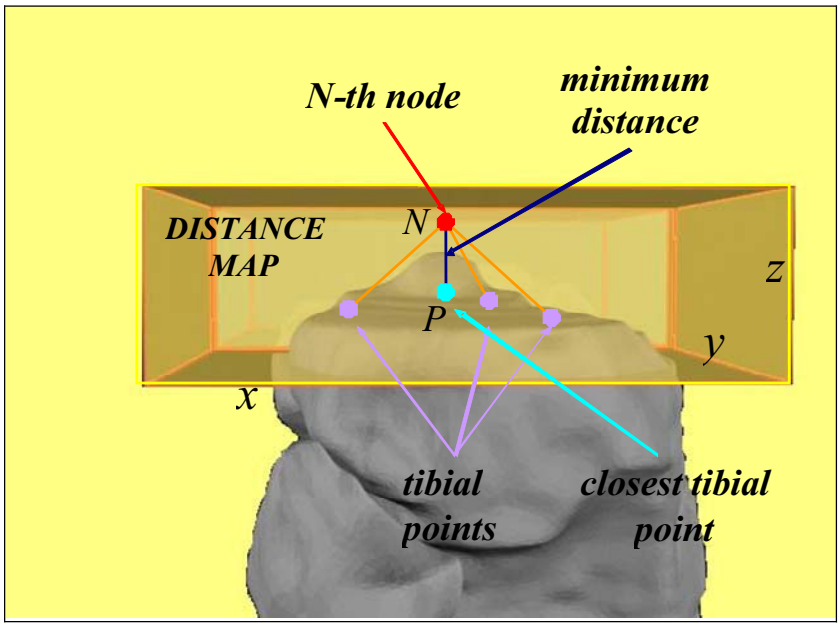

Figure 4.8: Scheme of the lateral distance map. Lateral tibial plateau (*gray*) is bounded by the Domain of the distance map (*yellow rectangle*). A node of the map (*red*), some tibial points (*violet*) and the tibial point closest to the considered node (*azure*) are shown.

In this study two Distance Maps were constructed around of the two tibial plateau and these were represented by two 3-D arrays (*L x M x N*) whose values were the distances from the closest point from each the tibial plateau. Each distance map size was about 40 x 55 x 15 mm and, with a resolution of 1 mm in each direction, the storage size of each Distance Map resulted about 300 KB.

At each node, the Euclidean distances from all the experimental points which describe the tibial plateau were evaluated. Then, the value of the minimum distance was stored in the structure data of the distance map at the indexes relative to the considered node. At the same indexes, in a similar structure data, the index relative to the closest tibial point was stored too, in order to can recover the position of the closest tibial point at each node.

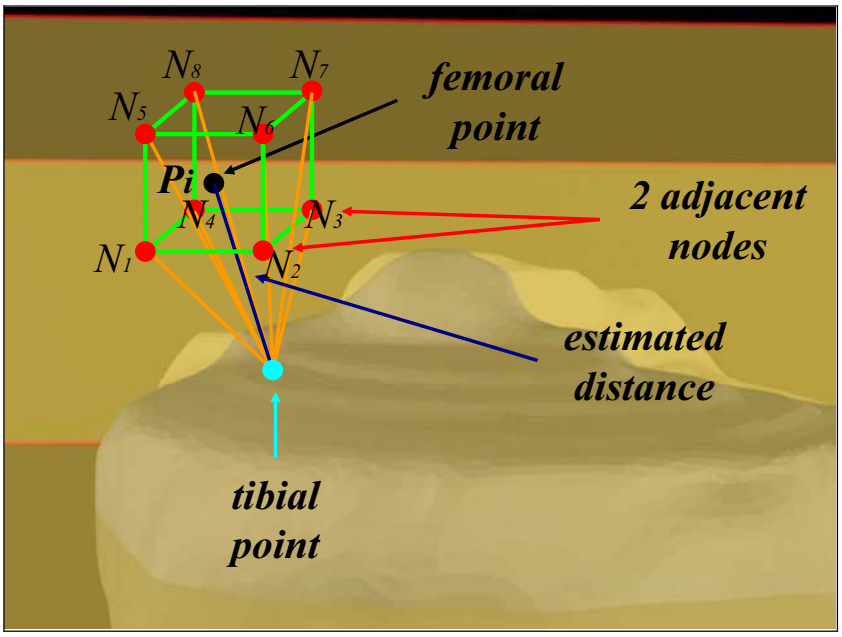

Figure 4.9: Scheme of the estimation of the distance (*blue*) of a femoral point (*black*) from the tibial plateau (*azure*) by means of the use of the distance map (*red*). From the spatial coordinates of the femoral point, the eight map nodes closest to the point (*red*) is identified. The estimation of the distance is performed with a tri-linear interpolation of the distances stored at the eight nodes. Here, all eight nodes point at the same tibial point (*azure*) but, generally, each node can point at a different tibial point. At the end, the final tibial point (*azure*), which is closest to the considered femoral point, is estimated as the barycentre of all tibial points obtained.

ii Proximity Between Femur and Tibia During Living Tasks

In order to reach the outlined aim, the estimation of the tibio-femoral contact during living activities by means of the use of distance maps, the subject-specific bony kinematics of the femur and the tibia were needed to be elaborated. In fact, since the two distance maps were constructed around the two tibial plateaus, these two objects needed to remain fixed in the space in order to had not make changes in the distance maps due to their movements in the space. This problem was simply solved describing the bony kinematics of the femur and the tibia in the anatomical reference system of the tibia. In this way, the femoral kinematics was described relatively to the fixed tibia and so the fixed distance map, both for the lateral and the medial side.

The standard expression of the position of a generic point *p* in the *global reference system* is:

$$^{glob}p = {}^{glob}R_{loc} \cdot {}^{loc}p + {}^{loc}o \tag{4.16}$$

where ${}^{glob}R_{loc}$ and ${}^{loc}o$ are the rotation matrix and the position of the origin of the *local reference system* the *global* one and ${}^{loc}p$ is the position of the generic point *p* in the *local reference system*. From the 3D video-fluoroscopy, the femoral and tibial reference systems (locals) with respect to the Nuclear Magnetic Resonance reference system (global) were known. Thus, it was possible to calculate, for each acquired frame, the position of the all femoral points, fixed points in the moving femoral reference system, in the fixed tibial reference system using the following expressions, Eq. (4.17), Eq. (4.18) and Eq. (4.19):

$$^{Tib}p = {}^{Tib}R_{Fem} \cdot {}^{Fem}p + {}^{Tib}o_{Fem} \tag{4.17}$$

$$^{Tib}R_{Fem} = {}^{g}R_{Tib}^{-1} \cdot {}^{g}R_{Fem} \tag{4.18}$$

$$^{Tib}o_{Fem} = {}^{g}R_{Tib}^{-1} \cdot \left({}^{Fem}o - {}^{Tib}o \right) \tag{4.19}$$

where ${}^{Tib}R_{Fem}$ and ${}^{Tib}o_{Fem}$ were the rotation matrix and the position of the origin of the femur reference system with respect to the tibia reference system, respectively.

Thus, for each frame of the experimental kinematics, each femoral condyle was represented as a Wx3 vector, where in each of the W rows there was spatial coordinates of the experimental points of the considered femoral

condyle. Thus, each *i-th* femoral point was evaluated as follows, see Figure 4.9:

1. if, the *i-th* point belongs to the distance map domain
2. then, find the indexes of the eight nodes closest to the point from its spatial coordinates using '*floor*' function and offsets
3. calculate the spatial interpolation between the eight values according to the relative distances of the point from the eight nodes
4. store the value of the interpolated distance and the index *i* in a Wx2 vector.

In the Wx2 vector at the end of the loop, the estimations of the distances of all femoral points of each condyle from the relative tibial plateau were stored and thus, the proximity between the femur and tibia was calculated, see Figure 4.10.

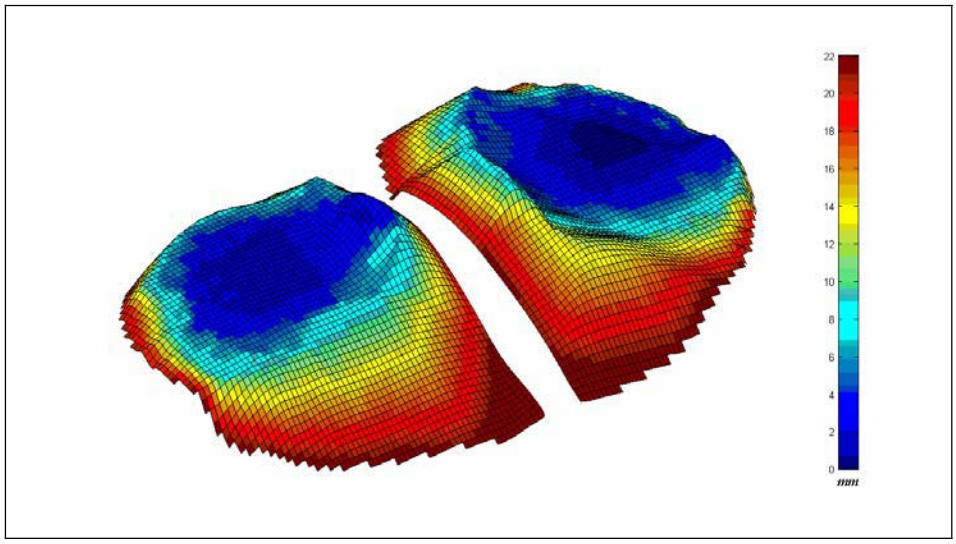

Figure 4.10: Colored proximity map between the femur and the tibia at the full extension position [mm].

In order to estimate the contact point, the Wx2 vector was increasingly sorted along the distances column. Thus, the femoral points at a distance smaller than the minimum distance (first row) plus a threshold defined in this study at 0.5 mm were selected. Finally, the contact point was estimated as the barycentre of the cloud of the selected points.

The positions of the contact point were calculated during the execution of three repetitions of the **chair rising/sitting** motor task and three repetitions of the **step up/down** motor task. The anterior-posterior locations of the medial and the lateral contact points were estimated for each acquired frame.

iii Results

The global behavior of the anterior-posterior translations of the contact point with respect to the flexion-extension angle were similar between the two considered motor tasks. Similar behaviors were obtained between the extension and the flexion movements too. Whereas, the behavior of the anterior-posterior translation of the lateral and the medial contact points were quite different, see Figure 4.11 and Figure 4.12. In fact, the lateral contact points, in both motor tasks, moved posteriorly with the increasing of the flexion angle, almost linearly for the firsts 20-30 degrees of flexion, a little plateau for further 10-20 degrees of flexion and then an ulterior posterior little translation. Instead, the medial contact points, in both motor tasks, moved both in the posterior direction and in the anterior one. From the full extension up to the maximum flexion angle reached during each living activity, about 70 degrees of flexion for the step up/down motor task and about 90 degrees of flexion for the chair rising/sitting motor task, the medial contact points swayed anteriorly and posteriorly, sometimes also of considerable quantities, without a clear tendency.

During the step up/down motor task, Figure 4.11, a little higher variability can be seen during flexions with respect to extension movements, both in the lateral and the medial side. Whereas, during the chair rising/sitting motor task, Figure 4.12, a clear tendency of the variability was not evident in order to make specific observations on the behaviour on one side with respect to the other one, or on one phase of the movement with respect to the other one. In fact, during this motor task, the highest repeatability was obtained on the medial side during the flexion movement, whereas during the extension movements on the same side the variability was similar to that obtained on the lateral side, without any difference due to the phases of the motor task.

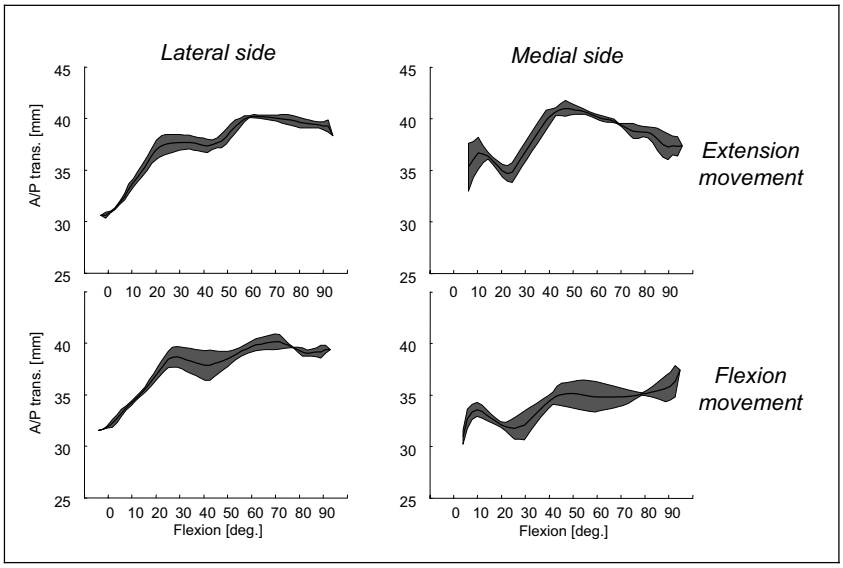

Figure 4.11: Anterior-posterior translation of the lateral (*left*) and the medial (*right*) contact points during the execution of the **step up/down** motor task with the extension (*top*) and the flexion (*bottom*) movements detached.

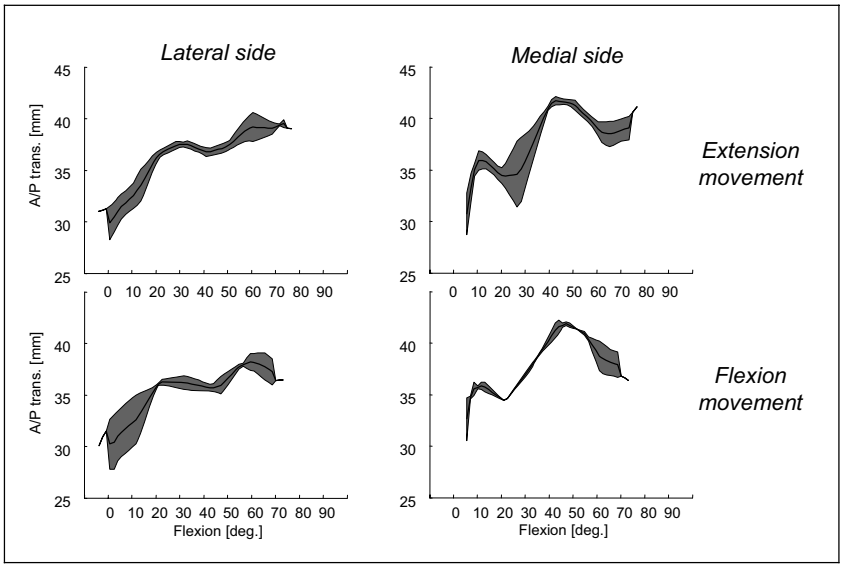

Figure 4.12: Anterior-posterior translation of the lateral (*left*) and the medial (*right*) contact points during the execution of the **chair rising/sitting** motor task with the extension (*top*) and the flexion (*bottom*) movements detached.

iv Discussion

A subject-specific model to evaluate the tibio-femoral contact was developed and implemented on a selected subject. It was based on specific experimental acquisitions performed by means of imaging technologies, such as NMR and vide-fluoroscopy. The peculiarity adopted in this model for the evaluation of the articular contact at the knee was the use of specific structures data called Distance Maps, which represent an object and its distance from nearby points. Once calculated, these structures data allowed to perform the evaluation of the distance of a generic point from the represented object much faster than standard methods, such as the research of the closest point of the object from the considered point. This feature allowed perform the evaluation of the proximity between femur and tibia several times, many as the frames acquired by the selected subject during the execution of living activities.

In the adopted model, each tibial plateau was represented by means of a 3D distance map. The bony kinematics of the femoral points were described in the tibial reference system in order to consider spatially fixed the two distance maps. Thus, all femoral points were evaluated by means of the distance map and the proximity of each femoral condyle from the relative tibial plateau was evaluated. Finally, the lateral and the medial contact points were estimated and its location during the execution of the step up/down and the chair rising /sitting motor tasks.

As seen in the results section, little differences in the anterior-posterior translation of contact points were obtained between the two considered living motor tasks. Little differences were also obtained for extension and flexion movements. Considering the behaviour of the anterior-posterior translation of the lateral and medial contact points, independently by the motor task or the phase of this, the lateral contact point clearly tended to move posteriorly with the increasing of the flexion angle, whereas the medial contact point moved less posteriorly and in a way less monotonous. This can be considered as the most meaningful result obtained with the devised model. In fact, the lateral side of the femur physiologically rolls on the tibia on the first degrees of flexion moving significantly the contact point in the posterior direction (*rolling phase*), then for higher flexion angles, the femur

slides on the tibia moving little more posteriorly the contact point (*sliding phase*). Whereas, the medial side of the femur tends to behave like a pivot point generating the *screw-home* movement coupled to the flexion-extension (i.e. the internal rotation of the tibia with the increasing of the flexion angle). The importance of the behaviour of both the contact points was not so obvious, in particular in loading *in-vivo* conditions.

The oscillations obtained by the medial contact point during these living activities could be due to the fact that the medial tibial plateau (bony component) was concave while the femoral condyle was convex. Usually, the congruency of these two articulating surfaces can generate more than a single contact point or even a contact area. This means that, in this case, the inaccuracies in the processes of reconstruction of the bony geometries and of bony kinematics, even if small, could generate some doubts on the correctness of the definition of the contact point as the closest point between of the two surfaces. But, considering for the estimation of the contact point all the couple of femoral and tibial points which their distance is smaller than the minimum distance plus a threshold, this problem can be limited. This because the threshold value allows to consider different contact points and thus, the final position of the contact point is a mediation of the positions of different closest point, as many as the threshold value has been able to recruit. Nevertheless, in this way, a large contact area, meant as the area in which the considered closest points take part to the estimation of the contact point, could be obtained, and thus the barycentre of this area can easily fluctuate around the pivot point.

As expected, little differences between the two considered living motor tasks were obtained in the anterior-posterior translation of contact points, because of the similarities between the two considered living activities. In fact, both the step up/down and the chair rising/sitting motor tasks consisted in providing the muscular force and the neural control to the lower limbs needed to raise up, against gravity, and down, according to gravity, the body weight. The great difference between these two activities was that the step up/down was a single leg motor task, whereas the chair rising/sitting was a two legs motor task. From this difference, it was possible to make some comment to the obtained variability of the anterior-posterior translation of the contact point. Since the chair rising/sitting motor task was a two leg activity and we focused our attention just at one of these, the repeatability

obtained in this motor task, meant also as the amount of the variability obtained for each side and phase of the motor task, could be invalidated by the unknown quantities in the other leg. In other words, since a living activity could not be reproduced always in the same way, even by the same subject, the two legs could behave differently each time the motor task was executed. Thus, considering just a single knee joint, no information about the variability due to the side or the phase of the movement can be done. On the other hand, it was important to obtain physiologically meaningful results during the chair rising/sitting. In fact, regarding the step up/down results, a bigger variability was obtained during the flexion phase with respect to that obtained during the extension phase. The greater repeatability obtained during the extension phase (step up movement) was probably due to a major activity of the muscles for controlling the movement. This muscular activity had the goal to perform the movement against the gravity force and thus, the concentric contraction of these were better controlled by the nervous system. Whereas the eccentric contraction of the muscles, which occurred during the flexion phase (step down movement), was less controlled by the nervous system for guiding this according to the gravity movement and thus, a minor repeatability was obtained.

The use of the 3D distance map for the evaluation of the tibio-femoral contact showed several advantages, but revealed some disadvantages too. For example, using 3D distance maps for describing the two tibial plateaus required to maintain fixed in the space the tibial geometry and so required to calculate the bony kinematics of the femur in the fixed tibial reference system. On the contrary, this approach allowed to manage the bony geometries as cloud of points, neglecting facets and normals of the mesh version and making the methodology simpler and computationally lighter. The computational weight paid in the pre-calculation of the distance map was spent in order to economize it much more during several evaluations of distances needed for each frame acquired by the video-fluoroscopy.

As reported before, about the definition of the borders of the domain, it was preferable that the domain included also the femoral points to be evaluated with the distance map. This choice was considered as ‘preferable’ because if a femoral point outside the domain wanted to be evaluated with the distance map an ulterior algorithm had to be written. As explained above, in this study, only the femoral points inside the domain were evaluated

because the outer femoral points could not take part to the contact zone. Nevertheless, the additional algorithm could qualitatively work as already proposed in the literature (Marai et al., 2004). From the spatial coordinates of the femoral point, the closest node on the boundary of the domain would be found and the Euclidean distance between the node and the femoral point would be calculated. Finally, the estimation of the distance between the femoral point outside of the domain and the object described by the distance map would be performed as the sum of the distance stored at the node and the distance between the node and the femoral point. Obviously, this was not the shortest distance between the femoral point and the tibia, but it would be considered a good approximation (Marai et al., 2004).

Thus, the devised model, based only on imaging technologies, was suitably used to reach the aim of the study, the evaluation of the tibio-femoral contact in a living subject during the execution of daily activities. The model produced physiologically meaningful results, and it showed that some biomechanical behaviours of the knee joint in passive and simulated loading conditions were present also during the execution of daily motor tasks, such as the step up/down and the chair rising/sitting. On the lateral side, the physiological rolling and sliding movements were obtained for little and higher flexion angle respectively, whereas on the other side, the physiological medial pivot seemed to be obtained.

Future improvements of the devised model will include methodologies for the estimation of the contact area and of the contact force (amount and direction), making hypotheses and/or *in-vivo* estimation the mechanical properties of the subject. Optimized algorithms for a faster calculus of the distance map will may be considered too. Moreover, an higher number of subjects, healthy and pathological, will be acquired in order to engineer all the needed processes for reaching reliable estimations of the investigated quantities.

In conclusion, this model, for the evaluation of the subject-specific tibio-femoral contact during the execution of daily living activities, will can become an important clinical device for suggesting effective pre-operative, surgical and rehabilitative procedures in pathological patients.

4.4 Conclusions

In this Chapter, two different approaches for modelling the tibio-femoral contact were developed and implemented using subject-specific data. As reported above, since the inputs of the model were the geometries and kinematics of the femur and the tibia, a material 'contact' between these two bodies never occurred. In fact, the 'contact' was defined as the condition when the two objects were closer than a threshold distance. The evaluation of the tibio-femoral 'contact' was performed by means of the quantification of the proximity between the geometries of the femur and the tibia for each relative pose according to the specific kinematics acquired from the subject. Once the proximity between the femur and the tibia was calculated, estimations of the contact point and area were performed and analyzed by means of threshold values properly defined for each single aim.

The first devised method employed the *thin plate splines* tool (TPS) to mathematically describe the articular surfaces of the femur. In the developed model, the proximity between each femoral condyle, described by means of a TPS form, and the relative tibial plateau, described with a simple plane, was calculated. The actual contact area (unknown) was estimated by means of two indicators, the first defined on the femoral surface and the other on the tibial one, which both dependant from the definition of the threshold distance.

The considered relative positions between the femur and the tibia were the position assumed by the subject during the NMR acquisition, (no body weight condition) and three positions at the maximum extension reached during the step up/down motor task (whole body weight condition).

The implemented model resulted to be suitable for the aim to be devised. The TPS method, which was used to interpolate the experimental data of the femoral condyles and to provide an analytical representation of these, showed the advantage to be capable to consider experimental data spatially disordered, and so to can suitably use the experimental data acquired on a specific subject. Nevertheless, the TPS method featured the disadvantage to produce artifacts using set of experimental points larger than 2000 points. For this particular problem, the subject-specific bony geometries, reconstructed from the NMR dataset by means of the software AMIRA,

needed to be elaborated in order to reduce the number of points. Moreover, since TPS method is based on the minimum energy deformation of a thin plate, it prevents to describe too curved surfaces. In fact, in the present study, only the part of femoral condyles which was known to be in contact with the tibia at the full extension was described by means of the TPS method. Thus, if the tibio-femoral contact at other flexion angles of the knee would to be evaluated, it would be necessary to select the relevant experimental points and perform the estimation of the new TPS forms, one for each considered position of the knee joint. In future improvements of the devised model, both the femoral and tibial articular surfaces will be represented by means of the TPS method. Thus, describing the bony geometries more anatomically, an higher level of specificity of the model will be reached.

The second method implemented to evaluate the tibio-femoral contact exploited the Euclidean Distance Transform (distance map) to represent the proximity of whatever point from each tibial plateau, in its nearby space. Differently by the method of the TPS, the use of the distance map allowed to overcome the problem due to the different poses of the femoral surface with respect to the tibial one during the execution of living motor tasks. In fact, since the use of the distance map allowed a very quick evaluation of the distance of all femoral points of each condyle with respect to the relative tibial plateau, the repetition of this process for each position assumed by the subject during the execution of the select motor task did not resulted too much computationally heavy. Moreover, this approach featured the capability to manage over-sampled geometries like those reconstructed by the NMR dataset with the software AMIRA.

In the adopted model, each tibial plateau was represented by means of a 3D distance map. The bony kinematics of the femoral points were described in the tibial reference system in order to consider the two distance maps fixed in the space. Then, all femoral points were evaluated by means of the distance map and the proximity of each femoral condyle from the relative tibial plateau was evaluated. Finally, the lateral and the medial contact points and their locations in the space were estimated during the execution of the step up/down and the chair rising /sitting motor tasks.

The use of the 3D distance map for the evaluation of the tibio-femoral contact showed several advantages, but revealed some disadvantages too.

For example, using 3D distance maps for describing the two tibial plateaus required to maintain fixed in the space the tibial geometry and so required to calculate the bony kinematics of the femur in the fixed tibial reference system. On the contrary, this approach allowed to manage the bony geometries as cloud of points, neglecting facets and normals of the mesh version and making the methodology simpler and computationally lighter. The computational weight paid in the pre-calculation of the distance map was spent in order to economize much more time during several evaluations of distances needed for each frame acquired by the video-fluoroscopy.

Thus, the devised model, based only on imaging technologies, was suitably used to reach the aim of the study, the evaluation of the tibio-femoral contact in a living subject during the execution of daily activities. The model produced physiologically meaningful results, and it showed that some biomechanical behaviours of the knee joint in passive and simulated loading conditions were present also during the execution of daily motor tasks, such as the step up/down and the chair rising/sitting. On the lateral side, the physiological rolling and sliding movements were obtained for little and higher flexion angle respectively, whereas on the other side, the physiological medial pivot seemed to be obtained.

Future improvements of the devised model will include methodologies for the estimation of the contact area and of the contact force (amount and direction), making hypotheses and/or *in-vivo* estimation the mechanical properties of the subject. Optimized algorithms for a faster calculus of the distance map will may be considered too. Moreover, an higher number of subjects, healthy and pathological, will be acquired in order to engineer all the needed processes for reaching reliable estimations of the investigated quantities.

In conclusion, this model for the evaluation of the subject-specific tibio-femoral contact during the execution of daily living activities will become an important clinical tool for suggesting effective pre-operative, surgical and rehabilitative procedures in pathological patients.

4.5 References

Amini, A. A., Chen, Y., Curwen, R. W., Mani, V., Sun, J., (1998). Coupled B-snake grids and constrained thin-plate splines for analysis of 2-D tissue deformations from tagged MRI. IEEE Transactions on Medical Imaging 17**,** 344-356.

Barber, C. B., Dobkin, D. P., Huhdanpaa, H., (1996). The Quickhull algorithm for convex hulls. Acm Transactions on Mathematical Software 22**,** 469-483.

Bookstein F.L., (1989). Principal Warps: Thin-Plate Splines and the Decomposition of Deformations. IEEE Transactions on Pattern Analysis and Machine Intelligence 11**,** 567-585.

Borgefors, G., (1984). Distance transformations in arbitrary dimensions. Computer Vision Graphics and Image Processing 27**,** 321-345.

Boyd, S. K., Ronsky, J. L., Lichti, D. D., Salkauskas, K., Chapman, M. A., Salkauskas, D., (1999). Joint surface modeling with thin-plate splines. Journal of Biomedical Engineering 121**,** 525-532.

Corazza, F., Stagni, R., Castelli, V. P., Leardini, A., (2005). Articular contact at the tibiotalar joint in passive flexion. Journal of Biomechanics 38**,** 1205-1212.

Danielsson, P. E., (1980). Euclidean distance mapping. Computer Graphics and Image Processing 14**,** 227-248.

Kozinska, D., Tretiak, O. J., Nissanov, J., Ozturk, C., (1997). Multidimensional alignment using the Euclidean distance transform. Graphical Models and Image Processing 59**,** 373-387.

Lavallee, S., Szeliski, R., (1995). Recovering the position and orientation of free-form objects from image contours using 3D distance maps. IEEE Transactions on Pattern Analysis and Machine Intelligence 17**,** 378-390.

Marai, G. E., Laidlaw, D. H., Demiralp, C., Andrews, S., Grimm, C. M., Crisco, J. J., (2004). Estimating joint contact areas and ligament lengths from bone kinematics and surfaces. IEEE Transactions on Biomedical Engineering 51**,** 790-799.

Meyer, C. R., Boes, J. L., Kim, B., Bland, P. H., Zasadny, K. R., Kison, P. V., Koral, K., Frey, K. A., Wahl, R. L., (1997). Demonstration of accuracy and clinical versatility of mutual information for automatic multimodality image fusion using affine and thin-plate spline warped geometric deformations. Medical Image Analysis 1**,** 195-206.

Mohr, R., Bajcsy, R., (1983). Packing volume by spheres. IEEE Transactions on Pattern Analysis and Machine Intelligence 5**,** 111-116.

Ragnemalm, I., (1993). The Euclidean distance trasform in arbitrary dimensions. Pattern Recognition Letters 14**,** 883-888.

Rosenfeld, A., Pfaltz, J., (1968). Distance functions on digital pictures. Pattern Recognition 1**,** 33-61.

Suter, D., Chen, F., (2000). Left ventricular motion reconstruction based on elastic vector splines. IEEE Transactions on Medical Imaging 19**,** 295-305.

Zuffi, S., Leardini, A., Catani, F., Fantozzi, S., Cappello, A., (1999). A model-based method for the reconstruction of total knee replacement kinematics. IEEE Transactions on Medical Imaging 18**,** 981-991.

Chapter 5: *In-vivo* Estimation of the Elastic Modulus of the Cruciate Ligaments

In this chapter, the problem of the estimation of the elastic modulus of the cruciate ligaments from a living subject was approached, and a novel method to reach this aim without using any invasive measurements was suggested. The aim of this study is not only the simple estimation of the elastic modulus parameter, even though only this would be an important result if the estimation is reliable. Actually, the main aim of this study is the development of a device (*arthrometer*) capable of measuring the loads applied to the patient's limb while joint motions are recorded, or rather, the development of a device capable to accurately measure of the knee joint laxity.

Knee joint laxity can result from soft tissue injury, such as a ligament tear, or from genetic factors (Bendjaballah et al., 1998; Almekinders et al., 2004). The location of a subject's passive knee laxity along a continuous spectrum is dependent on the mechanical properties of the existing structures, and the increased motion that often follows joint injury. At a threshold along the spectrum, a patient will be at risk for joint instability and further injury to joint structures. Links between instability and laxity may be better understood if laxity can be reliably and accurately quantified (Anderson et al., 1992). Current measures of laxity have not been compared to a 'gold standard' in all cases, and when they have, were found to overestimate the laxity values. This is attributed to soft tissue deformation. Consequently, a non-invasive measure of laxity, with an improved accuracy and repeatability, would be very useful in the clinical field and in the research sector.

5.1 Knee Laxity Measuring Device

As reported in a previous chapter, that one focused on the cruciate ligaments modelling, in order to develop a device able to estimate the elastic modulus of the cruciate ligaments in a living subject, an accurate acquisition of both bony kinematics and the applied forces to the knee need to be

available. Regarding the bony kinematics, the necessary accuracy and repeatability was already available by means of the 3D video-fluoroscopy, already successfully used in the cruciate ligaments modelling. Conversely, regarding the measurement of the net forces and torques at the knee, a new device and methodology need to be developed. Thus, merging the whole methodology developed for the cruciate ligaments modelling (Figure 5.1-left) with the measurement of the forces and torques at the knee joint (Figure 5.1-right), it will be possible to reach the aims cited above.

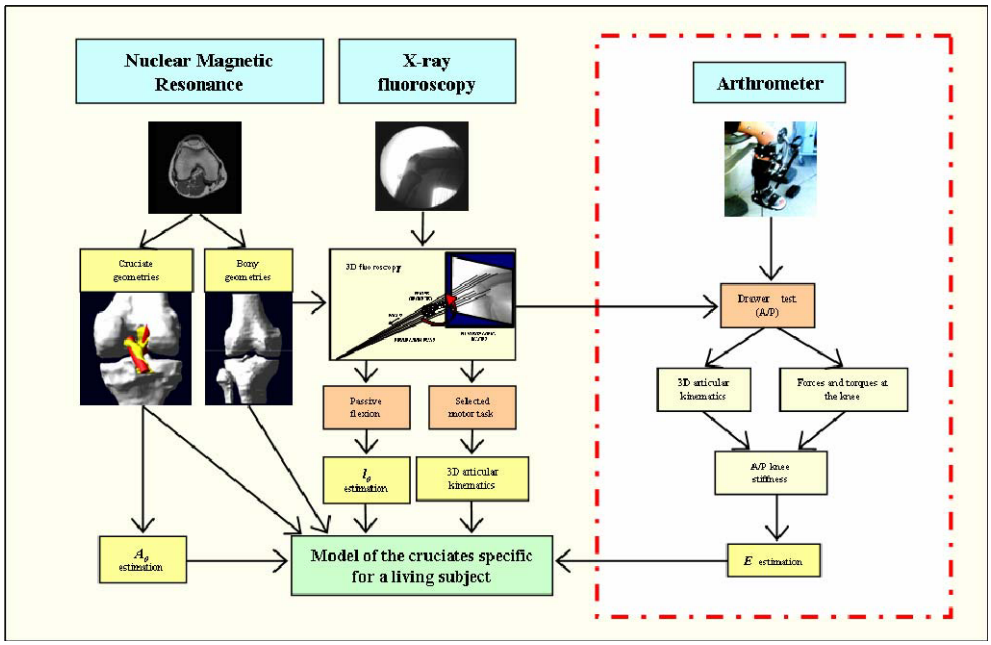

Figure 5.1: Whole scheme of the devised methodology to implement the subject-specific model of the cruciate ligaments of a living healthy subject.

In this new part of the model, it is necessary to develop a prototype of the arthrometer, which is the device capable of measuring the loads applied to the patient's limb while joint motions are recorded. Then, the anterior-posterior drawer test will be performed to the selected subject by means of the arthrometer during the acquisition of the bony kinematics with the 3D fluoroscopy. Thus, applying to the tibia an anterior/posterior force, a relative translation between the tibia and the femur, which is blocked to the table, will be imposed in the same direction. The imposed forces and the torques applied to the tibia will be synchronously recorded by means of the

arthrometer along with the kinematics data of the video-fluoroscopy. Thus, from the force and the kinematics data, it will be possible to calculate the stiffness in the anterior/posterior direction of the whole knee joint, which is proportional, in non-pathological subjects, to the elastic modulus of the cruciate ligaments. The proportionality coefficient will have to take into account both the geometry of the relative ligament (i.e. cross-sectional area and the reference length) and its orientation with respect to the anatomical reference system of the tibia. Thus, since these data can be already calculated from the elaboration of the NMR dataset and the 3D video-fluoroscopy, an *in-vivo* estimation of the elastic modulus will can be specifically performed on each selected subject.

5.2 Preliminary Developments

One of the first steps developed in this study was the designing and the construction of the arthrometer prototype. First of all, in order to measure forces and torques at the knee, a load transducer was necessary, preferably with the largest number of axes possible. Forces and torques have to be applied to the tibia through the load cell, and thus, the practical problem of how to transfer the forces, applied through the load cell, to the tibial segment arose. This problem was approached defining these two conditions: *i)* the tibia needed to be grasped with a comfortable but rigid structure, *ii)* the load cell needed to be firmly coupled to this structure. The first point was solved using a commercial rigid tibial brace for injured ankles, which was usable with different foot sizes and sides. The tibial brace was adopted as a cheap solution to firmly grasp the tibial bony segment. On the contrary, the second point was not completely solved yet. In fact, for the moment, the load cell is fastened to the tibial brace by means of three Velcro bands, but a firmer connection needs to be developed. Thus, this aspect have to be still significantly improved in order to increase the intrinsic rigidity of the arthrometer and to limit the sources of error as much as possible.

Once the first prototype was developed, it was tested in a gait analysis laboratory in order to assess rigidity, size, weight, and usability of the whole devised arthrometer. As already reported, the prototype of the arthrometer, see Figure 5.1, was composed by different parts: a handle which allowed to manually impose forces and torques, a *Bertec* six-component load transducer

to measure the three forces and the three torques manually imposed on the tibia through the handle, a commercial rigid tibial brace for injuries at the ankle, and a connection structure between the load cell and the tibial brace. During the tests, the bony kinematics were not recorded by means of a video-fluoroscopy, as it would be done, but using the stereo-photogrammetric system of the gait analysis laboratory. Obviously, the kinematic data of the bony segments resulted less accurate with respect those obtained with the 3D fluoroscopy, but since the aim of these tests was to assess the feasibility and the usability of the prototype and the methodology, we preferred to perform these tests in the condition as safe as possible for the subject and the operators.

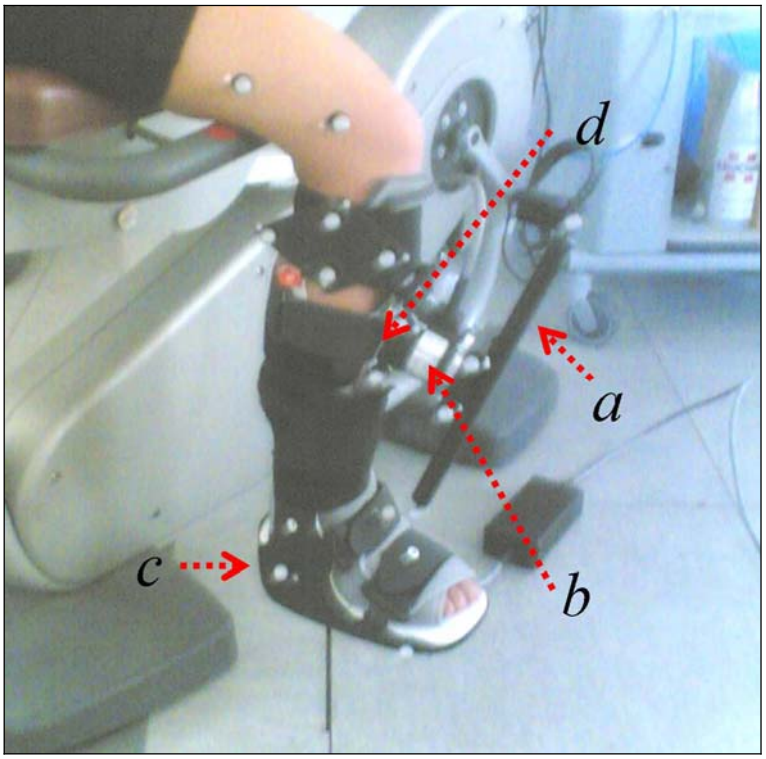

Figure 5.2: Mechanical device for the quantization of the drawer test: handle for the manual application of forces and torques (*a*), *Bertec* six-component load transducer (*b*), commercial rigid tibial brace (*c*), temporary coupling system (*d*). The test of the temporary coupling system was performed with stereo-photogrammetric acquisitions performed in a gait analysis laboratory.

The tests consisted in five trials, each one comprised four or five repetitions of the anterior drawer test performed by the operator, which attempted to impose an anterior tibial translation as pure as possible (i.e. trying to limit the flexion rotation). Thus, the operator tried to apply an anterior tibial translation as large as possible, without reaching discomfort in the subject. The data acquired during the fifth test were discarded because of the mechanical yielding of the structure which coupled the load cell and the tibial brace.

In order to calculate the anterior stiffness of the whole structure (i.e. the whole stiffness of the knee and the arthrometer) the calculus of the force component along the anterior direction and the calculus of the tibial translation along the same anterior direction was performed. Then, it was plotted the anterior force in function of the anterior translation and a linear regression was performed (Figure 5.5).

i Results

The maximum forces and torques acquired by the load cell were about 300 N and 45 Nm, obviously as anterior force and as flexion moment to compensate the anterior force applied below the centre of the knee. In fact, as visible, the anterior force (Figure 5.3) and the flexion torque (Figure 5.4) were the predominant quantities with respect to the other forces and torques.

In Figure 5.5, the estimation of the anterior stiffness obtained during the first test was shown and the estimated anterior stiffness was 8.04 N/mm. During the other tests, this parameter reached the values of 8.34 N/mm, 9.06 N/mm and 8.8 N/mm for the second, the third and the fourth test, respectively.

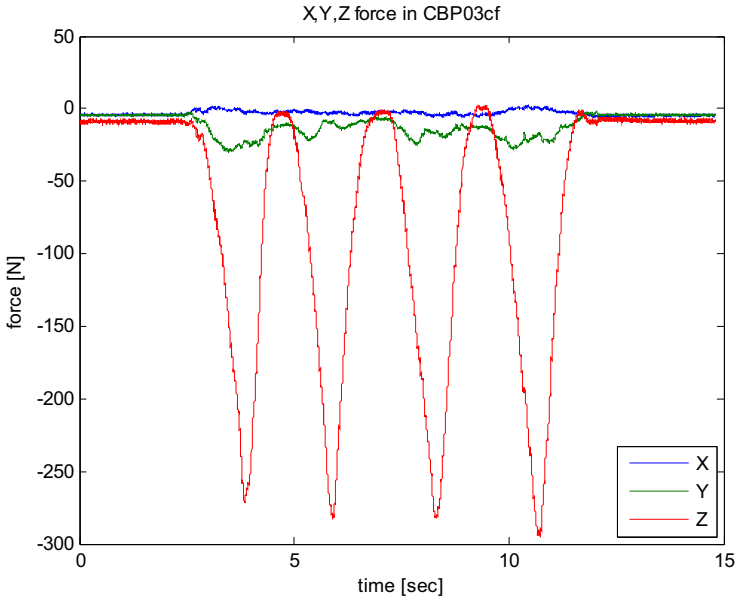

Figure 5.3: Distal(-)/Proximal(+) (*X*), Lateral/Medial (*Y*) and Posterior/Anterior (*Z*) tibial components of the forces acquired in the reference system of the load cell.

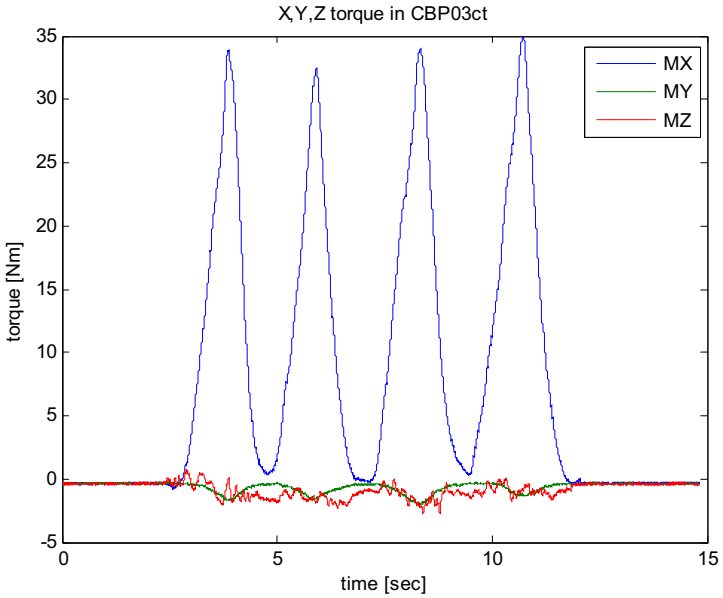

Figure 5.4: Flexion(-)/Extension(+) (*X*), External/Internal (*Y*) and Abduction/Adduction(*Z*) tibial torques acquired in the reference system of the load cell.

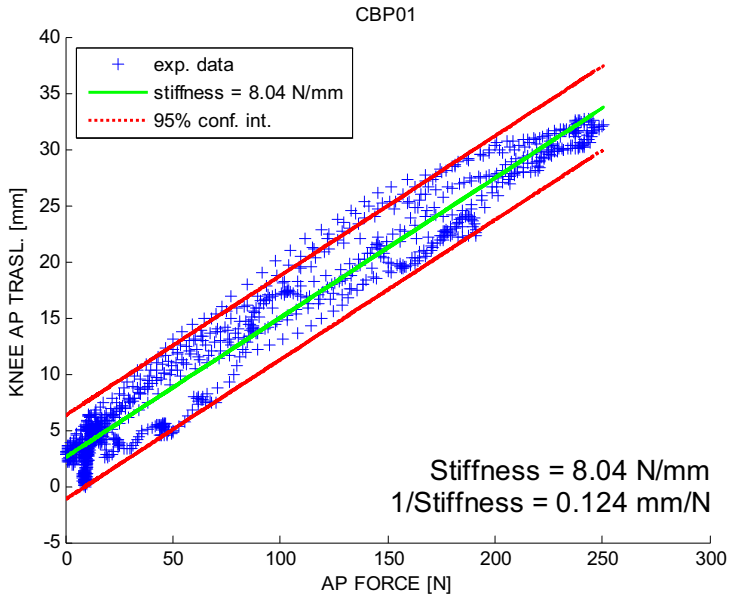

Figure 5.5: Anterior stiffness obtained during the third test and calculated from the linear regression (*green line*) of the experimental points (*blue crosses*).

ii Discussion

These preliminary tests were not aimed to assess the mechanical behaviour of neither the anterior cruciate ligament nor the intact knee of the select subject, but they were just aimed to better understand and evaluate the possible deficiencies of the methodology and the practical troubles that could occur during the use of this new device. Obviously, from the acquired data, just a simple evaluation of the repeatability of the measurements and a check of the order of magnitude of the quantities to be imposed and measured. Moreover, since during the fifth test the structure which connected the load cell with the tibial brace mechanically yielded, the necessity to develop a stiffer connection structure was confirmed.

As expected, the operator was able to impose anterior forces larger than the fixed minimal threshold of 200 N without produce discomfort in the subject. On the contrary, the measured flexion moments resulted larger with respect to those expected. Nevertheless, these were necessary in order to

compensate the anterior force that was applied at least 15 cm lower than the centre of the knee. This fact was verified considering the flexion-extension angle (Grood and Suntay, 1983) during the execution of the tests, which remained quite constant with little oscillations (lower than 5°) around the initial value (about 60° of flexion).

Considering the roughness in the calculation of the anterior stiffness parameter, a good repeatability was achieved, even more considering the early stage of the project and the large margins of improvement of the methodology. In fact, performing the kinematics acquisition with the stereo-photogrammetric system instead of the video-fluoroscopic system, a significant part of the relative translation between the femur and the tibia is probably due to the soft tissues artefacts, which derive from the hypothesis that the markers placed on the skin moved coherently with the underlying bones. Thus, it is very probable that just acquiring the bony kinematics by means of the 3D fluoroscopy technique, the repeatability of the devised methodology is meaningfully improved.

5.3 Conclusions and Future Works

In this preliminary stage of the present study, the development of a novel device (*arthrometer*) for the quantification of the drawer test was approached. This is not a completely novel concept. However, arthrometers currently available provide only a qualitative assessment. The arthrometer to be devised, conversely, is intended to provide quantitative accurate and repeatable measurements. Therefore, the proposed device is expected to provide various benefits. First of all, it will guarantee acquisition of more accurate information concerning joint laxity. This will enable improving the validation of existing and new biomechanical models of the knee. Secondly, once the device will be fully engineered, it can be introduced in clinical assessment, thus providing the clinicians with a more accurate assessment of knee joint function/pathology. In this way, orthopaedists will be able to take evidence-based clinical decisions. Moreover, another result that this methodology will be able to provide is just the capability to estimate the subject-specific stiffness and so the elastic modulus of the cruciate ligaments. Finally, a commercial exploitation of the proposed arthrometer

design will have to be considered, as the device has the potential of improving clinical and scientific investigation of knee biomechanics at large.

In conclusion, next developments of this research will be focused to improving the methodology overcoming those troubles encountered during the preliminary tests and to modify the prototype in order to can use it with the video-fluoroscopy, substituting all its metallic parts with non-metallic materials. Then, a series of new acquisitions will be performed on a set of living subjects with the modified arthrometer in order to test the arthrometer with this X-ray technology and also to assess the increasing of the meaningfulness of the acquired data. Moreover, all subjects will be also acquired by means of the NMR and video-fluoroscopy during the execution of daily living activities. Thus, a subject-specific model of the cruciate ligament will be implemented for each analysed subject using the methodology described in the relevant chapter. Finally, considering the estimation of the elastic modulus performed for each subject, a consistent validation process of the devised cruciate ligaments model, which will be actually and fully subject-specific, will be performed.

5.4 References

Almekinders, L. C., Pandarinath, R., Rahusen, F. T., (2004). Knee stability following anterior cruciate ligament rupture and surgery. The contribution of irreducible tibial subluxation. Journal of Bone and Joint Surgery - American Volume 86-A**,** 983-987.

Anderson, A. F., Snyder, R. B., Federspiel, C. F., Lipscomb, A. B., (1992). Instrumented evaluation of knee laxity: a comparison of five arthrometers. American Journal of Sports Medicine 20**,** 135-140.

Bendjaballah, M. Z., Shirazi-Adl, A., Zukor, D. J., (1998). Biomechanical response of the passive human knee joint under anterior-posterior forces. Clinical Biomechanics 13**,** 625-633.

Grood, E. S., Suntay, W. J., (1983). A joint coordinate system for the clinical description of three-dimensional motions: application to the knee. Journal of Biomedical Engineering 105**,** 136-144.

Conclusions

In the literature, the problem of the knee modelling has been tackled from several points of view and at different levels of complexity. Early 2D models of the knee joint were principally aimed to the evaluation of the knee kinematics and of the function of anatomical structures, such as ligaments, in the sagittal plane. Nevertheless, these models were limited because of their incapability to investigate motions and forces potentially significant which can physiologically occur out of the sagittal plane (i.e. internal/external and ab/adduction rotations). More complex 3D models considered several anatomical structures too (e.g. passive and active structures, articular surfaces and contact), but they often featured high computational weight and parameters derived from cadaver and/or non-homogeneous sources. In fact, the development of more complex models produced the necessity to define a larger number of parameters in order to anatomically describe and mechanically characterize the model.

Thus, researchers usually obtained these parameters both from experimental measurements (*in-vitro*, *ex-vivo* and rarely *in-vivo*) and/or considering data reported in the literature. This approach was adopted to qualitatively understand the function of several anatomical structures, also during the daily living activities. Nevertheless, even if a model is designed properly for a specific application, its potential can be invalidated by the errors due to inaccurate parameter definitions. In fact, this kind of error is often due to disagreement in the origin of the parameters and inputs, considered from different and non-homogeneous sources.

In this context, it is necessary to choose what kind of model we want to develop. A generic model is usually aimed to describe the function of a general knee ignoring the specificity of the subject, but the literature specific of this kind of knee model is already quite extensive. On the other hand, a subject-specific model is typically intended to investigate and quantify the peculiar characteristics of the analysed subject, which can be both normal and pathological.

In the present study, an high level of the subject-specificity of the developed models was the first target to be reached. In this way, the human cruciate ligaments and the tibio-femoral contact were modelled using specific data acquired by means of non-invasive imaging technologies from a selected subject. Thus, the models were as subject-specific as possible and able to investigate the functionality/pathology of the modelled anatomical structures of the specific subject without invasive measurements (exception made for a little X-ray dose).

Considering the cruciate ligaments model (Chapter 3), a 3D quasi-static model of the cruciate ligaments of the human knee joint was developed, assuming as foundations of the proposed methodology the measurements of the subject-specific anatomical geometries and of the *in-vivo* kinematic data. Special attention was paid to the geometrical and the mechanical parameters of the cruciate ligaments, each of these was modelled by means of 25 linear and elastic fibres. Other passive anatomical structures of the knee joint, such as collaterals, capsule, menisci and cartilages were neglected. No muscles were considered. The developed model of the cruciates ligaments was aimed to specifically evaluate elongation, force and recruitment of fibres at the cruciate ligaments during the execution of daily living activities. The possibility to perform different evaluations in this model, such as deformation and force at other passive structures, or contact location, force, and pressure at the articular surfaces, was neglected a priori.

Regarding the geometrical parameters of the cruciate ligaments, the cross-sectional area and the reference length were estimated by means of subject-specific nuclear magnetic resonance (NMR) and 3D video-fluoroscopy, respectively. Moreover, in this study, the problem of the estimation of the elastic modulus of the cruciate ligaments was proposed for living subject (Chapter 5). In fact, the elastic modulus of the soft tissues, like cruciate ligaments, is a critical parameter to evaluate, even by means of direct *in-vitro* measurements. Thus, since a subject-specific elastic modulus evaluation could not be obtained in *in-vivo* conditions, experimental measurements reported in the literature were considered to set the parameters of the model. Finally, the mechanical behaviour of the devised model was evaluated during simulations of the drawer test and the axial stability test. Moreover, the model was also employed in order to predict the forces of the cruciate

ligaments during the execution of the step up/down and the chair rising/sitting motor task, performed by the same selected healthy subject.

This work was intended as evaluation of the reliability of the devised methodology, including both experimental measurements and data processing. Although the devised model was simpler than other models presented in the literature, good comparison with the experimental data reported in the literature and physiologically meaningful predictions were obtained. In fact, considering the difficulty to characterize soft tissues, as demonstrated by the dispersion of experimental data reported in the literature, a more complex model would not necessarily imply more precise estimations. In this way, the hypothesis, which stated to use linear-elastic mechanical-properties for each ligament fibre, seems to be not so wrong. Even more true when the target of the study is to investigate a living subject without any invasive mechanical-measurement.

Regarding the estimation of the elastic modulus parameter by means of the arthrometer, see Chapter 5, a prototype of the device aimed to measure the forces applied to the subject's knee synchronously to the bony kinematics was developed and preliminary tested in the gait analysis laboratory. The devised prototype was composed by a six-component load transducer connected to a rigid tibial brace, and a handle needed to manually impose the forces to the tibia during the acquisition of the knee kinematics. In the performed tests, an operator performed the anterior drawer test to a selected subject and the applied force and the tibial translation in the anterior direction were recorded. Finally, the anterior stiffness of the knee was estimated. When the measurements will be more accurate and repeatable, the measurement of the anterior stiffness will can be related with the mechanical properties of the anterior cruciate ligament, and so with its elastic modulus.

The performed tests showed some crucial points to be fixed in the prototype of the arthrometer, such as the not satisfactory stiffness of the mechanical structure that connected the tibial brace with the load cell. Nevertheless, considering the accuracy of the stereo-photogrammetic system with respect to that of the fluoroscopy 3D, the results obtained in these preliminary tests were encouraging enough, even though we know that, regarding the development of this device, much work has yet to be done in order to improve its accuracy and repeatability.

In conclusion, the next step of this research consists in the acquisitions of a set of living subjects in order to increase the reliability and the accuracy of the proposed methodology and of the arthrometer. Thus, when the methodology and the arthrometer will be theoretically and mechanically improved, the selected subject will be acquired with the new mechanical device during the execution of the anterior/posterior drawer test and the forces and torques imposed manually to the tibia and the bony kinematics will be synchronously recorded. Thus, from these data, an *in-vivo* estimation of the elastic modulus of the cruciate ligaments specific of the subject will be performed, and the model will be actually subject-specific. Moreover, from the knowledge of the applied forces and torques and the relevant kinematics, the model of the cruciate ligaments will can be finally validated.

Considering the modelling of the tibio-femoral contact, two different approaches were implemented using the same subject-specific data. As reported in Chapter 4, since the inputs of the model were the geometries and kinematics of the femur and the tibia, a material 'contact' between these two bodies never occurred. In fact, the 'contact' was defined as the condition when the two objects were closer than a threshold distance. Thus, the evaluation of the tibio-femoral 'contact' was performed by means of the calculus of the proximity between the geometries of the femur and the tibia for each relative pose according to the specific kinematics acquired from the subject. Once the proximity between the femur and the tibia was calculated, estimations of the contact point and area were performed and analyzed by means of threshold values properly defined for each single aim.

The first devised method employed the *thin plate splines* tool (TPS) to mathematically describe the articular surfaces of the femur. In the developed model, the proximity between each femoral condyle, described by means of a TPS form, and the relative tibial plateau, described with a simple plane, was calculated. The actual contact area (unknown) was estimated by means of two indicators, the first defined on the femoral surface and the other on the tibial one, which both dependant from the definition of the threshold distance.

The considered relative positions between the femur and the tibia were the position assumed by the subject during the NMR acquisition, (no body

weight condition) and three positions at the maximum extension reached during the step up/down motor task (whole body weight condition).

The implemented model resulted to be suitable for the aim to be devised. The TPS method, which was used to interpolate the experimental data of the femoral condyles and to provide an analytical representation of these, showed the advantage to be capable to consider experimental data spatially disordered, and so to can suitably use the experimental data acquired on a specific subject. Nevertheless, the TPS method featured the disadvantage to hardly manage set of experimental point larger than 2000 points. For this particular problem, the subject-specific bony geometries, reconstructed from the NMR dataset by means of the software AMIRA, needed to be elaborated in order to reduce the number of points. Moreover, since TPS method is based on the minimum energy deformation of a thin plate, it prevents to describe surfaces too much curved. In fact, in the present study, only the part of femoral condyles which was known to be in contact with the tibia at the full extension was described by means of the TPS method. Thus, if the tibio-femoral contact at other flexion angles of the knee would to be evaluated, it would be necessary to select the relevant experimental points and perform the calculus of the new TPS forms, one for each considered position of the knee joint. In future improvements of the devised model, both the femoral and tibial articular surfaces will be represented by means of the TPS method. Thus, describing the bony geometries more anatomically, an higher level of specificity of the model will be reached.

The second method implemented to evaluate the tibio-femoral contact exploited the Euclidean Distance Transform (distance map) to represent the proximity of whatever point from each tibial plateau, in its nearby space. Differently by the method of the TPS, the use of the distance map allowed to overcome the problem due to the different poses of the femoral surface with respect to the tibial one during the execution of living motor tasks. In fact, since the use of the distance map allowed a very quick evaluation of the distance of all femoral points of each condyle with respect to the relative tibial plateau, the repetition of this process for each position assumed by the subject during the execution of the select motor task did not resulted too much computationally heavy. Moreover, this approach featured the

capability to manage over-sampled geometries like those reconstructed by the NMR dataset with the software AMIRA.

In the adopted model, each tibial plateau was represented by means of a 3D distance map. The bony kinematics of the femoral points were described in the tibial reference system in order to consider the two distance maps fixed in the space. Then, all femoral points were evaluated by means of the distance map and the proximity of each femoral condyle from the relative tibial plateau was evaluated. Finally, the lateral and the medial contact points and their locations in the space were estimated during the execution of the step up/down and the chair rising /sitting motor tasks.

The use of the 3D distance map for the evaluation of the tibio-femoral contact showed several advantages, but revealed some disadvantages too. For example, using 3D distance maps for describing the two tibial plateaus required to maintain fixed in the space the tibial geometry and so required to calculate the bony kinematics of the femur in the fixed tibial reference system. On the contrary, this approach allowed to manage the bony geometries as cloud of points, neglecting facets and normals of the mesh version and making the methodology simpler and computationally lighter. The computational weight paid in the pre-calculation of the distance map was spent in order to economize much more time during several evaluations of distances needed for each frame acquired by the video-fluoroscopy.

Thus, the devised model, based only on imaging technologies, was suitably used to reach the aim of the study, the evaluation of the tibio-femoral contact in a living subject during the execution of daily activities. The model produced physiologically meaningful results, and it showed that some biomechanical behaviours of the knee joint in passive and simulated loading conditions were present also during the execution of daily motor tasks, such as the step up/down and the chair rising/sitting. On the lateral side, the physiological rolling and sliding movements were obtained for little and higher flexion angle respectively, whereas on the other side, the physiological medial pivot seemed to be obtained.

Future improvements of the devised model will include methodologies for the estimation of the contact area and of the contact force (amount and direction), making hypotheses and/or *in-vivo* estimation the mechanical properties of the subject. Optimized algorithms for a faster calculus of the distance map will may be considered too. Moreover, an higher number of

subjects, healthy and pathological, will be acquired in order to engineer all the needed processes for reaching reliable estimations of the investigated quantities.

In conclusion, this model for the evaluation of the subject-specific tibio-femoral contact during the execution of daily living activities will become an important clinical tool for suggesting effective pre-operative, surgical and rehabilitative procedures in pathological patients.

List of Publications

Congress Presentations Available on International Journal

1. Stagni R., Fantozzi S., Lannocca M., *Bertozzi L.*, Cappello A.. Estimation of knee ligaments loads using the modelling approach applied on in-vivo accurate kinematics and morphology of a young subject. Modelling in Medicine and Biology VI archived in WIT Transactions on Biomedicine and Health (ISSN 1743-3525), 8, 381-399. In proceeding Biomedicine 2005, Bologna, Italy, 7-9 September 2005.
2. *Bertozzi L.*, Stagni R., Fantozzi S., Cappello A.. 3d knee model validation using drawer test to study cruciate ligaments biomechanic function in-vivo. In Press in Gait & Posture. In proceeding SIAMOC 2005, Tirrenia (Pisa), Italy, 29-27 October 2005.
3. *Bertozzi L.*, Stagni R., Fantozzi S., Cappello A., Investigation of the biomechanic function of cruciate ligaments using kinematics and geometries from a living subject during step up/down motor task. Springer-Verlag Lectures Note in Computer Science, 3994, 831-838. In proceeding ICCS 2006, Reading, United Kingdom, 28-31 May, 2006.
4. *Bertozzi L.*, Stagni R., Fantozzi S., Cappello A.. Estimation of knee cruciate loads during living activities: step up/down and chair rising/sitting motor tasks. Gait & Posture 24(1) S31-S32. In proceeding SIAMOC 2006, Empoli (Fi), Italy, 18-21 October 2006.
5. *Bertozzi L.*, Stagni R., Fantozzi S., Cappello A.. Evaluation of the elastic modulus variations in a subject-specific knee model using the drawer test. Journal of Biomechanics 39(1) S69-S70. In Proceeding 5th World Congress of Biomechanics, Munich, Germany, July 29th - August 4th 2006.
6. *Bertozzi L.*, Stagni R., Fantozzi S., Cappello A.. In-vivo evaluation of the tibio-femoral contact during daily activities: step up/down and chair rising/sitting motor tasks. In Proceeding SIAMOC 2007, 24-27 October 2007.

Congress Presentations not-Available on International Journal

1. *Bertozzi, L.*, Stagni, R., Fantozzi, F., Lannocca, M., Cappello, A.. "A 3D quasi-static model to investigate biomechanic function of the knee cruciate ligaments using subject specific geometry and kinematics data". In proceeding EMBEC 2005, Prague, Czech Republic, 20-25 November 2005.
2. *Bertozzi L.*, Stagni R., Fantozzi S., Cappello A.. Knee Model Sensitivity to Young Modulus of the Cruciate Ligaments during Anterior-Posterior Drawer Test. Oral Presentation at Knee2006, Berlin, Germany, 28-30 June 2006.

Original Papers on International Journal

1. *Bertozzi L.*, Stagni R., Fantozzi S., Cappello A., 2006. Investigation of the Biomechanic Function of Cruciate Ligaments Using Kinematics and Geometries from a Living Subject During Step Up/Down Motor Task. Springer Verlag Lectures Note in Computer Science, 3994, 831-838.
2. *Bertozzi L.*, Stagni R., Fantozzi S., Cappello A., 2007. Knee model sensitivity to cruciate ligaments parameters: a stability simulation study for a living subject. Journal of Biomechanics 40 (1) S38-S44.
3. *Bertozzi L.*, Stagni R., Fantozzi S., Cappello A., 2008. Evaluation of a cruciate-ligament model: sensitivity to the parameters during drawer-test simulation. Journal of Applied Biomechanics. In Press.
4. *Bertozzi L.*, Stagni R., Fantozzi S., Cappello A.. Evaluation of tibio-femoral contact in a living healthy subject. *To be submitted.*

Abstracts on International Journal

1. *Bertozzi L.*, Stagni R., Fantozzi S., Cappello A., 2006. Estimation of knee cruciate loads during living activities: step up/down and chair rising/sitting motor tasks. Gait & Posture 24 (1) S31-S32.

2. *Bertozzi L.*, Stagni R., Fantozzi S., Cappello A., 2006. Evaluation of the elastic modulus variations in a subject-specific knee model using the drawer test. Journal of Biomechanics 39 (1) S69-S70.

Chapter Book

1. *Bertozzi L.*, Stagni R., Fantozzi S., Cappello A., (2008). Biomechanical Modeling with In-Vivo Data. In: Cai, Y. (Ed.), Digital Humans, The State of the Art Survey. Springer.

Supervision of Master Thesis

1. Casaletto A., *Bertozzi L.*, Stagni R., "Modellazione del contatto nell'articolazione tibio-femorale" (*Modelling of the tibio-femoral contact*). Tesi di Laurea Specialistica in Ingegneria Biomedica - Università degli studi di Bologna – Polo di Cesena – Facoltà di Ingegneria 2. Marzo, 2007.

Biographical Notes

Luigi Bertozzi was born on 1980 in Rimini, Italy.

In 2002, he received the “Laurea Triennale” Degree in Bioengineering from the ALMA MATER STUDIORUM - Università di Bologna, Italy. The thesis was about X-ray micro-tomography applied to the investigation of the structure of the human trabecular bone.

In 2004, Luigi Bertozzi received the “Laurea Specialistica” Degree in Bioengineering, cum laude, from the ALMA MATER STUDIORUM - Università di Bologna, Italy. The thesis was focused on the evaluation of the biomechanic function of the human cruciate ligaments in a living subject.

In 2005, he started the PhD course in Bioengineering at the ALMA MATER STUDIORUM - Università di Bologna, in the Department of Electronics, Computer Sciences and Systems, working on the subject-specific modeling of anatomical structures of the human knee joint in healthy subjects.

Since 2008, Luigi Bertozzi has been working as post-doc at the ALMA MATER STUDIORUM - Università di Bologna, in the Department of Electronics, Computer Sciences and Systems. The research goal moves along the same direction of the PhD work, extending it with the evaluation of the biomechanic function of anatomical structures in pathological knees of living subjects.